OXIDATIVE TREATMENT OF ALGOGENIC ORGANIC MATTER

by

EYLEM KARAKAYA

BS. in Env. E., Yıldız Technical University, 2002

Submitted to the Institute of Environmental Sciences in partial fulfillment of
the requirements for the degree of
Master of Science
in
Environmental Technology

Boğaziçi University

2007

OXIDATIVE TREATMENT OF ALGOGENIC ORGANIC MATTER

APPROVED BY:

Prof. Dr. Miray Bekbölet . . . . . .

(Thesis Supervisor)

Prof. Dr. Işıl Balcıoğlu . . . . . .

Assoc. Prof. Dr. Zehra Can . . . . . .

DATE OF APPROVAL . . . . . .

(Day/Month/Year)

ACKNOWLEDGEMENTS

I must first thank my advisor, Prof. Dr. Miray Bekbolet, for sharing her vast knowledge and infinite patience with me. I appreciate all the unique opportunities she has generously provided me and I truly thank her for all she has taught me and all she has done for me.

I would also like to thank my dissertation committee, Prof. Dr. Işil Balcioglu and Assoc. Prof. Dr. Zehra Can, for their valuable time and the evolutions of the thesis.

I am indebted to Prof. Dr. Orhan Yenigun for his understanding and patience.

I am thankful to Prof. Dr. Bahar Kasapgil Ince for her support and permission for using microscope. Special thanks are also offered to Dr. Ayse Tomruk, Dr. Gulhan Ozkosemen, Dr. Ceyda Uyguner, and Dr. Altan Suphandag their guidance and assistance in much of my lab works.

This dissertation would not be complete without expressing acknowledgement and gratitude to my family; especially thanks go to my sisters Nazli, and my friends, Sitki and Ayca. I have to thank them for top-notch patience and wanting me to be happy. My thanks go out to Suna Erses, Nilgun Ayman Oz, Aslı Akoz and Aylin Alagoz for their encouragements and generous helps during my studies.

Funding for this research was provided by the Research Fund of Boğaziçi University, Project No. 05 Y 101 is gratefully acknowledged.

ABSTRACT

Nowadays, removal of organic substances from natural waters (NOM) is getting greater concern gradually because they form carcinogenic substances (DBP, THM, HAAs, etc.). Consequently, alternative methods have been tried to treat organic substances. Advanced treatment methods like titanium dioxide and photocatalytic oxidation are used as alternative methods through their non by-product formation characteristics. Experimental studies showed that, natural water content of organic materials contains humic acid, fulvic acid, hydrophilic acid, protein, lipid, amino acid and hydrocarbons.

The objective of this research was to characterize the spectroscopic properties of algal organic matter (AOM) which comes from the algae degradation as model compounds to represent the natural organic matter (NOM) in aquatic systems. The photocatalytic oxidation of AOM aqueous solution was carried out using TiO2 Degussa P-25 as the photocatalyst. The degradation kinetics was assessed based on pseudo first order kinetic models. The related data for all working solutions were comparatively presented in terms of UV-vis parameters such as Color436, Color400, UV365, UV280 and UV254. Furthermore, the molecular and structural characteristics of the AOM solution were monitored by spectroscopic techniques during photocatalytic oxidation. For all of the working solutions, higher removal rates were achieved in terms of UV254 values compared to that of Color436. According to obtained data, the aqueous solution of AOM was efficiently oxidized by photocatalytic due to TiO2 amount and dilution rates. However degradation time did not significantly affect removal efficiencies.

Moreover, considering the complexity of the algal derived organic macromolecules; they were fractionated into well defined subcomponents of known molecular sizes using ultrafiltration through membranes in the range of 1-100 kDa. The effect of photocatalytic oxidation on the molecular size fractions of algal organic matter was also evaluated on a comparative basis by UV-vis and fluorescence spectroscopy.

As confirmed by the spectroscopic evaluation of the molecular size distribution data, photocatalytic degradation of algal organic matter aqueous solution results in the formation of higher UV-absorbing compounds.

ÖZET

Günümüzde doğal sularda bulunan organik maddelerin giderimi (NOM) oluşturdukları kanserojen maddeler (DBP, THM, HAAs, vs.) yüzünden gün geçtikçe önem kazanmıştır. Bundan dolayı organik madde arıtımında alternatif yöntemler denenmektedir. İleri arıtma tekniklerinden biri olan titanyum diyoksit ile fotokatalitik parçalanma, yan ürün oluşturmamasından dolayı alternatif yöntem olarak uygulanmaktadır. Bugünkü deneysel çalışmalar göstermektedir ki, doğal sulardaki organik maddelerin içeriğinde, hümik asit, fulvik asit, hidrofilik asit, protein, lipit, aminoasit ve hidrokarbonlar bulunmaktadır.

Bu çalışmanın amacı, su kaynaklarında bulunan doğal organik maddeleri (NOM) temsil etmek için model olarak kullanılan ve alglerin bozunması sonucu oluşan alg organik maddesinin (AOM) spektroskopik ve florometrik olarak karakterizasyonunu yapmaktır. AOM solüsyonun fotokatalitik oksidasyonu TiO2 Degussa P–25 fotokatalizör kullanılarak yapılmıştır. Bozunma kinetiği olarak birinci dereceden reaksiyon kinetik modelleri üzerinden değerlendirilmiştir. Kullanılan solüsyonların verileri Renk436, Renk400, UV365, UV280 ve UV254 gibi UV-vis parametreleri üzerinden karşılaştırmalı olarak verilmiştir. Ayrıca, AOM solüsyonunun fotokatalitik oksidasyonu ile değişen moleküler ve yapısal özellikleri spektroskopik yöntemlerle izlenmiştir. Çalışılan tüm solüsyonlarda UV254 cinsinden giderimde Renk436 değerlerine kıyasla daha yüksek giderim hızına ulaşılmıştır. Elde edilen verilere göre, AOM solüsyonu TiO2 miktarına ve seyreltme oranına bağlı olarak fotokatalitik olarak verimli bir şekilde okside edilmiştir. Ancak bozunma zamanı giderimde ciddi bir değişikliğe sebep olmamıştır.

Ayrıca, AOM makro molekülünün karmaşık yapısı düşünülerek, ultrafiltrasyonla 1–100 kDa aralığında membranlar kullanılarak tanımlanmış molekül büyüklüklerindeki komponentlere ayrılmıştır. Fotokatalitik oksidasyonun, alg organik maddelerinin molekül fraksiyonlarına olan etkisi UV-vis ve flüoresan spektroskopisiyle değerlendirilmiştir.

Moleküler büyüklük dağılımı verilerinin spektroskopik olarak değerlendirilmesiyle onaylandığı gibi, alg organik maddelerinin fotokatalitik olarak parçalanması yüksek UV absorbe eden bileşiklerin oluşumuna neden olmaktadır.

TABLE OF CONTENTS

LIST OF TABLES

LIST OF FIGURES

LIST OF ABBREVIATIONS AND SYMBOLS

Symbol	Explanation	Units used
μ	Specific growth rate	(d^{-1})
[S]	Concentration of solute	(mg L^{-1})
1/n	Freundlich adsorption intensity parameter	
a	$KMnO_4$ consumed by sample	(mL)
AHA	Aldrich Humic Acid	
AOP	Advanced Oxidation Processes	
b	$KMnO_4$ consumed by blank	(mL)
BLF	Black Light Fluorescent Lamp	
C	Concentration	(mg L^{-1})
C_e	Concentration of solute in spectrophotometric measurements remaining in the solution at equilibrium	(m^{-1})
COD	Chemical Oxygen Demand	(mgO_2 L^{-1})
$Color_{400}$	Absorbance at 400 nm	(m^{-1})
$Color_{436}$	Absorbance at 436 nm	(m^{-1})
Da	Dalton	
DBP	Disinfection By-Product	
DOC	Dissolved Organic Carbon	
EM	Emission wavelength	(nm)
EOM	Extracellular Organic Matter	
EX	Extraction wavelength	(nm)
F	Titration factor of $KMnO_4$ solution	
FI	Fluorescence Index	
FA	Fulvic acid	
FTIR	Fourier transformation infrared	
HA	Humic acid	

HMW	High Molecular Weight	
HPLC	High Pressure Liquid Chromatography	
HS	Humic Substances	
IOM	Intracellular Organic Matter	
k	Pseudo first order reaction rate constant	(m^{-1})
K_F	Freundlich adsorption capacity constant	
LMW	Low Molecular Weight	
MSD	Molecular Size Distribution	
MW	Molecular Weight	
NF	Nanofiltration	
NMR	Nuclear Magnetic Resonance	
NOM	Natural Organic Matter	
OD	Optical Density	
Py-GC-MS	Pyrolysis-Gas Chromatography-Mass Spectroscopy	
q_A	Adsorbed amount of per unit weight of adsorbent	(m^{-1} g^{-1})
R	Pseudo first order reaction rate	($m^{-1}min^{-1}$)
RHA	Roth Humic Acid	
RO	Reverse Osmosis	
t	Irradiation time	(min)
t_1	First sampling time	(d)
$t_{1/2}$	Half-life	(min)
t_2	Second sampling time	(d)
t_d	Doubling time	(d)
THM	Trihalomethane	
THMFP	Trihalomethane Formation Potential	
TOC	Total Organic Carbon	(mg C L^{-1})
UF	Ultrafiltration	
UV_{254}	Absorbance at 254 nm	(m^{-1})
UV_{280}	Absorbance at 280 nm	(m^{-1})
UV_{365}	Absorbance at 365 nm	(m^{-1})

V	Sampling volume	(mL)
X_1	Cell concentration at t_1	(cell d^{-1})
X_2	Cell concentration at t_2	(cell d^{-1})
$\Delta\lambda$	Bandwidth	(nm)

1. INTRODUCTION

Organic matter, both particulate and dissolved, is composed of non-humic and humic substances. Non-humic organic substances include carbohydrates, proteins, peptides, amino acids, fats, waxes, resins, pigments and other low molecular weight compounds. These are labile and easily degraded by microorganisms. Natural organic matter (NOM) occurs in all natural water sources when animal and plant material breaks down. Natural organic matter contains humic acids, fulvic acids, polysaccharides, hydrophilic acids, proteins, lipids, amino acids and hydrocarbons. Natural organic matter characteristics of source waters, such as molecular weight distribution and humic content, can vary due to some geographical or source-related (surface vs. groundwater) differences.

NOM affects water quality by providing precursor material for disinfection by-products (DBPs), substrate for biogrowth, and complexation sites for heavy metals. To understand these processes better and to control their effects on drinking water quality, it is necessary to understand the chemistry of NOM (Benjamin et al., 2000).

NOM is derived from both allochtonous (watershed or terrestrial) and autochtonous (algal or in situ) sources. Allochtonous NOM generally exhibits more of a humic signature while autochtonous NOM largely consists of algogenic organic matter (AOM). It is well known that AOM exhibits some humic like material along with some lower and higher molecular size components of low UV absorptivity. Although much has been learned about the chemical characteristics of terrestrially derived NOM, knowledge about autochthonous AOM still remains limited.

Algae derived organic matter constitutes a different source contributing to the broad array of substances that form natural organic matter in fresh water systems. For this reason in this study algae (Chlorella sp., Scenedesmus sp. etc.) were utilized in order to get information about NOM.

Up to date, model humic substances either as commercially available humic acids or as humic and fulvic acid standards have been used to represent natural organic matter in drinking water supplies (Uyguner and Bekbolet, 2004a; Uyguner and Bekbolet, 2005a). Due to the importance of NOM, both terrestrial and aquatic origin humic substances have been investigated. However, gathered data reveal differences between model compounds and real natural water systems (Uyguner and Bekbolet, 2004b). Accordingly, different types of organic matter such as algogenic organic matter in water and commercially available chemicals such as lignosulfonic acid, pyrogallol and gallic acid require further investigation.

Recent studies of advanced oxidation processes for the degradation of model humic substances mostly cover the kinetics of the reaction and evaluation of different kinetic models focusing on their spectroscopic characterization using UV- vis and fluorescence spectroscopy (Uyguner and Bekbolet, 2004a; Uyguner and Bekbolet, 2005a; Uyguner and Bekbolet, 2005c). Also, Widrig et al. (1996) studied the removal of AOM by ozonation and coagulation. Even though pre-ozonation enhanced organic matter removal, AOM was not easily removed by coagulation, and higher coagulant doses were required.

With reference to the previously conducted studies, in this study removal of AOM will be achieved by photocatalytic oxidation using TiO_2. The kinetics of the reaction will be evaluated and comparatively discussed with respect to recently studied humic matter based natural organic matter removal (Uyguner and Bekbolet, 2004a; Uyguner and Bekbolet, 2005a).

2. THEORETICAL BACKGROUND

2.1. Natural Organic Matter

Natural organic matter (NOM) is used to describe the complex mixture of organic material present in all drinking water sources such as humic acids, hydrophilic acids, proteins, lipids, amino acids and hydrocarbons. NOM is a complex mixture of dissimilar organic species found in all potable water sources (Benjamin et al., 2000).

To understand the biogeochemistry of natural organic matter, humic substances, and their interactions with their surrounding environment, it is essential to know the nature of the studied material (McDonald et al., 2004).

NOM in surface-water ecosystems is composed of two broad fractions: the readily utilizable NOM or 'labile pool' and the residue that is 'refractory' and not as easily utilized (Ogura, 1975; Geller, 1986). Though an operative definition of labile NOM is somewhat elusive, the labile pool is generally thought to consist mainly of sugars, amino acids, peptides and other simple compounds (Moran and Hodson, 1990), and accounts for less than 20% of the total NOM. The labile pool is rapidly utilized and is degraded within hours to days. Sondergaard and Middelboe (1995) defined labile NOM as the amount of NOM that could be decomposed by bacteria within a week or two; it has been shown to support the majority of bacterial secondary production (Moran and Hodson, 1990). An alternative definition of labile NOM was suggested by Servais et al. (1989), who determined the labile NOM by filter-sterilizing a water sample containing the NOM to be tested, inoculating it with autochthonous bacteria, and measuring the decrease of NOM over four weeks due to carbon oxidization by bacteria.

The refractory pool, which is composed mostly of higher molecular-weight humic and fulvic acids, is more abundant, but it turns over more slowly and has been considered

relatively less important as a substrate for bacterial growth (Moran and Hodson, 1990) than the labile pool. Nevertheless, at least some components of the refractory pool may be altered photochemically to produce more bioavailable compounds (Lindell et al., 1995; Wetzel et al., 1995; Moran et al., 2000), and several studies have suggested that humic substances are more important components of the biodegradable NOM pool than previously thought (Meyer et al., 1987; Amon and Benner, 1996; Volk et al., 1997). Some high-molecular-weight organic compounds appear to be readily utilized by bacteria in both the ocean and in streams (Travnik, 1990; Tulonen et al., 1992; Amon and Benner, 1996; Meyer et al., 1997; Volk et al., 1997).

A growing body of evidence suggests that the rate at which bacteria degrade different varieties of organic compounds depends not only on the nature of the carbon compounds, but also on bacterial physiology (Leff and Meyer, 1991). Maurice and Leff (2002) found that bacteria in the stream were able to use higher molecular-weight, aromatic-rich components of the NOM. Therefore different bacterial communities have different abilities to utilize high- versus low molecular-weight NOM components. This data suggest that NOM quantity and chemical characteristics may be important in determining microbial growth rates, but that the relative importance of these two factors depends on microbial community composition. For example, Cottrell and Kirchman (2000) found that different bacterial phylogenetic groups are dominant in different basic types or 'qualities' of oceanic organic matter samples.

Much research to date has shown that lower molecular weight fractions of NOM are the most bioavailable for uptake (Saunders, 1976; Hobbie, 1988; Meyer et al., 1997; and references therein). Contrary to this, several studies have shown that higher molecular weight fractions are readily taken up by bacteria in marine and fresh waters (Tranvik, 1990; Tulonen et al., 1992; Amon and Benner, 1996; Meyer et al., 1997; Volk et al., 1997).

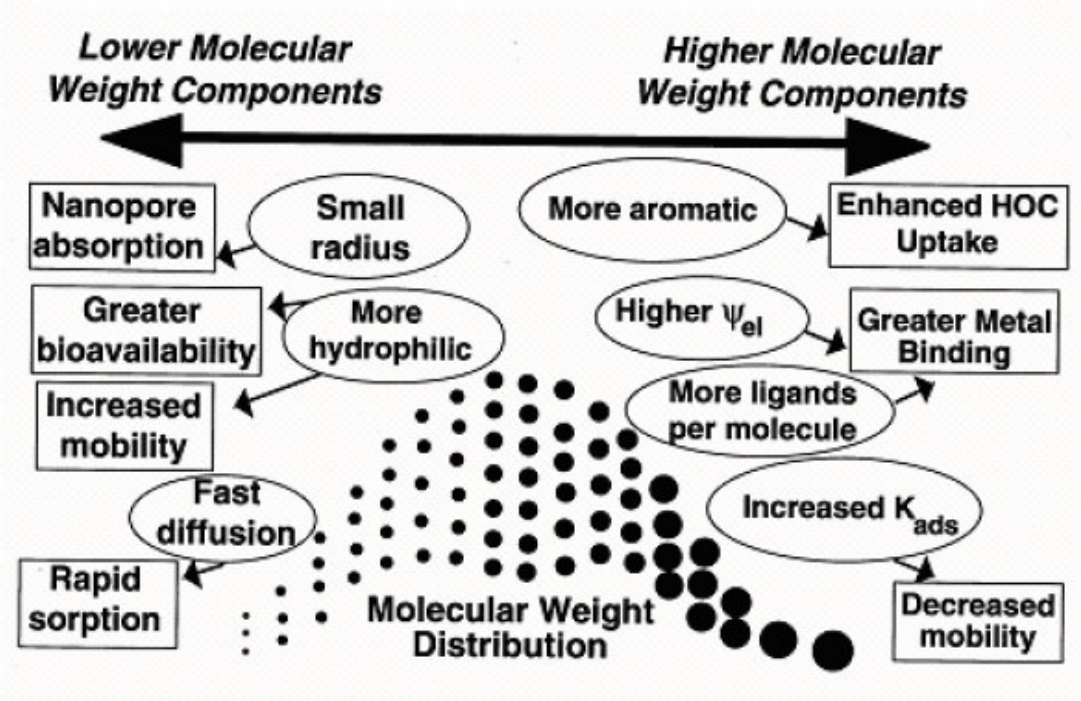

Figure 2.1. Molecular weight has a number of noticeable effects on both NOM properties and behavior (Cabaniss et al., 2000).

The interactions between bacteria and NOM are important to the dynamics of the global C cycle (Azam, 1998). Hence, factors that affect NOM production and consumption chemical composition, molecular weight, and inorganic nutrient concentrations - have an influence on ecosystem C fluxes (Amon and Benner, 1996). Bacterial-NOM interactions are also important because bacterial adsorption of NOM may have an effect on contaminant mobility. Microbial adsorption has the potential to decrease aqueous concentrations of both metals and organic acids (Fein, 2000). Therefore, an increasing amount of work is being done to determine what effect bacterial adsorption has on physicochemical properties of NOM (Frost et al., 2004; Maurice et al., 2004).

In aquatic ecosystems, NOM represents one of the largest active organic carbon reservoirs; the amount of NOM (commonly measured as dissolved organic carbon (DOC) in

aquatic systems is nearly equal to the amount of CO_2-carbon that exists in Earth's atmosphere (Farrington, 1992).

NOM plays an important role in a wide range of biogeochemical reactions, such as mineral growth and dissolution (Jardine et al., 1989; Zhou et al., 2001) NOM has also an important role in controlling metal and pollutant mobility, attenuating potentially damaging UV radiation, and fueling microbial based food webs (Findlay et al., 1986; Azam, 1998). Microbial productivity linkages to NOM cycling are of great importance in wetland (Mann and Wetzel, 1995), river and stream (Meyer et al., 1987; Kaplan and Bott, 2000), lacustrine (Tranvik, 1989; Tulonen et al., 1992; Bertilsson and Tranvik, 1998), and oceanic environments (Azam, 1998).

Fe is able to bind to the aliphatic and aromatic carboxyl and hydroxyl functional groups of NOM, thus enabling it to form dissolved complexes. Micromolar concentrations of Fe can be found in fresh surface waters (Pullin and Cabaniss, 2001). Even though in aerobic environments, Fe is often a limiting nutrient for microbial growth (Schwertmann and Cornell, 1991).

The occurrence of natural organic matter in raw drinking water can be problematic for water utilities because of NOM's role in the transport and concentration of inorganic and organic pollutants, its potential for serving as a substrate for biological growth in distribution systems, the increased chemical costs that result from the increased coagulant and oxidant demands, and its role as a precursor for potentially harmful disinfection by-products (DBPs).

2.1.1. Relationship Between Natural Organic Matter and Disinfection By-products

The variety of the components in NOM changes from water to water which leads to variation in the reactivity with chemical disinfectants such as chlorine, ozone and chlorine dioxide. The understanding of the structure and abundance of these components is therefore vital in the understanding of how to predict and control disinfection by-products (DBPs) in water treatment processes. Precursors for disinfection by-products can be organic or inorganic.

Organic precursors for DBPs include natural organic matter such as algal-derived organic matter (AOM), and humic and fulvic materials. Bromide ion and chlorite are inorganic precursors. DBPs are formed when these precursors are present in water disinfected at treatment plants. Trihalomethanes (THMs), the most common family of DBPs, are derived from organic matter and may include bromated compounds.

Toxicological studies on laboratory animals showed that certain DBPs have negative effects on animal health, leading the U.S. Environmental Protection Agency (U.S.EPA) to implement THM regulations for drinking water in 1979. More recently, epidemiology research has shown weak associations between several cancer sites and exposure to chlorinated surface water and its byproducts in humans. Many DBP compounds are regulated by the U.S.EPA because of their carcinogenic and mutagenic nature. The currently regulated disinfection byproducts are trihalomethanes, haloacetic acids, chlorite, and bromide.

Disinfection byproduct levels can vary greatly depending on the source of the water. Surface waters from rivers and lakes produce higher DBP levels than groundwater because of higher organic matter content. Water quality (carbonate alkalinity, ammonia, bromide, pH, temperature) and treatment conditions (contact time, disinfectant dose, removal of natural organic matter before disinfectant application, and/or prior addition of disinfectant) also play important roles in DBP levels.

Removing DBP precursors and modifying disinfection practices can reduce disinfection byproduct formation. Ozone-biofiltration, membranes, granular activated carbon, sedimentation, coagulation, lime-soda softening, and adsorption can all remove organic matter.

Bekbolet and Ozkosemen (1996) later determined the trihalomethane potentials (THMFP) of the photocatalytically treated humic acid solutions. They concluded that the destructive removal of humic acid in aqueous medium by TiO_2/UV process was an effective method to keep the THM levels below the maximum contaminant level of 100 $\mu g\ L^{-1}$(U.S.EPA).

2.1.2. Treatment of Natural Organic Matter

One of the primary challenges faced by the drinking water treatment industry today is the formation of suspected carcinogenic DBPs, which occurs as a result of reactions between natural organic matter and oxidants/disinfectants such as chlorine. Because of this, removal of NOM in particular AOM has a significant role on drinking water treatment systems. Beside the other technologies, UV and fluorescence spectroscopy can be used on unaltered samples and therefore require much less time and effort per analysis. Fluorescence spectroscopy is an extremely sensitive method that permits NOM to be studied in solution at DOC concentrations less than 1 mg L^{-1}. The fluorescence emission of NOM is governed primarily by the identity and concentration of aromatic functional groups in NOM molecules, but nitrogenous groups might be significant as well.

Effective removal of soluble natural organic matter (NOM) from low turbidity waters can be achieved by aluminum coagulation provided due attention is paid to coagulation and flocculation. To obtain maximum NOM removal studied with different pH influencing chemicals such as acid, alum and lime. Adjusting the pH downwards to between 4 and 5 prior to the coagulant addition allows to the formation of soluble NOM-aluminum complexes that link to each other, thereby forming large insoluble bridges complexes that also act as nuclei for flocculation (Gregor et al., 1997).

Chemical structures of hydrophobic acids which consist in NOM affect chemical reactions with coagulants. The removal of NOM with aluminum coagulants can involve hydrolysis, complexation, and precipitation and adsorption reactions (Sen, 2004).

The effectiveness of water treatment processes in the removing natural organic matter depends on its molecular size, polarity and charge density, and with properties of the raw water such as turbidity and hardness. The more hydrophobic NOM fractions were the most easily removed by polymer. The performance of cationic polymers improved significantly with increasing charge density and molecular weight. An alum/polymer combination is the most attractive treatment option (Bolto et al., 1999). Another study of Bolto et al. (2002) is the

removal of natural organic matter (NOM) by coagulation with cationic organic polymers and with alum, and by adsorption on anion exchangers.

2.1.3. Studies on Natural Organic Matter

Despite NOM's abundance and importance in aquatic systems, we do not yet understand quantitatively how the chemical composition of NOM affects its bioavailability, or how bacterial degradation affects NOM properties and reactivity. Several studies have focused on how the quantity of NOM affects microbial communities (Tranvik, 1990; Leff and Meyer, 1991; Sabater et al., 1993; Eiler et al., 2003; Young et al., 2004). However, relatively few studies have investigated how NOM physicochemical properties may influence its bioavailability (Leff and Meyer, 1991; Leff, 2000; Young et al., 2004). Research to date has focused on determining how NOM bioavailability varies with fundamental properties such as elemental composition (Kroer, 1993; Hunt et al., 2000), and with processes such as photochemical reactions (Lindell et al., 1995; Bertilsson and Tranvik, 1998). Several authors have used tangential-flow ultrafiltration to examine how molecular size of NOM affects bioavailability. Using 1000 Da cutoff membranes to separate low molecular weight-LMW- (<1000 Da) and high molecular weight-HMW- (>1000 Da) fractions of NOM, Meyer et al. (1987) showed that bacterial growth and NOM consumed were greatest in LMW enriched samples. Amon and Benner (1996) used ultrafiltration and also found that bacterial efficiencies were consistently higher in LMW fractions than HMW fractions. Covert and Moran (2001) used ultrafiltration to show that the bacterial communities living on LMW fractions of NOM were different than those communities living on HMW fractions of NOM. Young et al. (2004) showed that NOM biodegradation was influenced by source-specific microbial species and NOM physicochemical characteristics. Young et al. (2004) study is also the first to show that the bacteria were able to consume the humic/fulvic type components of the NOM, rather than the low molecular weight, organic compounds present in NOM.

Takahashi et al. (1995) has shown that, ozonation of natural organic matter (NOM) results with a strong rapid decrease in color and UV-absorbance due to a loss of aromacity and

depolymerization, increase in biodegradability, and reduction in THMFP (trihalomethane formation potential) (Camel and Bermond, 1998).

O'Melia et al. (1999) examined the adsorption of NOM on oxide surfaces is investigated. The adsorption of NOM on oxides depends significantly on complex formation reactions between specific sites on oxide surfaces and functional groups on the NOM. Frequently there is a stoicheiometric relationship between the required coagulant dosage and the TOC or the water to be treated. Other important factors include pH and the concentration of divalent cation. Ozone may benefit or retard coagulation, depending on coagulant type and the water quality characteristic that is dominate in setting the optimum coagulant dosage.

According to Chin et al. (1994) molar absorptivity of NOM was investigated. They determined it using a UV-vis wavelength of 280 nm because $\pi \rightarrow \pi^*$ electron transitions occur in this UV region for typical terrestrially-derived humic substances also absorbance at this wavelength is sensitive to the aromatic nature of the NOM. Other studies have used wavelengths including 205, 254, 272 and 280 nm to show that the molar absorptivity of NOM at various UV wavelengths correlate with 13C-NMR-measured aromaticity (Traina et al., 1990; Chin et al., 1994; Peuravuori and Pihlaja, 1997).

2.2. Humic Substances

The term humic substance refers to the organic material in the environment those results from the decomposition of plant and animal residues. Humic substances which are the dominant type of organic matter occur ubiquitously in soil, aquatic environment and certain sediments (Suffet and MacCarty, 1989). They are natural dark paramagnetic, macromolecular, heterogeneous substances with a high degree of polydispersity, extremely complex structure and unique biological and physicochemical features (Slavinska et al., 2002).

Humic substances play important manifold roles in the C-cycle, solar energy transformation, metal ions immobilization and fate of xenobiotics and radionuclides due to their multifunctional physicochemical and biological properties. Results of recent

investigations provided the evidence that humic substances can no longer be recognized only as a transformer of solar energy into heat, storage of nutrients for plants and microbes, soil-structure-forming factor and plant-growth stimulator. For agriculture, ecology and environmental protection the interaction of solar radiation with the surface of ecosystems constitutes the crucial point. Therefore they are the most important solar light absorbers (Slavinska et al., 2002). The humic materials absorb most of the solar energy between the region 300 and 500 nm in which a number of photochemical processes can be initiated (Gaffney et al., 1996).

Humic substances become different from one geographical location from another area. Even the characteristics of humic substances from a given area vary with climatic conditions, such as seasons, rainfall and saltwater intrusion into estuaries (McCoy, 1996).

According to Gjessing (1976) the term humic substances are also defined as the product of a heteropolycondensation of carbohydrates, proteins, fatty acids, lignin, tannins and many other materials depending on their origin. Thus, any structures formulated for humic substances should reflect structures that can occur in plants and microorganisms or their degradation products. The main classes of chemical constituents comprising plant litter are cellulose, hemicelluloses (non-cellulosic polysaccharides), phenolic compounds such as tannins and lignin, water-soluble compounds such as sugars, amino acids and aliphatic acids, ether- and alcohol-soluble compounds such as fats, oils, waxes, resins and pigments, and proteins. Other components of plant litter that are thought to be refractory and may therefore form part of humic substances include carbon black, sporopullenins, cutans, suberans, and algaenans that have been identified in the outer walls of a number of microalgae (McDonald et al., 2004).

The view that humic substances are too complex for determine their chemical structure. The distribution of functional groups may also be important in determining the solubility and aggregation behavior of humic substances (McDonald et al., 1992). Therefore humic substances have been isolated and given special names depending on their solubility at variety of pH value and they can be classified three classes;

- Humic acid: The fraction of humic substances that is not soluble in water under acidic conditions (pH < 2.0) but become soluble at greater pH.
- Fulvic acid: The fraction of humic substances that is soluble in water under all pH conditions.
- Humin: The fraction of humic substances that is not soluble in water at any pH value (Suffet and MacCarty, 1989).

Typically 90 percent of the dissolved humic substances in natural waters consist of fulvic acid, and the remaining 10 percent consist of humic acid. In contrast to this composition, humic substances from soils that humic acid is very large excess over the fulvic acid (Sen, 2004). When referring to humic substances, the term molecular weight is often used, however, it should be used with caution, as humic substances are composed of a complex mix of substances and have not as yet been properly chemically defined, therefore only average molecular weights can be determined. One of the constitutions of humic substances is humic acid referred to as being the high molecular weight fraction, range from 1500 to 5000 Da in streams, and from 50,000 to 500,000 Da in soils. The other one is fulvic acid referred to as moderate molecular weight substances ranging from 600 to 1000 Da in streams and 1000 to 5000 Da in soils (McDonald et al., 2004).

In recent studies, humic substances, particularly fulvic acids, were generated by algae and contributed to the multitude of diverse compounds that comprised the dissolved humic substances (McDonald et al., 2004).

2.2.1. Differences Between Humic Acid and Fulvic Acid

Humic acids, which are a subgroup of humic substances, are heterogeneous and polydisperse macromolecules comprise a wide area (Choudry, 1982). They have an important role in binding and fate of inorganic and organic compounds in natural environment (Van Loon and Duffy, 2000).

Humic acids may operate as concentration and transport agents for trace toxic materials. Humic substances also have a strong tendency to become adsorbed on hydrous oxides, clays and other surfaces. Humic acids are high molecular weight compounds of complex nature. Structurally, they may be considered as condensation products of phenols, quinones and amino compounds (Suphandag, 1998).Humic acids contain more hydrogen, carbon, nitrogen, and sulfur and less oxygen than fulvic acids (Sen, 2004).

Fulvic acid has probably a lower molecular weight but more hydrophilic functional groups than humic acid and humin. Fulvic acids can adsorb or trap other organic substances, such as alkanes, fatty acids, phthalates, and possibly also carbohydrates, peptides, and pesticides because of the their and functional groups of structure (Suphandag, 1998). The structures of fulvic acids are more aliphatic and less aromatic than humic acids. According to Chen and Schnitzer (1976) and McDonald et al. (2004) fulvic and humic acids behave like flexible, linear, synthetic polyelectrolyte in aqueous systems .The total acidities of fulvic acids (900-1400 meq/l00g) are considerably higher than that of humic acids (400-870 meq/l00g) (Tripping, 2002).

Table 2.1. Mean elemental compositions of different humic substances from different origin expressed as weight percentage (All values are on ash-free and moisture free basis) (Rice and MacCarty, 1991).

	Humic Acid				Fulvic Acid			
Element	*Soil*	*Fresh-water*	*Marine*	*Peat*	*Soil*	*Fresh-water*	*Marine*	*Peat*
C	55.4	51.2	56.3	57.1	45.3	46.7	45	54.2
H	4.8	4.7	5.8	5.0	5.0	4.2	5.9	5.3
N	3.6	2.6	3.8	2.8	2.6	2.3	4.1	2.0
S	0.8	1.9	3.1	0.4	1.3	1.2	2.1	0.8
O	36.0	40.4	31.7	35.2	46.2	45.9	45.1	37.8

As can be seen from Table 2.1, depending on their origin, the carbon content of humic acid is higher than that of fulvic acid whereas the oxygen content exhibits a lower weight percent. Humic acids contain more hydrogen, nitrogen, and sulfur and less oxygen than fulvic acids in fresh water.

Esparza-Soto and Westerhoff (2003) studied on biosorption of HA, which was sorbed higher than FA, and FA increased under the presence of calcium. Similar effects have been reported during the biosorption of humic acids in the presence of metals by dried fungal biomass and activated carbons.

In many studies, HA and FA were selected because of several reasons: they have been extensively characterized; they are representative of aquatic humic substances; their high molecular weight may be representative of particulate/colloidal wastewater organic matter (Esparza-Soto and Westerhoff, 2003).

2.2.2. Relationship Between Dissolved Organic Carbon and Humic Substances

Humic substances can comprise a significant of the dissolved organic carbon (DOC) (McDonald et al., 2004) so that many scientists express the concentration of humic substances as dissolved organic carbon (DOC) or total organic carbon (TOC). Typical freshwater concentrations may be in range of 1-25 mgL^{-1} expressed as DOC (Gjessing, 1976). Because humic substances compose from 25% of the dissolved organic carbon concentration (DOC) in ground waters to as much as 90% of (DOC) in wetlands (Thurman, 1985).

The humic fraction of DOC is considered problematic in water because it can readily react with chlorine to form carcinogen compounds and it can complex/partition heavy metals and hydrophobic polychlorinated organics, affecting their fate and transport (Zhou and Banks, 1993).

2.2.3. Treatment and Studies on Humic Substances

Environmental scientists have been working on treatment technologies, to reduce, destroy, and to prevent humic substances. The presence of humic substances in a water supply is undesirable not only for their environmental health effects but also for their interferences with the water treatment processes. Humic substances adversely affect the quality of drinking water in many ways. For instance, they impart color, serve as precursors to the formation of chlorinated compounds, possess ion exchange, and complexion properties that include association with toxic elements and micro pollutants, and precipitate in distribution systems (Vik and Eikebrokk, 1989).

In destroying humic matter; chlorine has been the classic choice. While effective, the formation of trihalomethanes (THM) from this reaction is a concern, even in industrial settings. THM compounds are not readily removed by ion exchange and can penetrate to the process. Ozonation is also effective in biocontrol and destruction of humic matter. No THM compounds are formed. In some cases, hydrogen peroxide has also been used, with similar effects and limitations as ozone.

Besides the traditional treatment methods such as activated carbon adsorption, coagulation precipitation, ion-exchange and biological degradation, advanced oxidation processes (AOP) which are ultrafiltration (UF), nanofiltration (NF) and reverse osmosis (RO) are applied for the removal of humic acids (Arai et al., 1986; Backlund et al., 1992; Gilbert 1988; Kusakabe et al., 1990; McCoy, 1996).

Coagulation is a widely used process for the removal of humic substances in water treatment and has been an area of interest for so many years (Black et al., 1963; Hall and Packham, 1965; Van Benschoten and Edzwald, 1990; O'Melia, 1999). Various types of coagulants, mainly Fe (III) and Al (III) are used in the coagulation-flocculation of humic material. Up to 90 percent removal of the humic acids fraction has been achieved with both Al (III) and Fe (III) (Hunt and O'Melia, 1988; Stephenson and Duff, 1996; O'Melia et al., 1999; Vilge-Ritter et al., 1999).

Most of organic compounds are removed from water by activated carbon adsorption. Carbons with high percentages of macrospores have the highest capacities for adsorption of humic substances. The adsorbability of individual compounds depends on a polarity and molecular size and structure, and pH. Pore size distribution is also the most important factor in the adsorbability of humic substances onto activated carbon (Sen, 2004).

Latest studies on the oxidative destruction of the humic substances in natural waters cover the application of advanced oxidation methods such as UV, UV and H_2O_2, ozone and radiation (Arai et al., 1986; Gilbert, 1988; Backlund, 1992).

Cloete et al. (1999) has recently proposed photocatalytic oxidation as an alternative for the destruction and removal of humic substances in drinking water. The photocatalytic oxidation was followed in terms of TOC analysis, UV absorbance at 254 nm and THM formation potential. A significant reduction was observed in all three responses which confirmed the removal of humic substances from the water samples via photocatalytic oxidation.

Recently, the photocatalytic degradation of humic acids in aqueous TiO_2 suspensions have been extensively studied (Bekbolet, 1996; Bekbolet and Balcioglu, 1996; Bekbolet and Ozkosemen, 1996; Bekbolet et al., 1998).

Ozone is one of the strongest chemical oxidants known. Ozone is used in water and wastewater treatment for disinfection, for decolorization, and as pretreatment for filtration and adsorption processes. Ozone reacts quickly with humic substances to produce oxidized by-products of low molecular weight that generally are more easily biodegradable, polar, and hydrophilic than their precursors (Gracia et al., 1996). The action of ozone on humic substances leads to decrease of molecular weight, increase of the carboxylic functions, degradation of color and UV absorbance (Langlais et al., 1991).

Traina et al. (1990) found that UV absorptivity at 272 nm provides a good estimate of the percent aromatic C content of humic acids, and later Chin et al. (1994) showed a strong

correlation between molar absorptivity, total aromaticity, and weight-average molecular weights for humic substances.

Studies on humins have shown that they are similar to humic acids except that they are strongly bound to metals and clays, rendering them insoluble (Gaffney et al., 1996).

2.3. Algal Derived Organic Matter

2.3.1. Relationship Between Algae and Organic Matter

It is known that in aquatic environments, macromolecular organic matter such as humic substance, are prevalent in marine and lacustrine sediments and are believed to originate from algae or bacteria. Thus, alga-derived macromolecular compounds deposited in aquatic environments probably contribute to total organic matter content of the aquatic systems.

Surface waters, such as lakes and rivers, plant and animal life are active in and around them. After these living things die, bacteria and fungi decompose their carbohydrate and protein legacy into simpler components. Some of these organic compounds are formed in the water itself; others are leached into the water from the surrounding soil. The composition, structure and molecular weight of these compounds vary greatly, depending on many factors, which are the type of biomass decomposed, the temperature and oxygenation of the water and other environmental factors, such as the supply of nutrients and trace elements in the water (McCoy, 1996).

Algae give out anabolic products into the surrounding environment, which are known as extracellular organic matter (EOM). Cell biopolymers within the algae are known as intercellular organic matter (IOM). The EOM and IOM are together referred to as algogenic organic matter (AOM) (Tulonen, 2004). The characterization of physicochemical properties of AOM is necessary in understanding its role in the fate, reactivity, and transport of inorganic

and organic pollutants. Molecular size and light absorptivity can yield important information regarding the chemical reactivity and diffusivity of AOM (Young, 2005).

The soluble AOM includes glycolic acid, carbohydrates, polysaccharides, amino acids, peptides, organic phosphorus, enzymes, vitamins, hormonal substances, inhibitors, and toxins. The release rates of AOM are quite variable depending on the algal growth phase, type of algae, and physiological and environmental conditions (Her et al., 2004).

2.3.2. Algae Growth

Algae are abundant and diverse in drinking water supplies including lakes, reservoirs, rivers, and streams. In all aquatic habitats, Low concentrations of algae are important primary producers of organic matter at the base of the food chain and also food source for freshwater fish and crustaceans. When growth is stimulated by an enrichment of nutrients or by optimal environmental conditions that favor the production of accelerated growth, algae blooms can occur.

In non-limiting nutrient environment algae will reproduce and increase in number. The growth curves relate the change in the number of microorganisms with time as influenced by a set of intrinsic and extrinsic parameters (or conditions) that dictate the growth, survival, and control of desirable and undesirable microorganisms in food systems. If the logarithm of the density (count) of algae is plotted against time, a characteristic curve such as that shown in Figure 2.2 results. This curve represents an environment desirable for algae growth, and is characterized by four main phases which are illustrated as Figure 2.2:

- The lag phase that encompasses the lag time in which the cells are adjusting their physiology and biochemistry to exploit the environment in which they find themselves.
- The exponential (log) phase where the cells grow in their environment as rapidly as possible and at a relatively constant rate.

- The stationary phase where the reproduction rate is equal to death rate. The accumulation of waste metabolites leads to some reduction in the growth rate of the microorganisms.
- The death phase where a further increase in the accumulation of toxins increases bacterial lysis and the rate of cell death exceeds the rate at which the cells divide.

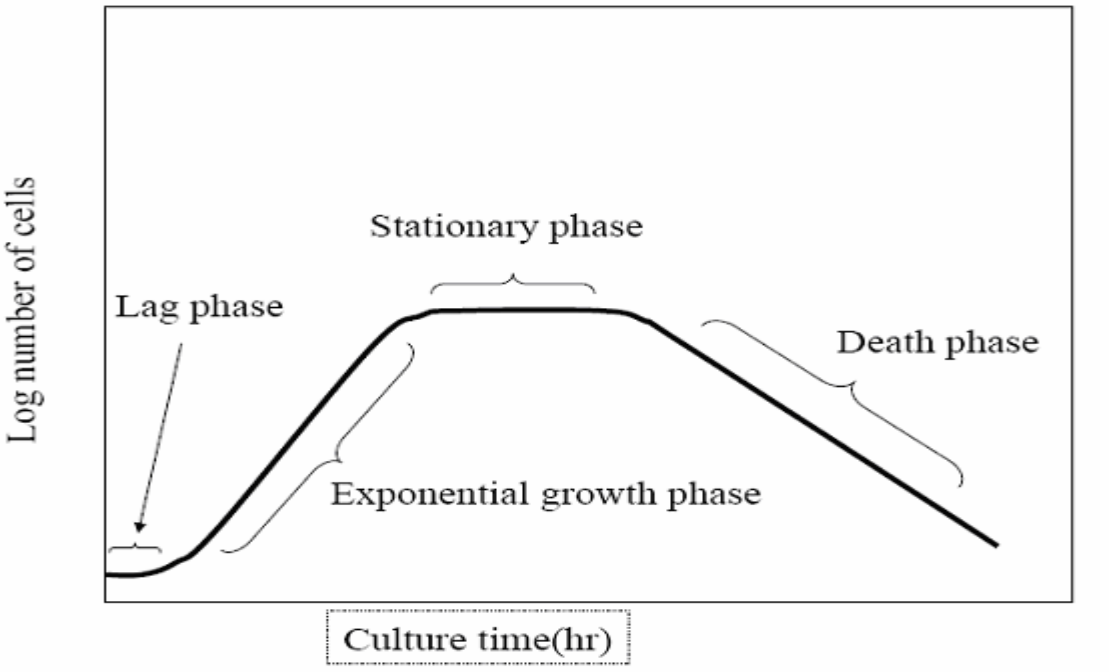

Figure 2.2. Typical batch growth curve.

The typical growth curve is valuable in explaining some trends observed in processing operations, and assist in assessing methods for improving the overall process effectiveness and risk assessment.

Excess algae growth can impart taste and odor problems to potable water. Moreover algae blooms can create very large quantities of organic matter in source water. This will substantially increase the total organic carbon (TOC) content. Recently studies have related increases in algal production to increases in disinfectant by-product formation (Akhlaq et al., 1990; Edzwald et al., 1985; Goel et al., 1995; Hoehn et al., 1980; Hoehn et al., 1984). Beside

the algae harms a summary of algae benefits are; the first link in the aquatic food chain, useful indicators of pollution, help remove excess nutrients, produce oxygen, constitute the raw material to manufacture agar, iodine, diatomaceous earth, and various food products, and can provide spawning habitat for fish.

2.3.3. Culturing and Monitoring of Algal Growth

Studying the growth kinetics of microorganisms is usually carried out experimentally using laboratory growth medium (growth curve studies). In laboratory studies, algae growth system generally consists of two type culture methods which are batch and continuous.

The most common culture system is the batch culture, due to its operational simplicity and low cost. This is a closed system in which there is no input or output of materials. The algal population cell density increases constantly until the exhaustion of some limiting factor, while other nutrient components of the culture medium decrease over time. Batch culture systems are highly dynamic and their accuracy of growth rate determination was highest in an artificial medium as compared to cells grown in natural surface water.

Continuous culture systems have been widely used to culture microbes for industrial and research purposes. This method of culturing algae differs from the batch culture method in that fresh medium is added to the culture at a constant rate and old media (and some of the algae cells) is removed at the same rate in order to maintain a constant volume. The culture therefore never runs out of nutrients. The principal advantage of continuous culture is that the rate of dilution controls the rate of microbial growth via the concentration of the growth-limiting nutrient in the medium.

The suppliers of batch culture were illustrated in the following Figure 2.3.

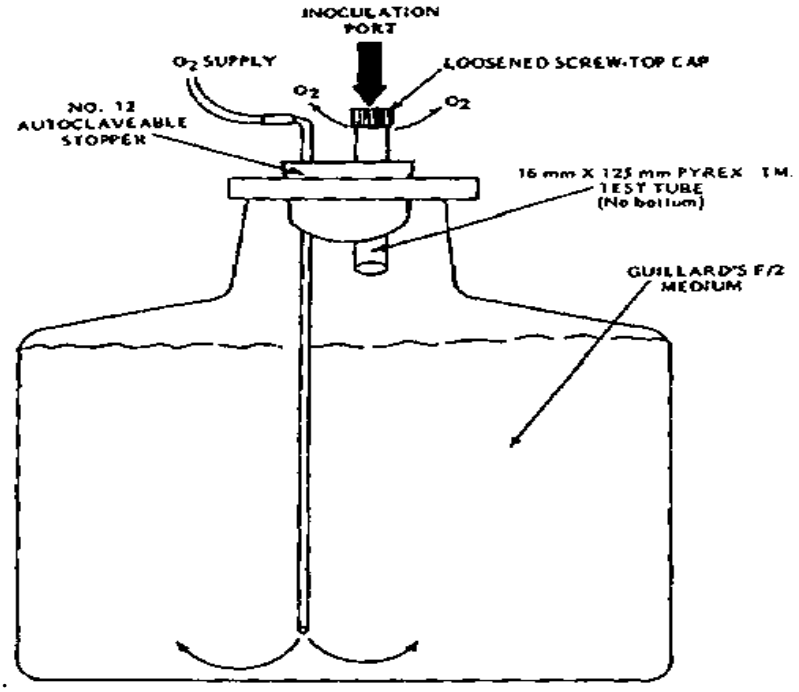

Figure 2.3. The mechanism of batch culture.

Algae may be quantified by various methods such as visual observations microscopically by cell counting; photometrically by absorbance measurement; and by ATP quantification, fluorometrically or electronically, using counting devices. Enumeration of algal cells with an electronic particle counter or microscopic chamber (hemacytometer or blood cell counter) is time consuming and many environmental laboratories do not have the resources to purchase an electronic particle counter (Mayer et al., 1998; Markle et al., 2000). Whereas, absorbance and fluorescence, for which affordable instruments can be used to determine biomass for algae tests (U.S.EPA, 1993). Today phytoplankton biomass typically is estimated by measuring the fluorescence of chlorophyll a either *in vivo* or *in vitro* the principle photosynthetic pigment present in all algae. Measurement by fluorescence, the absorption of light energy at one wavelength and its instantaneous mission at a longer wavelength, is a highly specific, convenient, and sensitive analytic technique. Measurement of chlorophyll fluorescence in vitro is based on its extraction from disintegrated cells in an organic solvent such as methanol, ethanol, or acetone and on its subsequent determination by spectrophotometry and fluorometry, or chromatography (Jacobsen, 1978; Otsuki and

Takamura, 1987). Acetone is typically used as an extraction solvent and the most commonly used extractive method developed by Strickland and Parsons in 1972. However, it has some disadvantages such as: being time consuming, requiring a standard sampling procedure, a necessity of a large volume of sampling and exposures possible quantitative changes during sample storage (Gregor and Marsalek, 2004). Therefore in this study, beside *in vivo* measurement of chlorophyll, hot methanol extraction method was used for measurement of chlorophyll determination.

In vivo fluorescence is re-radiation of light absorbed by algal pigments in intact cell. *In vivo* analysis is the direct measurement of chlorophyll in algal cells without extraction or chemical treatment. These measurements can be taken using discrete samples or continuous-flow. The obvious advantage of *in vivo* analysis is rapid, on-the-spot measurement eliminating the delays for extraction and laboratory measurement. For quantitative determinations, the *in vivo* data are compared with other measurements, including fluorometric extractive data.

Quantification of algae by photometry with absorbance measurement is inexpensive and a frequently used method but it offers lower precision and sensitivity than fluorescence measurement. Various absorbance wavelengths have been suggested for determination of algal biomass (Mayer et al., 1997; Geis et al., 2000).

Light is an important environmental variables that can directly effect the growth of algal populations as medium. Mayer et al. (1998) recommended light intensity is usually between 60 to 120 $\mu E\ m^{-2}s^{-1}$ and is less for freshwater blue green algae and marine algae than for freshwater green species.

According to Cleuvers et al. (2002) algae convert light energy to food through photosynthesis; light is a limiting factor in alga test and is as essential as growth media. In other words, due to light absorption of colored substances, availability of light for the algae is diminished; this will inevitably result in reduced algal growth.

Dominguez-Bocanegra et al. (2004) also analyzed impact of environmental factors such as light intensity, aeration and nutrients on the growth and astaxanthin production of unicellular clear water microalgae *Haematococcus pluvialis*. Maximum growth of *Haematococcus pluvialis* was obtained at 28 ºC under continuous illumination (177 µmol photon $m^{-2}s^{-1}$) of white fluorescent light.

2.3.4. Treatment of Algae and Algal Organic Matter

Algae are ubiquitous and abundant in ecosystems. Because of their ubiquity and reactivity, algae have a large effect on determining the fate of inorganic and organic pollutants. Occasional algal blooms, comprised of blue-green algae (*cyanobacteria*) and/or green algae, causes significant challenges in drinking water treatment due to the release of organic compounds (algogenic organic matter, AOM). These organic compounds interact with disinfection materials, for example chlorine, and cause carcinogenic compounds.

Preozonation of water supplies containing algae may lead to microflocculation or impair coagulation depending on algae type, concentration and molecular weight of extracellular organic matter, and ozone dose (Edzwald, 1993). The similar study carried out by Widrig et al. (1996). Their study was about removal of AOM by preozonation and coagulation. Under acidic condition and high coagulant dose, the DOC removal was achieved about 20-50 %. Also, preozonation effects on the removal of DOC were not found to be significantly.

AOM was effectively removed by ultrafiltration membranes process due to membrane fouling (Chow et al., 1997).

2.3.5. Studies on Algae and Algal Organic Matter

The relationship between algae and inorganic pollutants, such as metals, has been well-studied; less is known about the complex relationship between algae and NOM. Because of the lack of knowledge, recent studies focus on understanding this relationship.

Her et al. (2003) investigated characterizing algogenic organic matter by various methods and evaluated depending on NF membrane fouling. According to obtained data, AOM contains large amount of proteins and polysaccharides and reflects a wide molecular weight range of components with less aromatic and more hydrophilic fractions.

Bouteleux et al. (2005) investigated effects of adding AOM on drinking water. This study examined whether algal organic matter (AOM) added in drinking water can compromise water biological stability by supporting bacterial survival. AOM, likely to be present in treatment plants during algal blooms, and thus potentially in the treated water may compromise water biological stability.

Lake et al. (2001) showed that there is a strong link between the end of the algal bloom and the presence of coliforms in the distribution system, leading to a situation incompatible with health standards. Algal products in the treated water were suspected of providing a good nutritional source for bacterial regrowth in the distribution system.

2.4. Advanced Oxidation Processes

Advanced oxidation process for the oxidative removal of organic substances is gaining importance in water treatment. Ozonation, photooxidation, and photocatalytic oxidation are all topics investigated under oxidative removal of organic material (Zhou and Smith, 2002).

The advanced oxidation processes which depend on the formation of hydroxyl radicals ($^{\cdot}OH$) are applied for total elimination of organic compounds both in water and wastewater treatment. Highly reactive $^{\cdot}OH$ species are attack on non-selectively to almost all organics and result in rapid degradation. Beside the applying only one process, the combination of various oxidation techniques are applied in advanced oxidation processes Such as UV, UV/H_2O_2 , ozonation, O_3/UV, O_3/H_2O_2 and photocatalytic oxidation (TiO_2/UV Process). All AOPs have in common, that the formation of hydroxyl radicals is the rate-limiting step. Recent developments in the domain of chemical water treatment have led to an improvement in

oxidative degradation procedures for organic compounds dissolved or dispersed in aquatic media, in applying catalytic and photochemical methods.

2.4.1. UV Process

In direct photochemical transformations the light-absorbing substance is changed due to the electronic excitation of the molecule and its ability to lose or gain electrons is often altered. Photooxidation reactions upon electronic excitation of the organic substrate imply in most cases an electron transfer from the excited state (C*) to ground state molecular oxygen (O_2), with subsequent recombination of the radical ions or hydrolysis of the cation, or homolysis to form radicals. The free radicals generated can then react with dissolved oxygen in water:

$$C + h\nu \longrightarrow C^* \quad (2.1)$$

$$C^* + O_2 \rightarrow C^{\bullet+} + O_2^{\bullet-} \quad (2.2)$$

$$R\text{-}X + h\nu \rightarrow R^{\bullet} + X^{\bullet} \quad (2.3)$$

$$R^{\bullet} + O_2 \longrightarrow RO_2 \quad (2.4)$$

The absorption cross section of the organic molecule, the quantum yield of the process, the photon rate at the wavelength of excitation and the concentration of dissolved molecular oxygen are important parameters in determining the rate of photooxidation (Legrini et al., 1993).

In practice, treatment of contaminated waters by UV alone is not widely used. Ultraviolet photolysis procedures are generally of low efficiency when compared to the procedures involving hydroxyl radical formation. Also degradation of organic compounds to new organic molecules and inorganic products may be a disadvantage. This is due to the fact that the products formed may be more toxic and more resistant to biodegradation. Another limitation for ultraviolet photolysis is the absorption of light by the target molecule in competition with other absorbers in solution. This creates a real problem in highly polluted wastewaters. Most

contaminated waters contain a variety of pollutants to be destroyed and their removal by photodegradation is not always cost effective in terms of process economics.

2.4.2. Photocatalytic Oxidation (TiO_2/UV Process)

Photocatalytic oxidation, which is an advanced oxidation method, has been applied in water, and wastewater treatment studies (Eggins et al., 1997). Photocatalysis relies on oxidative degradation reactions, where organic radicals are generated upon photolysis of the organic substrate or by reactions with generated hydroxyl radicals. These radicals are subsequently trapped by dissolved molecular oxygen and lead via peroxyl radicals and peroxides to an enhancement of the overall degradation process and finally lo complete mineralization (Legrini et al., 1993).

In photocatalysis, a suspension of a particulate metal oxide or other insoluble inorganic semiconductor powder is irradiated with natural or artificial UV light. This excitation promotes an electron from a bonding or no bonding level in the solid to a highly delocalized level, creating a localized oxidizing site (a hole) and a mobile reducing site (an electron). The holes react with the electron donors in the electrolyte to produce powerful oxidizing free radicals such as •HO (Bahnemann et al., 1994).

ZnO, ZnS, TiO_2, and CdS are the examples of semiconductors used as photocatalysis. Because of its stability, non-toxicity, and low energy band-gap, TiO_2 is accepted to be one of the most suitable semiconducting materials for photocatalysis.

The semiconductor photocatalytic process is based on aqueous phase hydroxyl radical chemistry and couples low energy UV-A light with semiconductors acting as photocatalyst. The overall process has been proved to destroy many organic compounds completely to carbon dioxide. The overall process can be summarized as follows:

$$\text{Organic pollutants} + O_2 \xrightarrow{\text{Semiconductor + UV - A light}} CO_2 + H_2O + \text{mineral acid} \qquad (2.5)$$

Titanium dioxide is a crystalline solid. It begins to melt at over 1800 degrees Celsius. It is polymorphous. It exists in three modifications or crystal structure, rutile, Anatase or brookite. Only the Anatase and rutile modifications are of any note, technically, or commercially. The most important use for titanium dioxide is as a pigment for providing brightness, whiteness and opacity to such products as paints, coatings, plastics, textiles, paper, inks, fibers, food and cosmetics and the material is colorless. Titanium dioxide must be developed to an ideal particle size, so that one may realize its special properties. Normally, the particle size is one half the wavelengths of visible light or about 0.3 microns (Kronos Inc., 1996).

Titanium dioxide is inert, and may be disposed in landfills or recycled. It is not toxic in any form, but may be dangerous if ingested in the powder form. Titanium dioxide, as a chemical has dielectric properties, high ultraviolet absorption and high stability which allow it to be used in specialty applications, such as electroceramics, glass, and wastewater treatment.

The main mechanism of the photocatalytic destruction process is the photo generation of electrons and holes in the photocatalyst. The absorption of bandgap light (380 nm) by a TiO_2 particle excites an electron to the conduction band leaving a positive hole in the valance band.

$$TiO_2 + h\nu \rightarrow TiO_2^* (e_{cb}^- - h_{vb}^+) \quad (2.6)$$

$$(e_{cb}^- - h_{vb}^+) \rightarrow e_{cb}^- + h_{vb}^+ \quad (2.7)$$

These photogenerated species constitute a redox-pair and take part in photoredox reactions. Molecular oxygen which must be present in all oxidative degradation processes is the accepting species in the electron-transfer reaction from the conduction band of the photocatalyst to oxygen. The electrons are rapidly captured by the molecular oxygen to form either superoxide anion radical or hydrogen peroxide.

$$O_2 + e_{cb}^- \rightarrow O_2^- \quad (2.8)$$

$$O_2 + 2e_{cb}^- + 2H^+ \rightarrow H_2O_2 \quad (2.9)$$

On the other hand photogenerated H_2O_2 has been reported to promote the generation hydroxyl radicals in TiO_2 activated photocatalytic systems.

$$H_2O_2 + O_2^- \longrightarrow OH^- + HO\bullet + O_2 \quad (2.10)$$

Although the presence of H_2O_2 on the TiO_2 has been observed, Matthews (1991) reported that HO• generated from H_2O_2 are negligible compared with HO• generated from holes. It has also been shown that the addition of hydrogen peroxide considerably enhances the rate of photodegradation, most probably via the reaction given as follows, or by surface-catalyzed dismutation of H_2O_2.

$$H_2O_2 + e_{cb}^- \rightarrow OH_{aq}^- + HO\bullet \quad (2.11)$$

$$H_2O_2 + h\nu \rightarrow 2\ HO\bullet \quad (2.12)$$

Beside e_{cb}^- reactions, the holes react with electron donors in the electrolyte to produce powerful oxidizing free radicals such as HO•. This reaction mechanism appears to be of greater importance in oxidative degradation processes, most probably due to the high concentration of H_2O and OH^- molecules adsorbed at the particle surface. In the presence of an organic pollutant in aqueous media, the electron transfer from adsorbed substrate RX and electron transfer from adsorbed solvent molecules (H_2O and OH^-) can be described by:

$$RX + h_{vb}^+ \rightarrow RX^+ \quad (2.13)$$

$$H_2O + h_{vb}^+ \rightarrow HO\bullet + H_{aq}^+ \quad (2.14)$$

$$OH^- + h_{vb}^+ \rightarrow HO\bullet \quad (2.15)$$

Organic pollutants adsorbed onto the surface of the titanium dioxide particles will then be oxidized by HO• radicals.

The TiO_2/UV process is known to have many important advantages like available TiO_2 at a relative modest price and high reaction rate if large surface areas of the photocatalyst can be used. Low quantum yield of this process, however, provides the advantage of being

operational in the UV-A domain (320-400 nm) with a potential use of solar radiation. But, the particle size of the added photocatalyst requires centrifugation or microfiltration techniques for its separation from the treated liquid and therefore serious technical and economical problems for a further development of this procedure. This can be overcome by immobilization of catalyst on beads, inside tubes of either glass or teflon.

2.4.2.1. Kinetics of Photocatalytic Degradation. The photocatalytic degradation of various organic solutes obeys pseudo first-order kinetics (Matthews, 1991).

$$-dS / dt = k [S] \quad (2.16)$$

Where k is the pseudo first-order decay constant and [S] is the concentration of solute.

The half-life for the reaction is given as:

$$t_{½} = 0.693 / k \quad (2.17)$$

Bekbolet et al. (1998) investigated the influence of common inorganic ions, namely, chloride, nitrate, sulfate, and phosphate ions on the photocatalytic removal of color from humic acid solutions and the degradation expressed as pseudo first-order reaction kinetics.

Boyacioglu (1997) studied the influence of pH dependent on the photocatalytic degradation of 10 mg L^{-1} humic acid in aqueous media. Boyacioglu reported that, at low pH values, irradiation with 0.25 mg mL^{-1} TiO_2 for 1 hour resulted in 95 percent $Color_{436}$ and 62 percent removal TOC removal.

Karabacakoglu (1998) investigated the influence of hardness cations on the photocatalytic degradation of humic acid. It was reported that, the increase in the removal rate was due to the changes in the humic acid structure due to the presence of divalent cations. Recently, Bas (2001) investigated the adsorption and desorption behavior of humic acid onto

two structurally different TiO_2 powders as a contributor to the photocatalytic degradation of humic acids. For adsorption, Degussa P-25 was reported to be more effective.

The photocatalytic efficiencies of two crystal forms of titanium dioxide; anatase and rutile were compared by Dincer (1998) using humic acid as a model compound. Relatively higher removal rates were observed with Anatase Degussa P-25 photocatalyst and its efficiency on the photocatalytic degradation of humic acid was concluded. Also Suphandag (1999) studied about adsorption efficiencies of different structure of titanium dioxide due to pH. Furthermore, adsorption characteristics of humic acids following photocatalytic oxidation was examined by Bekbolet et al. (1996), where the Freundlich isotherm constants for raw and irradiated humic acid were compared after activated carbon adsorption. The results showed that photocatalytic pretreatment of humic acids do not contribute the adsorption process.

A new development is the synergistic combination of an oxidant, especially TiO_2, with UV irradiation (McCoy, 1996). Humic acids can efficiently removal in aqueous media by photocatalytic oxidation with illuminated titanium dioxide. For example; Bekbolet (1996) reported that; after 1 hour of radiation, 40% TOC and 75% $Color_{436}$ removal for 50 mg/L humic acid solution was reached.

Recently, the destruction of humic acids has become an important task and TiO_2 catalyzed photodegradation of humic acids has been subject to many projects utilizing artificial light sources as well as solar light (Bekbolet et al., 2002).

2.4.3. Adsorption

Adsorption is a significant phenomenon in most natural, physical, biological, and chemical processes. Examples include removal of taste and odor producing organic materials and other trace organic contaminants such as trihalomethanes, pesticides and chlorinated organic compounds, removal of residual organic contaminants from treated wastewater effluents, and the treatment of leachates, industrial wastewaters, and hazardous wastes.

Sorption of solids, particularly active carbon, has become a widely used operation for purification of waters and wastewaters.

Adsorption isotherms describe the equilibrium conditions for an adsorbate (that which is adsorbing) onto the surface of an adsorbent. The adsorption of molecules on to a surface is a necessary prerequisite to any surface mediated chemical process. Usually the amount of material adsorbed is some complex function of the concentration of the adsorbate.

All three of the adsorption isotherms have been widely used to analyze adsorption data from wastewater studies. In general, the Langmuir and BET equations do not apply to dilute solutions or mixed solutes as well as the Freundlich equation. Therefore, the Freundlich isotherm is the most widely used nonlinear adsorption equilibrium model (Singh, 1984). It describes adsorption events occurring on heterogeneous surfaces composed of different adsorption sites, with adsorption on each site following the Langmuir isotherm. The model has the general form:

$$q_A = K_F C_e^{1/n} \qquad (2.18)$$

where;

q_A: The amount of solute adsorbed per unit weight of solid adsorbent
C_e: The concentration of the solute remaining in the solution at equilibrium
K_F: The constant which relates to adsorption capacity
1/n: The constant which relates to adsorption intensity

Freundlich equation is basically empirical but is often useful as a means for data description. Data is usually fitted to the logarithmic form of the equation as follows:

$$\log q_A = \log K_F + 1/n \log C_e \qquad (2.19)$$

A plot of log q_A versus C_e should yield a straight line whose slope is 1/n and whose intercept is log K_F. The intercept is roughly an indicator of adsorption capacity and the slope of adsorption intensity.

Suphandag (1998) studied the adsorption capacity of humic acid on three different semiconductor powders, namely Degussa P-25, Merck and Hombikat UV100. This study exhibited that, for each TiO_2 samples, with increasing pH of the humic acid solution, the adsorption efficiencies decreases. The same observations were obtained by Yildirim (2000). In this investigation, adsorption properties of humic acid onto titanium dioxide were analyzed depending on pH and ionic strength of the medium and highest adsorption efficiency values were gained at acidic condition. Furthermore, the similar study was investigated by Suphandag (2006) that the sorption isotherms of humic acid (HA) onto titanium dioxide were analyzed at acidic, neutral and basic pH ranges. In the study, the combined effects of pH and increasing ionic strength were evaluated in order to asses the effect of changing solution matrix on the molecular structure of humic acid.

Bekbolet et al. (2002) investigated the photocatalytic efficiencies of TiO_2 powders on the decolorization of humic acids. Decolorization rate of humic acid by photocatalytic oxidation in terms of pseudo first-order kinetics in the presence of Degussa P-25 was found to be more efficient than in the presence of Hombikat UV100 specimen. The results of the adsorption experiments for Degussa P-25 indicated higher adsorption capacity for humic acid at pH 6.7.

3. MATERIALS AND METHODS

3.1. Materials

All chemicals used in this study are analytical grade.

3.1.1. Humic Acid

Aldrich humic acid (AHA) was used for the preparation of humic acid solution. Humic acid stock solution (1000 mg L^{-1}) was prepared by dissolving humic acid sodium salt in distilled-deionized water and filtering through paper. 20 mg L^{-1} humic acid solution, which was used during the experiments, was prepared in a 1 L volumetric flask by the dilution of the stock humic acid solution with distilled-deionized water.

Stock humic acid solution was stored in a dark glass container and was protected from light to prevent decomposition.

3.1.2. Titanium Dioxide Powder

Degussa P-25 TiO_2 was used as the photocatalyst. The primary particle size was 20-30 nm, and BET surface area was 50±15 $m^2 g^{-1}$. The crystal structure of the TiO_2 was composed of 70% anatase and 30% rutile.

3.1.3. ANOM Solution

ANOM solution was prepared by 250 mL of 20 mg L^{-1} AHA and 250 mL of extracted aqueous solution of AOM diluted to 1 L with distilled water.

3.2. Methods

3.2.1. Laboratory Equipments

Following laboratory instruments and equipments were used during different steps of the experiments.

Amicon Model 8010 Ultrafiltration Stirred Cell System: It was used for molecular size fractionation.

BOS N_2 Gas Tube: It was used for experiment of molecular size fractionation.

Hach 2100P Turbidimeter: It was used for measurement of turbidity of AOM aqueous solution.

Hach COD Digester: It was used for low COD experiment.

Hach DR/2010 Portable Datalogging Spectrophotometer: UV-visible absorption spectra were recorded, chosen different wavelength, employing quartz cuvettes 2.5 cm optical path length.

Hettich EBA 20 Centrifuge: It was used for the removal of photocatalyst, the suspensions were centrifuged for 10 min at 5500 rpm.

Hettich Universal 16A Centrifuge: It was used for AOM extraction experiment at 4000 rpm for 10 min.

Junke and Kunkel IKAMAG RH Magnetic Stirrer: It was used for the continuous mixing of the suspensions throughout the reaction time during photocatalytic treatment. It also used Molecular Size Fractionation via Ultrafiltration and $KMnO_4$ experiments.

Memmert Oven: It was used to dry the glassware.

Memmert Top-Shaker: The adsorption experiments of ANOM solution and TiO_2 suspensions were carried out on the Memmert water-bath shaker.

Olympus BX50 microscope: It was used for algal cell counting.

Perkin Elmer Lambda 35 UV-vis Spectrophotometer: UV-visible absorption spectra were recorded employing quartz cuvettes 1.0 cm optical path length.

Perkin Elmer LS 55 Luminescence Spectrometer: Fluorescence spectra were recorded employing quartz cuvettes 1.0 cm optical path length.

Scaltec SBA 31 Balance: Balance was used for weighing certain amounts of titanium dioxide.

Selecta Plactronic Hot Plate: It was used for AOM extraction experiment.

Shimadzu TOC-V Wp Total Organic Carbon Analyzer: It was used for analyzing TOC.

Thoma Hemacytometer: It was used for microscopically with cell counting.

Ultra Sonic Waterbath LC30: The homogeneous suspension was provided by sonification of the slurry.

WTW pH Meter- pH 526: The pH values were measured to observe pH changes during the experiments. The pH meter was calibrated with pH 4 and pH 7 buffer solutions.

Sterile Millex – HA Millipore Filter: The suspensions were filtered through 0.45 µm Millipore syringe filter to remove the residual photocatalyst after centrifuging.

Syringe: Syringes were used to filter the suspensions.

3.2.2. Preparation of Algal Culture

In this study, mixed culture of unicellular green algae primarily composed of *Chlorella* sp. and *Scenedesmus* sp. were grown in batch mode in 2 L Erlenmeyer flask containing 2 L of algal growth media. Composition of algal growth media is presented in Table 1.

Table 3.1. Composition of algal growth media (modified from Guillard, 1975).

Compound	Molar Concentration in Final Medium
$NaNO_3$	8.83×10^{-4} M
$NaH_2PO_4 \cdot H_2O$	3.63×10^{-5} M
$Na_2SiO_3 \cdot 9H_2O$	1.07×10^{-4} M
$FeCl_3 \cdot 6\ H_2O$	1×10^{-5} M
$Na_2EDTA \cdot 2\ H_2O$	1×10^{-5} M
$CuSO_4 \cdot 5\ H_2O$	4×10^{-8} M
$Na_2MoO_4 \cdot 2\ H_2O$	3×10^{-8} M
$ZnSO_4 \cdot 7\ H_2O$	8×10^{-8} M
$CoCl_2 \cdot 6\ H_2O$	5×10^{-8} M
$MnCl_2 \cdot 4\ H_2O$	9×10^{-7} M

For inoculation, samples were collected from research ponds in Botanic Faculty of Istanbul University. The experiment was started within 48 hour after collection. Later on, 100 mL from inside of samples was taken for inoculation and added to Erlenmeyer flask.

The reactor was cultured under a continuous air and light regime, 100 Watt/ 1340 lumen, and maintained at room temperature as 25 ºC. Continuous aeration was achieved by bubbling air into the algal suspension. The bubbling air was also prevented flocculation in the reactor. Beside the air, flask was hand shaken at least once daily to prevent settling of the cells.

To compensate the volume loss due to the evaporation, volume correction was made with medium before measurements.

3.2.3. Measurement of Algal Growth

The algae growth was measured with four different methods: 1) in vivo chlorophyll fluorescence intensities with a fluorimeter (Perkin Elmer LS55 Luminescence Spectrometer). 2) optical density (OD 600) with a spectrophotometer (Perkin Elmer Lambda 35 UV-vis Spectrophotometer and Hach DR/2010). 3) microscopically with cell counting by a Thoma hemacytometer under binocular light microscope Olympus BX-50.

3.2.3.1. Fluorometric Measurements. According to the Standard Methods for the Examination of Water and Wastewater (APHA, 1998) direct fluorescence was measured from a 5 mL aliquot with a 430 nm excitation filter and 663 nm emission filters. A low/high fluorescence level compared to control indicated a reduced/increased level of photosynthetic pigments and also algal growth.

3.2.3.2. Spectrometric Measurements. The subsequent growth rate was recorded by measuring optical density at 600 nm (OD 600) with a spectrophotometer during the experiments.

3.2.3.3. Microscopic Analysis. Algal cells were observed by an epifluoroscence microscope (Olympus BX-50 with Olympus computer using a Spot Insight color cooled digital camera with PC archive and measurement software. Enumerations of algal cells were made by a Thoma hemacytometer under binocular light microscope.

3.2.4. Algal Organic Matter Extraction Method

When algal growth reached approximately 10^7 cell mL^{-1}, algal solution was extracted according to research of Myklestad and Swift (1998). In this extraction firstly, the settlement of algal flocks were waited by stopping the air of the solution. When two layers occurred supernatant was separated by siphoning method. Then concentrated algae solution was

obtained by centrifuge (Hettich Universal 16A Centrifuge) for 10 min and at 4000 rpm. The pellet was washed twice with Millipore water. Afterwards, the solution was heated on a hot plate up to 60 -70 °C for one or two hour since its color became brownish. And the solution was waited in a dark place for degradation approximately one day. When settlement occurred, the upper solution was taken and centrifuged (Hettich EBA 20 Centrifuge) for 10 min and 5500 rpm. Obtained pellet was separated from supernatant and the pellet was discarded. The remaining solution was filtered using 0.45 μm Millipore Millex-HA cellulose based membrane filters. Filtered solution was kept in a dark bottle because of containing organic substances which came from algae degradation. The final solution was called aqueous solution of AOM (algal organic matter).

3.2.5. Photocatalytic Degradation Experiments

The light source was 125 W Black Light Fluorescent Lamp (BLF) having an output spectrum of 320 to 440 nm with a maximum emission at 365 nm. The intensity of incident light as measured by potassium ferrioxalate actinometry (Hatchard and Parker, 1956) was 2.85×10^{16} quanta s^{-1}. In all of the experiments, the distance between the lamp and the surface of the suspension in the reactor was kept constant at 16.5 cm (Bekbolet, 1996). Photochemical experiments were performed in a 25 ml cylindrical Pyrex reaction vessel with a diameter of 5.5 cm and height of 3.5 cm. A Junke and Kunkel IKAMAG RH magnetic stirrer provided continuous stirring. A mirror casing enclosed the photoreactor, and the whole system was placed in a box. The inner walls of the box were covered with Al-foil.

All raw samples were photocatalytically treated. 25 mL of samples was added into the photo reactor containing various amount of titanium dioxide. For the homogenization of the slurry, Ultrasonic LC30 water bath sonicator was used for 1 min. This homogeneous mixture was placed on the magnetic stirrer for continuous stirring through out the reaction period. At the end of each reaction period, volume loss due to the evaporation of water was compensated by distilled/ deionized water.

In order to separate TiO_2 from the solution, the reactor content was centrifuged at 5500 rpm for 10 min using HETTICH EBA 20 centrifuge. Then, the cleared liquid was filtered using a 0.45 μm Millipore Millex-HA cellulose based membrane filters, which was attached to 10 mL syringe. The clear solution obtained was analyzed with the UV-vis spectrophotometer for residual absorbance at 436, 400, 280 and 254 nm ($Color_{436}$, $Color_{400}$, UV_{280} and UV_{254}).

3.2.6. Adsorption Experiments

Batch adsorption experiments were carried out using flasks filled with 25 mL ANOM solution and TiO_2 ranging from 0.2 mg mL^{-1} to 1.0 mg mL^{-1} was added into each flask. One extra flask was filled with only ANOM solution for comparative purpose. Each sample was sonicated for homogenization of TiO_2 in the slurry. The stoppered flasks were immersed into the water-bath and shaken for 24 hours at room temperature. The samples, taken out of water-bath, were then centrifuged for 15 minutes in 10000 cycles min^{-1}. The supernatant was then filtered through 0.45 μm Millipore syringe filter. Filtered samples were analyzed with the UV-vis spectrophotometer for residual absorbance at 436, 365, 280 and 254 nm to monitor the same parameters used in photocatalytic degradation.

3.2.7. Molecular Size Fractionation via Ultrafiltration

Molecular size fractionation of the raw and photocatalytically treated AOM aqueous solution were performed using a 10 mL Amicon Model 8010 ultrafiltration stirred cell. Firstly, the samples were filtered through 0.45 μm (approximately 450 kDa) Millipore cellulose acetate membrane filters. Then, filtration was repeated by using Millipore YM series cellulose membrane filters with 25 mm diameter, which were 1 kDa, 10 kDa, 30 kDa, 100 kDa with a sequence of decreasing pore size.

The cell was operated on a magnetic stirrer. A nitrogen gas tube which was attached to the stirred reactor was used for the required pressure. At the beginning of each filtration all the membranes were rinsed with deionized water. Each filtered samples were collected separately and characterized by UV-vis and fluorescence spectra.

3.2.8. Chemical Oxygen Demand Analysis

COD measurement was performed by using dichromate closed reflux method according to the Standard Methods for the Examination of Water and Wastewater (APHA, 1998). Samples were refluxed with potassium dichromate ($K_2Cr_2O_7$) and sulfuric acid (H_2SO_4) for two hours at 150 ºC in HACH COD Digester. Interference from chloride was prevented with the addition of mercury sulfate ($HgSO_4$). Silver sulfate (Ag_2SO_4) was used as catalyst. Absorbance values were measured colorimetrically at 420 nm by using HACH DR/2010 Portable Data Logging Spectrophotometer.

COD measurement was also realized by potassium permanganate ($KMnO_4$) consumption according to the Laboratory Manual for the Examination of Water, Wastewater and Soil (Rump and Krist, 1992). In this method potassium permanganate ($KMnO_4$) was oxidizing agent and the experiment was depended on its consumption.

3.2.9. Analytical Methods

3.2.9.1.Total Organic Carbon (TOC) Analysis: Total organic carbon (TOC, mg L^{-1}) measurements of samples were performed on a Shimadzu TOC-V Wp Total Organic Carbon Analyzer. Calibration of the instrument was done using potassium persulphate in the concentration range of 0-5 mg L^{-1}.

3.2.9.2. UV-vis Measurements: UV-vis absorption spectra were recorded on a Perkin Elmer Lambda 35 UV-vis Spectrophotometer employing quartz cuvettes 1.0 cm optical path length. Aqueous solution of AOM and ANOM solutions were characterized by UV-vis spectroscopy. Absorbance values at 436 nm ($Color_{436}$), 400 nm ($Color_{400}$), 365 nm (UV_{365}), 280 nm (UV_{280}) and 254 nm (UV_{254}) were recorded for the evaluation of UV-vis parameters.

3.2.9.3. Fluorescence Measurements: Fluorescence spectra in the emission and synchronous scan modes were recorded on a Perkin Elmer LS 55 Luminescence Spectrometer equipped with a 150 W Xenon arc lamp and a red sensitive photomultiplier tube. A 1-cm pathlength

quartz cell was used. The method of measuring fluorescence is that the cuvette holder excites the sample over the entire path length and reads the emitted light at right angles. Both the excitation and the emission slits of the instrument were 10 nm. A scan speed of 400 nm min^{-1} was used with a slit width opening of 10 nm. Opening the slit wider allows more light energy from the xenon light source to excite the molecules in the sample. A larger slit width applies more excitation light energy to a sample, and a less–well defined spectral purity of the excitation and emission bands (e.g. broader emission bands rather than sharper bands) results (Westerhoff et al., 1999). Synchronous scan spectra were recorded in the excitation wavelength range of 300-650 nm excitation wavelength range using the bandwidth of $\Delta\lambda$=18 nm between the excitation and emission monochromators (Senesi, 1990). The scan speed was 400 nm min^{-1}. The emission spectra were scanned over the range of 400-600 nm at a constant excitation wavelength of 350 nm (Senesi, 1990; Hautala et al., 2000). Since all of the spectra were recorded on the same instrument using the same experimental parameters, a comparative discussion of the spectra is acceptable although, no corrections for fluctuation of instrumental factors and for scattering effects (e.g. primary and secondary inner filter effects) were applied to the data (Senesi, 1990; Peuravuori et al., 2002).

4. RESULTS AND DISCUSSION

In this study, aqueous solutions of extracted algal organic matter (AOM) were used. A mixed algae culture which was inoculated from natural waters sample was used to obtain algal organic matter. Algal growth was observed daily according to the methods outlined in the materials and methods section. When the required growth ratio was reached, extraction operation was conducted. Attainment of extracted algal organic matter was carried out according to the procedure outlined in the previous section (i.e. material and method section). In order to comply with the objective of NOM modeling, aqueous solution of AOM was mixed with humic acid solutions (AHA) in appropriate ratios. This aqueous solution is referred to as ANOM.

In the second section, aqueous solution of AOM was characterized with respect to its UV-Vis and fluorescence spectroscopic properties as it is presented in Table 4.1, Figures 4.1 and 4.2. Due to the complexity of the algal organic matter, it was further fractionated into molecular sizes using membranes filters within diameter from 0.45 µm to 500 Dalton for ultrafiltration. This process was described in the materials and methods section. Moreover, the spectroscopic properties of each size fraction were further characterized and compared by UV-vis and fluorescence spectroscopy.

In the third part, photocatalytic oxidation of ANOM and diluted ANOM solutions was done using TiO_2 Degussa P-25 as the photocatalyst. The obtained data were presented as removal efficiencies graph. Degradation of ANOM solution was also presented as UV-Vis scan graph. Degradation kinetics of ANOM solution was calculated by using pseudo first order kinetic models. Moreover, in this section, the molecular size distribution profiles of the partially oxidized algal organic matter were comparatively presented in the specified UV-vis properties and synchronous scan fluorescence spectra graphs.

In the last part, adsorption properties were examined in photocatalysis of ANOM solution based on Freundlich adsorption equilibrium model.

4.1. Growth of Algal Culture

As it is described in latter sections (3.2.2, 3.2.3 and 3.2.4), the algae was grown and extracted to obtain AOM aqueous solution which was used during experiments.

The algae growth was monitored daily by microscope and particle counting was processed by Thoma hemacytometer under binocular light microscope. Absorbance measurements at 600 nm were carried out using spectrophotometer.

During the counting process, algae growth was monitored by absorbance and cell numbers for 20-25 days. A calibration graph obtained by cell number versus absorbance readings would be used for enumeration of algae during degradation experiments. The linear portion of the growth curve was fit to a linear regression equation to obtain the calibration curve. Duplicated experiments were performed. The calibration curve yielded the following equation;

$$\text{Cell number } (x10^4) = 1035.7\ Abs_{600} + 37.43 \qquad R^2 = 0.96 \tag{4.1}$$

where,
Cell number = counted cell number of algae (cells mL^{-1})
Abs_{600}= absorbance value at 600 nm (cm^{-1})

The results were quantified in terms of algal specific growth rates (μ) calculated from measurements of total cell numbers. The cell concentrations at two different time periods were employed for the calculation of the growth rate as expressed by;

$$\mu = \ln (X_1 / X_2) / \ t_1 - t_2 \tag{4.2}$$

where,

μ = specific growth rate (d^{-1})

X_1 = cell concentration at t_1 (cells mL^{-1})

X_2= cell concentration at t_2 (cells mL^{-1})

t_1 = first sampling time (d)

t_2 = second sampling time (d)

Also the doubling time t_d (d) can be defined as,

$$t_d = \ln 2/\mu \quad (4.3)$$

If the rate of growth is proportional to the number or mass of organisms present, then growth can be said to be first-order with respect to cell mass:

$$k = \mu\, c \quad (4.4)$$

where,

k = rate of growth, mg $L^{-1}d^{-1}$

μ = specific growth rate coefficient, d^{-1}

c = biomass concentration, mg L^{-1}

A calibration curve of absorbance against time gave a growth rate coefficient which is k=0.156 d^{-1}, (R^2 =0.93). The results of duplicate analysis revealed a growth graph based on cell numbers versus time, and the related growth rate coefficient was calculated as k=0.120 d^{-1}, (R^2 =0.75).

A representative growth curve was illustrated in Figure 4.1.

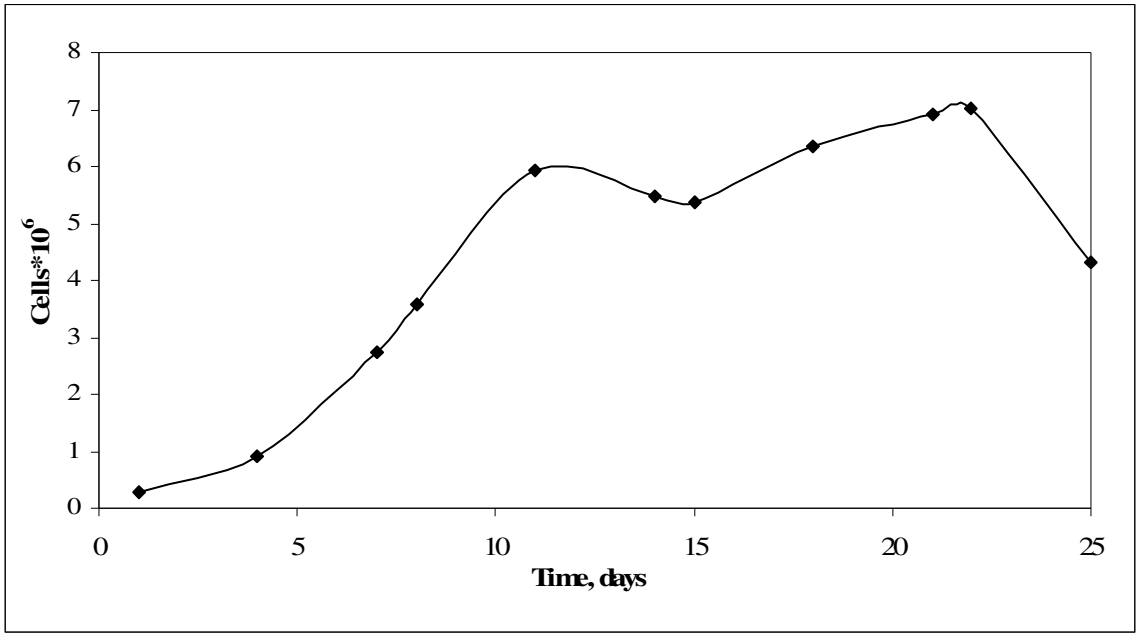

Figure 4.1. Algae growth on a daily basis.

According to section 2.3.2, the typical growth curve was demonstrated in Figure 2.2. In Figure 4.1, expected growth can be seen in first 11 days period of obtained curve. From the day 11 to day 22, the curve indicates a stationary trend. The stationary phase is explained as the equilibrium of growth rate to death rate. In the same way, after the last day of stationary phase period the curve is representing dead phase.

The UV-vis spectrum and enumeration of the algae growth versus time was presented by Figure 4.2. The absorbance values measured at 600 nm increased daily and the maximum absorbance values were obtained after 22 days.

The fluorescence spectra of algal organic matter turned out to be more useful than the UV-vis spectra due to the better peaks resolution. As it could be seen from Figure 4.3, the synchronous scan spectra of algal organic matter followed increasing fluorescence intensity over time, indicating a positive relationship with the algal growth.

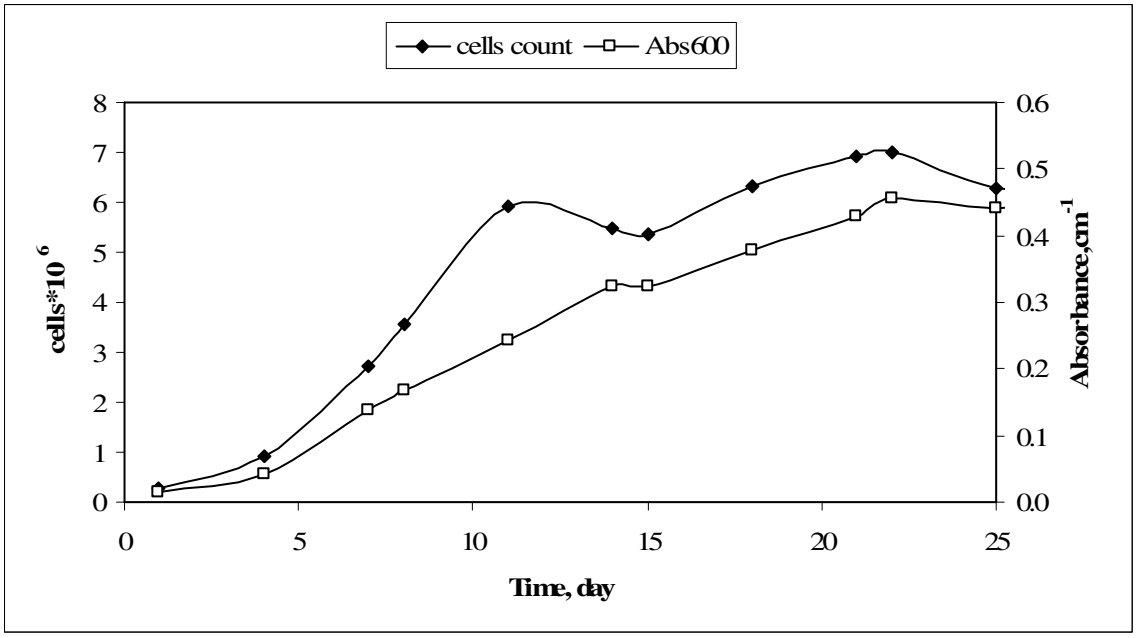

Figure 4.2. The UV-vis spectrum and enumeration of the algae growth with respect to time.

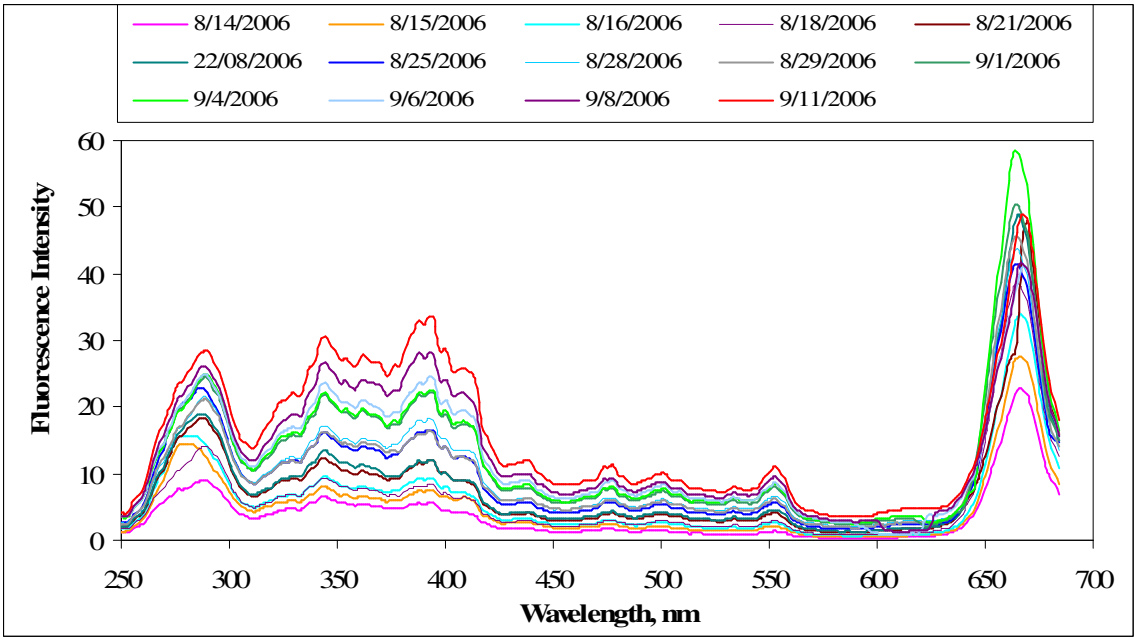

Figure 4.3. Synchronous scan fluorescence spectra of algae growth with respect to time.

As can be clearly seen from the fluorescence intensity figure above, the peak was about 663 nm. This peak value indicates the amount of chlorophyll which has a similar wavelength with the chlorophyll experiment described in Standard Methods for the Examination of Water and Wastewater (APHA, 1998).

Maximum absorbance peak value was found to be parallel to the increase in number of algae because of increasing amount of chlorophyll. Liu et al., (2005) studied on synchronous-scan fluorescence spectra of *Chlorella vulgaris* solution and found that the initial peak was observed at EX 236.6/ EM 326.6 related to the presence of the algal organics substances (Stephan et al., 1998).

4.2. Analysis of Algal Organic Matter (AOM) Aqueous Solution

In order specify to AOM and ANOM solutions, some experiments were carried out according to the methods outlined in the materials and methods sections (i.e. 3.2.8 and 3.2.9). These results are shown in Table 4.1.

In Table 4.1, aqueous solution of AOM exhibited almost neutral medium conditions because of pH value as 6.7± 0.3. The turbidity was also found to be 6.4 ±1.9 NTU. It can be clearly seen in Table 4.1 that the low absorbance values detected in the visible region as explained by $Color_{400}$ and $Color_{436}$ indicate a colorless solution. At these wavelengths, the solution had 0.8 and 0.6 m^{-1} absorbance values. Beside these low values, it had 16.5 and 18.0 m^{-1} absorbance values for UV_{280} and UV_{254}, respectively.

Aqueous solution of AOM was specified with measurements of $KMnO_4$, COD and TOC values as 65.59, 51.22 and 13.90 mg L^{-1}, respectively (Table 4.1).

Table 4.1. The general properties of AOM aqueous solution.

Physical Properties:	
Turbidity, NTU	6.4 ±1.9
Temperature, ^{o}C	30
Chemical Properties:	
pH	6.7± 0.3
Chemical Oxygen Demand	
Permanganate Consumption Value, mg O_2 L^{-1}	65.59
Dichromate Method, mg O_2 L^{-1}	51.22
Total Organic Carbon, mg C L^{-1}	13.90
Spectroscopic Properties:	
$Color_{436}$, m^{-1}	0.6
$Color_{400}$, m^{-1}	0.8
UV_{365}, m^{-1}	2.2
UV_{280}, m^{-1}	16.5
UV_{254}, m^{-1}	18.0

In addition, aqueous solution of AOM was specified according to its UV-vis and fluorescence spectroscopic properties. The same specifications were also used for molecular size fractionated aqueous solution of AOM. The ultrafiltration membranes, in the range of 0.45 µm to 500 Da., were used for fractionation.

4.2.1. UV-vis Spectroscopic Properties of AOM Aqueous Solution

In literature, UV-vis absorption is commonly accepted as conventional and versatile for characterization of organic matter in natural waters (Traina et al., 1990; Uyguner and Bekbolet, 2005a; Uyguner and Bekbolet, 2005b).

Absorption of light in the UV range by organic substances is caused by π-electrons and reflects aromatic and carboxylic electron systems as well as their conjugates (Frimmel et al., 2002).

Absorbance values of UV_{254} and $Color_{436}$ are generally used for the quantification of humic substances (Bekbolet 1996; Bekbolet and Balcioglu, 1996; Bekbolet and Ozkosemen, 1996; Bekbolet et al., 1998; Bekbolet et al., 2002; Kerc et al., 2003; Uyguner and Bekbolet, 2004a, Bekbolet et al., 2005; Uyguner and Bekbolet, 2005a; Uyguner and Bekbolet, 2005b; Uyguner and Bekbolet, 2005c). UV_{254} is measured for determination of total organic carbon which represents the natural organic matter content in surface waters (Najm et al., 1994). UV_{280} is also measured to represent total aromaticity, because, $\pi \rightarrow \pi^*$ electron transition occurs in this UV region (270-280 nm) (Chin et al., 1994; Traina et al., 1990). This knowledge sheds light on all the spectrophotometric results in this research and also same wavelengths were used for evaluation of AOM and ANOM solutions.

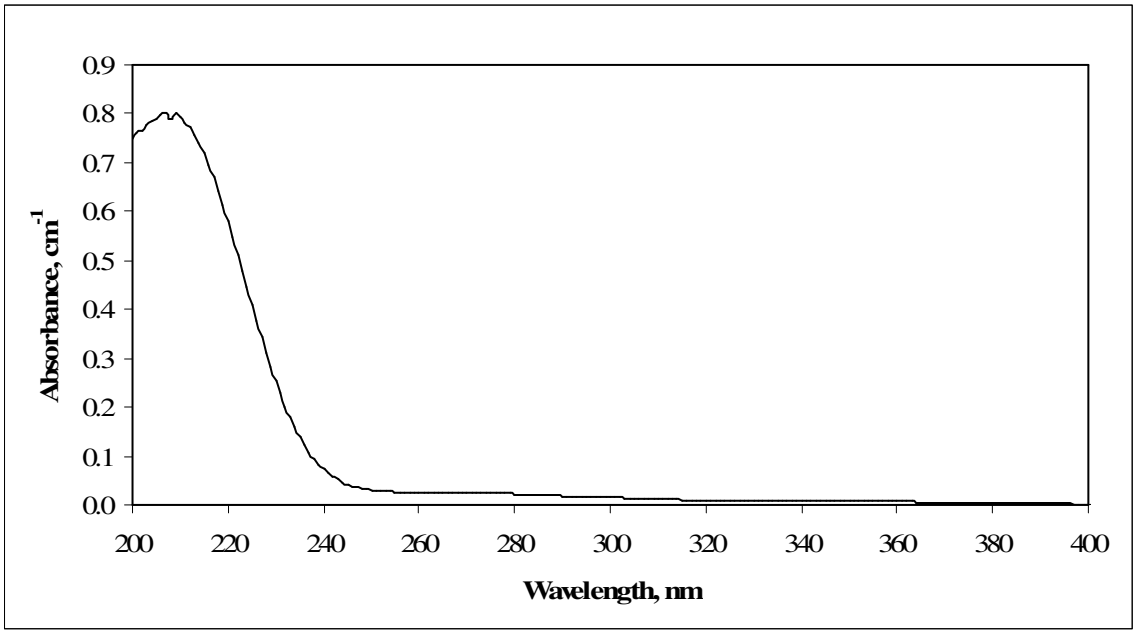

Figure 4.4. UV-vis spectra of AOM aqueous solution.

As can be seen in Figure 4.4, the absorbance spectra of aqueous solution of AOM had one distinctly broad peak around 210 nm following a declining pattern with increasing wavelength. Up to 250 nm the absorbance values decreased rapidly. Furthermore it expressed relatively lower absorbance values approaching to zero at wavelengths greater than 360 nm.

According to Table 4.1 and Figure 4.4, the absorbance values of UV_{280} and UV_{254} were normally higher than the values of $Color_{436}$ and $Color_{400}$ revealing low $Color_{436}$ and $Color_{400}$ values. It can be said that aqueous solution of AOM is almost colorless.

4.2.2. Fluorescence Spectroscopic Properties of AOM Aqueous Solution

The fluorescence of organic substances contains information about the structure, functional groups, conformation, and heterogeneity of compound (Senesi et al., 1991; Mobed et al., 1996).

Fluorescence mechanism depends on molecule absorption and emitting capabilities. Therefore fluorescence reveals the relationship between absorbed and emitted photons at specified wavelengths. The relationship is explained that after a molecule absorbs light photons from the UV-visible region, it is excited and then rapidly emits light photons while it is returning to its ground state. This technique gives precise results, besides it is inexpensive and easily applied.

In previous investigations, Uyguner (2005) and the others supported that humic acids provide a much better defined peak resolution in the synchronous scan fluorescence spectra. In addition to obtain more specific characterization about aqueous solution of AOM, the synchronous scan fluorescence spectra were used.

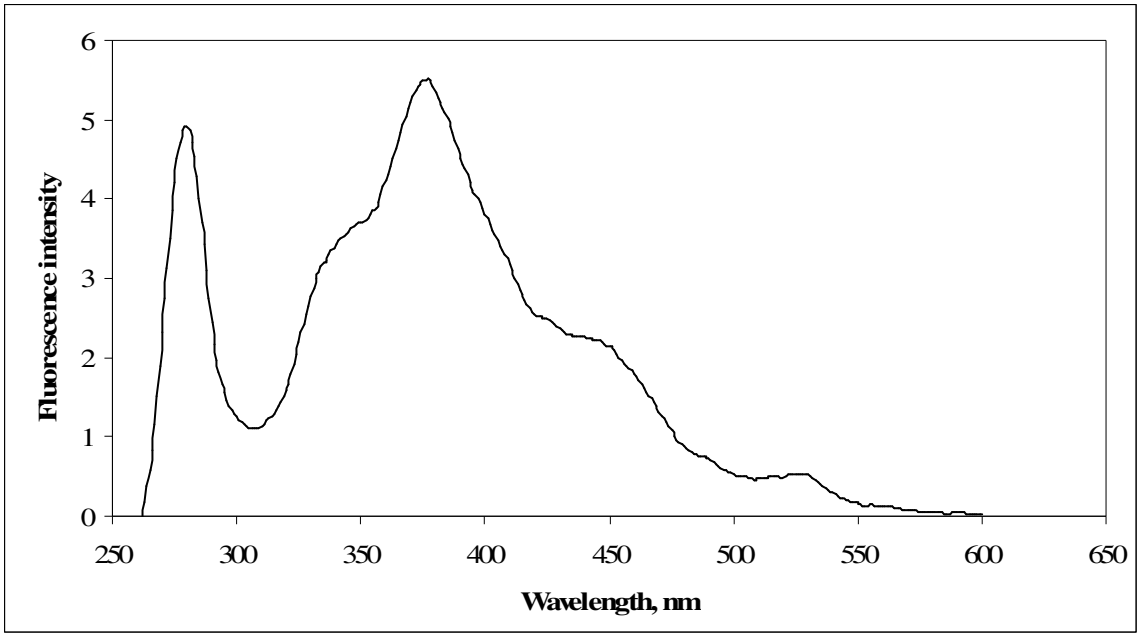

Figure 4.5. Synchronous scan fluorescence spectra of AOM aqueous solution.

As can be seen from the Figure 4.5, the fluorescence spectra of AOM aqueous solution mainly had two peaks at 280 and 375 nm and their values could be considered as close to each other. Nevertheless the initial peak was sharper than the other. The second peak (λ_{max}: 375 nm) covered two distinct shoulders at around wavelengths less than 350 nm and more than 430 nm. After 375 nm the fluorescence intensity gradually decreased with increasing wavelength. The fluorescence intensity decreased to insignificant values after wavelength grater than 550 nm. When wavelength was longer than 600 nm, the intensity values approximated to zero.

4.2.3. UV-vis Spectroscopic Properties of the Molecular Size Distribution of AOM Aqueous Solution

In this study, molecular size distribution of AOM aqueous solution was measured. The ultrafiltration method was applied using membranes aiming further fractionation in the range between 0.45 µm to 500 Da. After fractionation, UV-vis spectroscopic determinations were

carried out for the specification of the UV-absorbing moieties and color forming groups of AOM aqueous solution

In agreement with survey results, aqueous solution of AOM exhibited a declining pattern, furthermore, the absorbance values decreased with decreasing molecular size except for 30 kDa. The results were presented in Figure 4.6. The wavelength (λ: 210 nm) at which the maximum absorbance values were attained did not change with respect to molecular size fractions. The UV-vis spectra of the molecular size fractions of humic substances followed a similar declining pattern as previously reported (Uyguner and Bekbolet, 2005a).

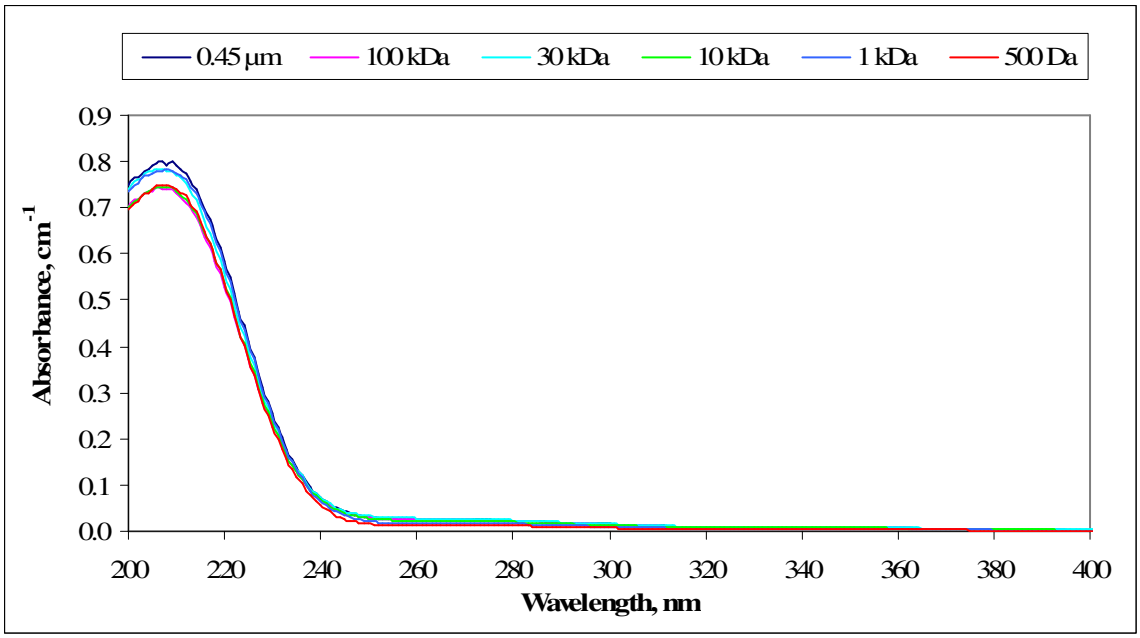

Figure 4.6. UV-vis spectra of the molecular size fractions of AOM aqueous solution.

As it is presented below in Figure 4.7, the absorbance of AOM aqueous solution increased with decreasing wavelength. It can be concluded that, dominant part of the organic matter is mainly consisted of AOM fractions covering 30 kDa particles.

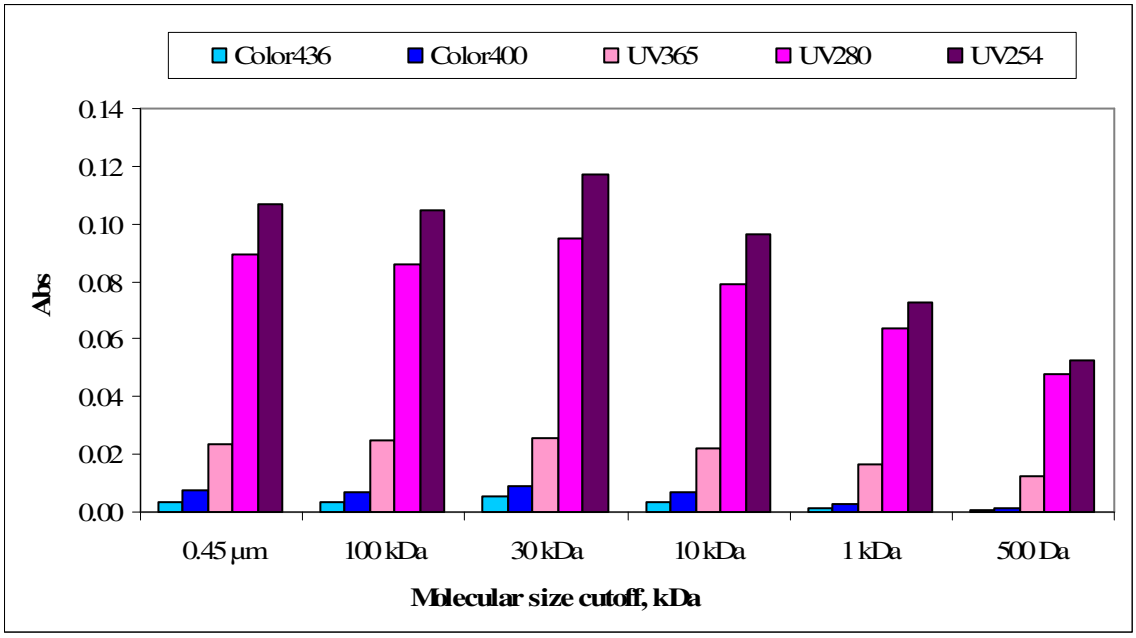

Figure 4.7. $Color_{436}$, $Color_{400}$, UV_{365}, UV_{280} and UV_{254} values for AOM aqueous solution with respect to molecular size distribution.

According to Figure 4.7, for $Color_{436}$ and $Color_{400}$ absorbance values were approaching to zero for 1 kDa and 500 Da which could be regarded as colorless. As mentioned before, $Color_{436}$ and $Color_{400}$ are defined parameters to express color forming moieties in organic matter structure. AOM aqueous solution exhibited a decreasing trend for UV_{280} and UV_{365} for all molecular sizes. The spectra of the higher molecular size fractions; 0.45 µm, 100 kDa and 10 kDa displayed almost equal $Color_{436}$ values as 0.0037, 0.0035 and 0.0038, respectively. All the fractions had relatively lower absorbance values that approaches zero for wavelengths greater than 450 nm. On the other hand, UV_{254} values expressed quite similar values as 0.1065, 0.1049 and 0.0961 for the size fractions of 0.45 µm, 100 kDa and 10 kDa respectively. It is evident from the spectroscopic measurements that higher molecular size fractions (0.45 µm and 100 kDa) possessed have almost the same absorbance values (Figure 4.7).

4.2.4. Fluorescence Spectroscopic Properties of the Molecular Size Fractions of AOM Aqueous Solution

Synchronous scan spectra provide a possibility for each fluorescent component to be identified in a spectral range. Therefore, the synchronous scan fluorescence spectra were used for characterization of molecular size fractions of AOM aqueous solution (Figure 4.8).

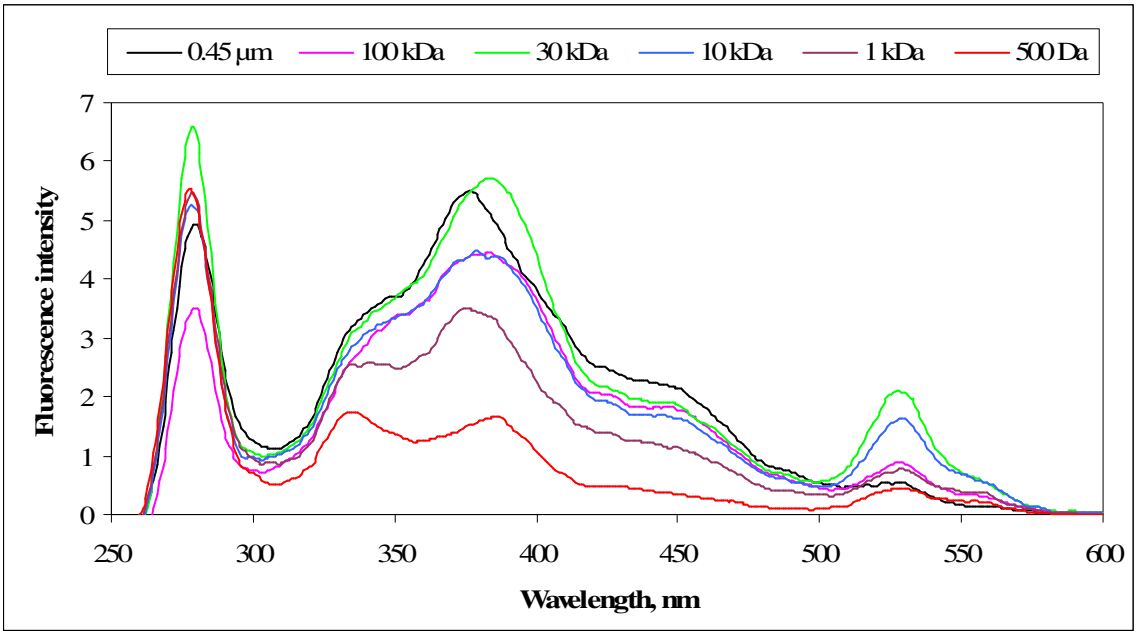

Figure 4.8. Synchronous scan spectra of molecular size fractions of AOM aqueous solution.

As it was clearly seen from, the presence of absorption peaks at about 280 and 530 nm wavelengths were found to be significant for each molecular size fraction. Furthermore, around 390 nm wavelength, 0.45 µm and 30 kDa size fractions displayed a considerable higher peak formation whereas 100 kDa and 10 kDa molecular size fractions exhibited absorption shoulders. In the range of 330 nm to 400 nm the shoulder was slightly sharpened for 1 kDa and 500 Da which could also be considered as peak (Figure 4.8).

In Figure 4.8, fluorescence intensities of AOM aqueous solution followed random patterns, irrespective of their size fractions. Mainly three fluctuating composite peaks were

observed based on molecular sizes, except for 30 kDa. Initially, the fluorescence intensity generally increased with decreasing molecular size about 280 nm wavelengths. In this region the maximum intensity reached as high as 6.58 for 30 kDa to lower values around 3.49 for 100 kDa molecular size fractions.

The spectra of each size fraction, except for 30 kDa, exhibited decreasing trend in terms of fluorescence intensity for wavelengths 500>λ>300 nm. In this region the intensity profiles of 100 kDa and 10 kDa of molecular sizes showed similar profile and minimum and maximum intensity values were at 500 kDa and 0.45 µm respectively (Figure 4.8). For the wavelength region greater than 500 nm the intensity values of 100 kDa and 1 kDa size fractions were found to be close to each other. However, the intensities of all sizes diminished to zero when the wavelength approached to 600 nm (Figure 4.8).

According to the findings of Uyguner et al (2005), the decrease in the fluorescence intensity of lower molecular size fractions of humic acid and the formation of a minor intensity peak around 550 nm might be caused from the depletion of the aromatic and/or polyphenolic contents which are mostly of high molecular size and also the enrichment of its carbohydrate materials which do not give fluorescence. Similarly, in this study the formation of a minor intensity peak around 530 nm was observed. The results are able to give information about the consistence of AOM aqueous solution.

4.3. Analysis of ANOM Solution

4.3.1. UV-vis Spectroscopic Properties of ANOM Solution

ANOM solution was formed from extracted algal organic matter (AOM) which was 25% of total volume, the other 25% of total volume was 20 mg L^{-1} Aldrich humic acid, and the rest 50% of total volume was distilled water.

In the following sections, 1:2, 1:3, 1:4 and 1:5 dilutions of ANOM solution were used for investigation of the concentration effect on the photocatalytic degradation of AOM

aqueous solution. In this part, ANOM solution was specified by using same experimental methodology described for aqueous solution of AOM.

Table 4.2. The general properties of ANOM solution.

Physical Properties:	
Turbidity, NTU	-
Temperature, ^{o}C	30
Chemical Properties:	
pH	6.54
Chemical Oxygen Demand	
Permanganate Consumption Value, mg O_2 L^{-1}	34.71
Dichromate Method, mg O_2 L^{-1}	19.67
Total Organic Carbon, mg C L^{-1}	15.38
Spectroscopic Properties:	
$Color_{436}$, m^{-1}	7.02
$Color_{400}$, m^{-1}	9.39
UV_{365}, m^{-1}	13.08
UV_{280}, m^{-1}	30.39
UV_{254}, m^{-1}	35.43

As it can be seen from Table 4.2, as ANOM solution was compared to AOM aqueous solution, the organic matter value of ANOM solution was almost the half value of AOM aqueous solution because of the dilution factor. However, pH values of two solutions were not different from each other, significantly. The ANOM solution properties displayed relative order of values as 34.71, 20.50 and 15.38 mg L^{-1} for $KMnO_4$ consumption value, COD and TOC measurements.

In the previous section in Table 4.1, the AOM aqueous solution exhibited a colorless property which was explained by having low absorbance values in the visible region as $Color_{400}$ or $Color_{436}$. On the other hand, all the absorbance values of ANOM solution were more than values of AOM solution because of humic acid which was present in ANOM solution. For $Color_{436}$ and $Color_{400}$, the ANOM solution had 7.02 and 9.39 m^{-1} values. Besides, ANOM solution expressed more aromaticity than color forming moieties as 30.39 and 35.43 m^{-1} values for UV_{280} and UV_{254}, respectively (Table 4.2).

In a recent study (Uyguner et al., 2005), the UV-vis spectra of the studied humic substances showed a gradually decreasing absorptivity. In relation to this trend, UV-vis spectra of ANOM solution displayed the same manner which could be attributed to the presence of humic acid.

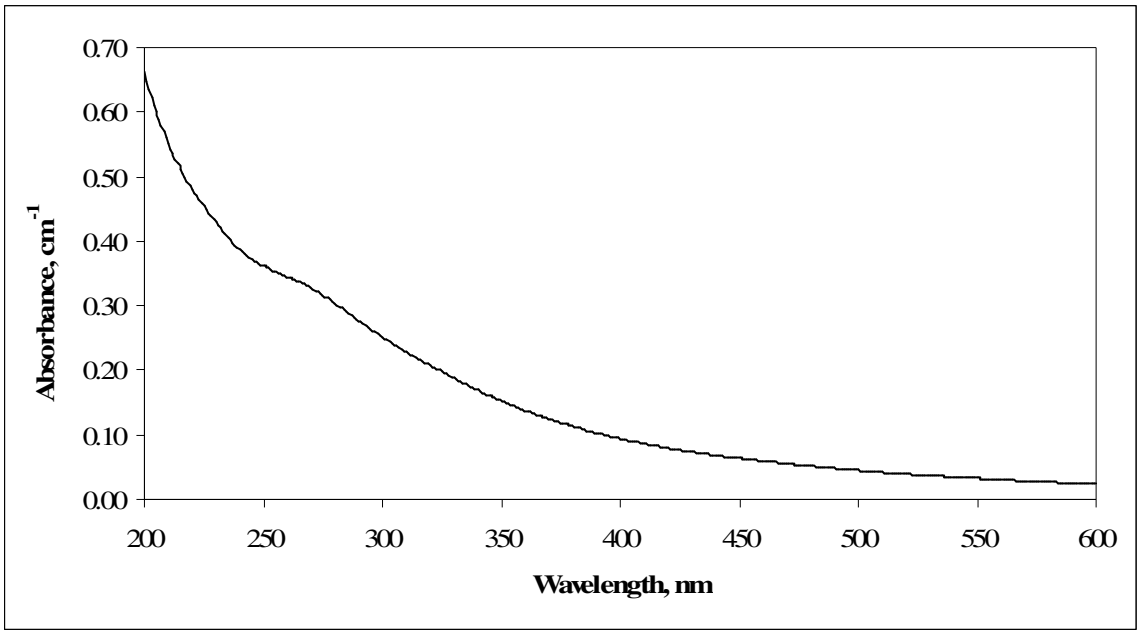

Figure 4.9. UV-vis spectra of ANOM solution.

As it can be seen in Figure 4.9, the UV-vis spectra of the studied ANOM solution were in declining trend and also absorbance values of ANOM solution were demonstrated at defined wavelengths in Table 4.2.

As it is mentioned in the previous sections, UV_{254} represents a parameter expressing total organic carbon content and UV_{280} represents total aromaticity. The color forming chromophoric groups of organic substances are usually expressed with $Color_{436}$ and/or $Color_{400}$ values (Bekbolet et al., 1998). Under the light of this fact, AOM and ANOM solution values could be compared. The values of AOM aqueous solution were 0.180, 0.165, 0.008 and 0.006 while ANOM solution values were 0.354, 0.304, 0.094 and 0.070 for UV_{254}, UV_{280}, $Color_{400}$ and $Color_{436}$, respectively. According to these data it can be said that color and aromaticity of AOM aqueous solution was less than ANOM solution which was consistent with the higher aromatic content of humic acid.

4.3.2. Fluorescence Spectroscopic Properties of ANOM Solution

In literature, the synchronous scan fluorescence spectroscopy is more convenient and has been extensively used for the characterization of humic substances (Senesi, 1990; Pullin and Cabaniss, 1995; Santos et al., 2001; Peuravuori et al., 2002).

Preliminary studies were conducted on raw and oxidized humic substances for the selection of the appropriate excitation wavelengths for the emission and the synchronous scan spectra and observed the effect of concentration of humic substances on the fluorescence spectra (Uyguner and Bekbolet, 2005b; Uyguner and Bekbolet, 2005c). Therefore, same method was applied on ANOM solution which partly consisted of humic acids for characterization of AOM aqueous solution in this study.

Synchronous scan spectra not only offer a potential use to reduce overlapping interferences but also provide a possibility for each fluorescent component to be identified in a spectral range. The synchronous scan fluorescence spectra for ANOM solution were shown in Figure 4.10.

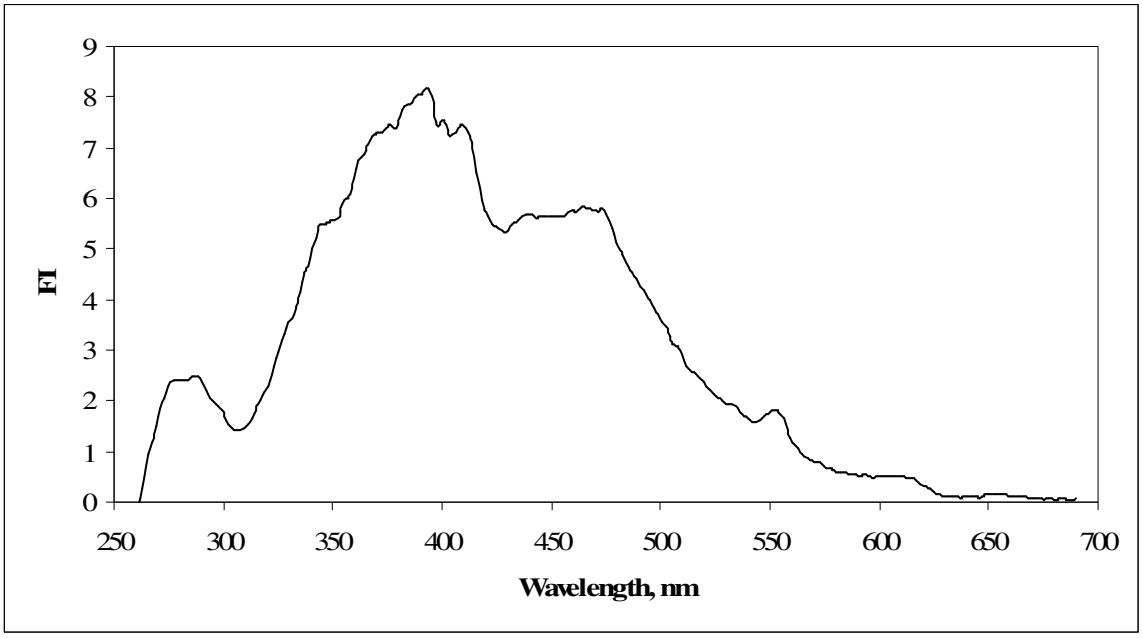

Figure 4.10. Synchronous scan fluorescence spectra of ANOM solution.

It is obvious from Figure 4.10 that initial peak was around 280 nm and also in the range of 345 to 430 nm ANOM solution displayed a broad absorption peak. A maximum intensity, 8.19, was observed at 393 nm. After the broad shoulder had formed in 430-465 nm, the fluorescence intensity decreased with respect to increasing wavelengths. Furthermore, the presence of a slight peak was also observed at about 550 nm wavelength region.

4.3.3. UV-vis Spectroscopic Properties of 1:2 Diluted ANOM Solution

In this study, the sample was obtained from ANOM solution by 1:2 dilutions with distilled water. Its character is presented as ANOM solution in Table 4.3.

Table 4.3. The general properties of 1:2 diluted ANOM solution.

Physical Properties:	
Turbidity, NTU	-
Temperature, ^{o}C	30
Chemical Properties:	
pH	6.82
Chemical Oxygen Demand	
Permanganate Consumption Value, mg O_2 L^{-1}	29.53
Dichromate Method, mg O_2 L^{-1}	12.90
Total Organic Carbon, mg C L^{-1}	-
Spectroscopic Properties:	
$Color_{436}$, m^{-1}	3.90
$Color_{400}$, m^{-1}	5.26
UV_{365}, m^{-1}	7.14
UV_{280}, m^{-1}	15.88
UV_{254}, m^{-1}	18.78

According to the table above, 1:2 diluted ANOM solutions exhibited almost neutral pH conditions of 6.82. It can be clearly seen in Figure 4.11 that, low absorbance values in the visible region which represents color features of substances as $Color_{436}$ and $Color_{400}$ resulted in quite light color of 1:2 diluted ANOM solution. At these wavelengths, the solution had 3.90 and 5.26 m^{-1} values. Beside these low values, 1:2 diluted ANOM solution expressed 15.88 and 18.78 m^{-1} values for UV_{280} and UV_{254}, correspondingly (Table 4.3).

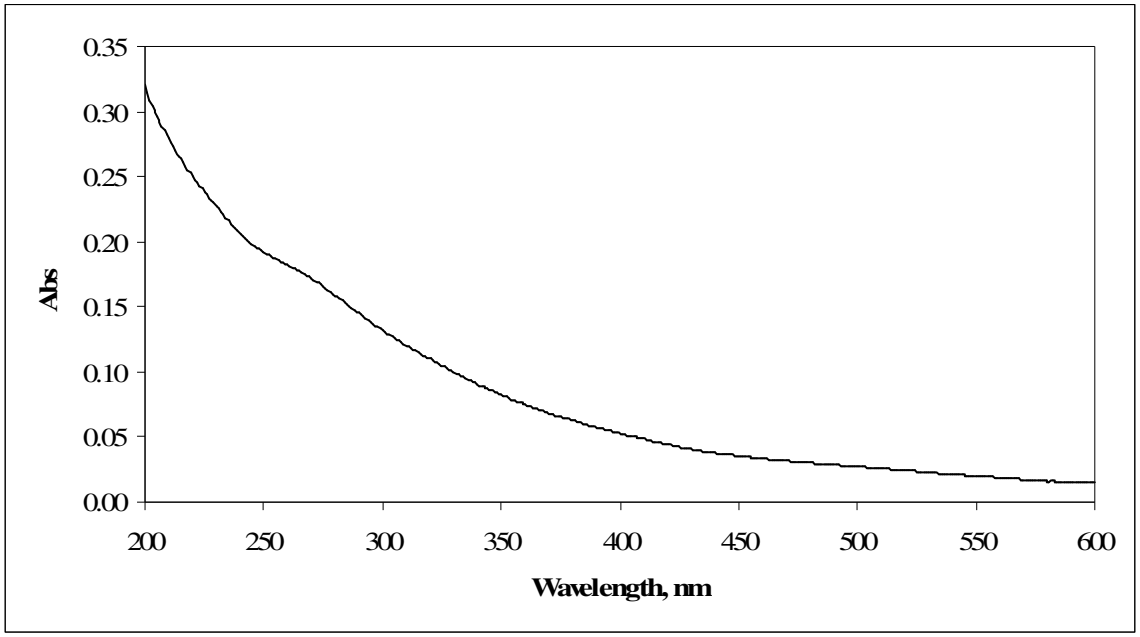

Figure 4.11. UV-vis spectra of 1:2 diluted ANOM solution.

The absorbance values of 1:2 diluted ANOM solutions continuously decreased with increasing wavelengths however slight change was observed at 250-280 nm. As mentioned before, the absorption values measured at these wavelengths could be used for the explanation of the presence of the aromatic groups in the complex organic structures (Figure 4.11).

It was obviously seen from in Figure 4.11 and Table 4.3 that the values of ANOM solution for UV_{254} and UV_{280} were higher than $Color_{400}$ and $Color_{436}$ but could also be considered as similar to values of AOM aqueous solution. Considering the data, 1:2 diluted ANOM solution was found to be more aromatic in character and also had more color forming moieties then aqueous solution of AOM.

4.3.4. Fluorescence Spectroscopic Properties of 1:2 Diluted ANOM Solution

Synchronous scan fluorescence spectra of 1:2 diluted ANOM solution were demonstrated in Figure 4.12.

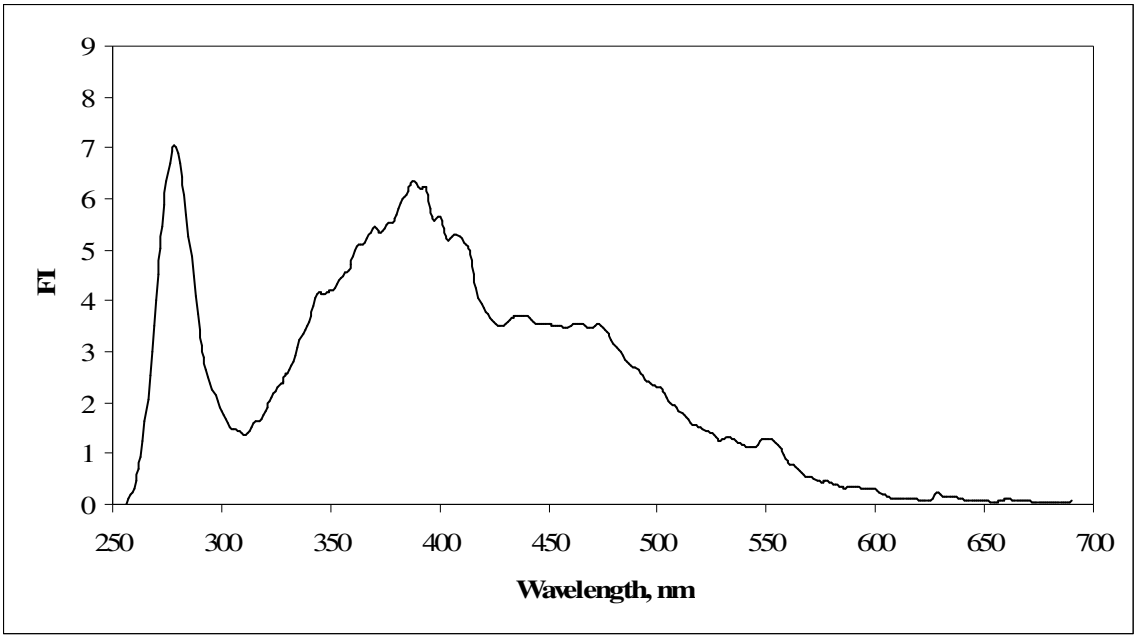

Figure 4.12. Synchronous scan fluorescence spectra of 1:2 diluted ANOM solution.

Fluorescence spectra of 1:2 diluted ANOM solution was found to be exhibiting a significantly higher FI from raw ANOM solution at a wavelength region about 280 nm. In this region it had a sharp peak at 280 nm and also maximum intensity value of 6.99. A broader peak was also observed around 390 nm with a minor shoulder around 550 nm. In 430-475 nm wavelength region, fluorescence intensity was slightly changed resembling a shoulder effect in this region and then continuously decreased with increasing wavelength. The fluorescence intensity values approached to zero for wavelength region of 600-700 nm (Figure 4.12).

4.3.5. UV-vis Spectroscopic Properties of 1:3 Diluted ANOM Solution

The studied sample was obtained 1:3 diluted to ANOM solution with distilled water. The properties of solution were shown in Table 4.4.

Table 4.4. The general properties of 1:3 diluted ANOM solution.

Physical Properties:	
Turbidity, NTU	-
Temperature, ^{o}C	30
Chemical Properties:	
pH	6.81
Chemical Oxygen Demand	
Permanganate Consumption Value, mg O_2 L^{-1}	17.90
Dichromate Method, mg O_2 L^{-1}	8.47
Total Organic Carbon, mg C L^{-1}	-
Spectroscopic Properties:	
$Color_{436}$, m^{-1}	2.26
$Color_{400}$, m^{-1}	2.98
UV_{365}, m^{-1}	4.12
UV_{280}, m^{-1}	9.38
UV_{254}, m^{-1}	10.90

It can be obviously seen from in Table 4.4, that 1:3 diluted ANOM solution was neutral with a pH value of 6.81. 1:3 diluted ANOM solution exhibited 17.90 and 8.47 mg L^{-1} for $KMnO_4$ consumption value and COD respectively. UV-vis spectroscopic parameters revealed very similar color property alongside with comparatively higher UV_{254} and UV_{280}. UV-vis spectra of 1:3 diluted ANOM solutions and also its absorbance values at specific wavelengths were demonstrated in Figure 4.13.

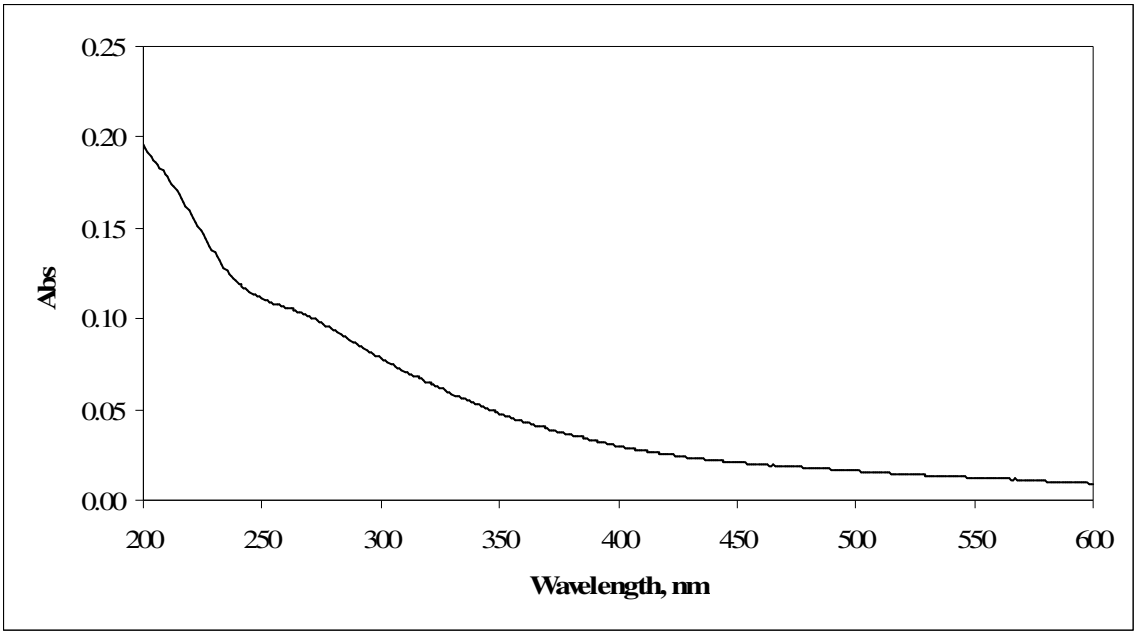

Figure 4.13. UV-vis spectra of 1:3 diluted ANOM solution.

As can be seen in Figure 4.13 that the UV-vis spectra of 1:3 diluted solution displayed similar absorbance properties compared to other diluted ANOM solutions of which the absorbance values were gradually decreased with increasing wavelength and had lower color forming moieties than UV absorbing aromatic centers.

4.3.6. Fluorescence Spectroscopic Properties of 1:3 Diluted ANOM Solution

The synchronous scan fluorescence spectra of 1:3 diluted ANOM solution was illustrated in Figure 4.14.

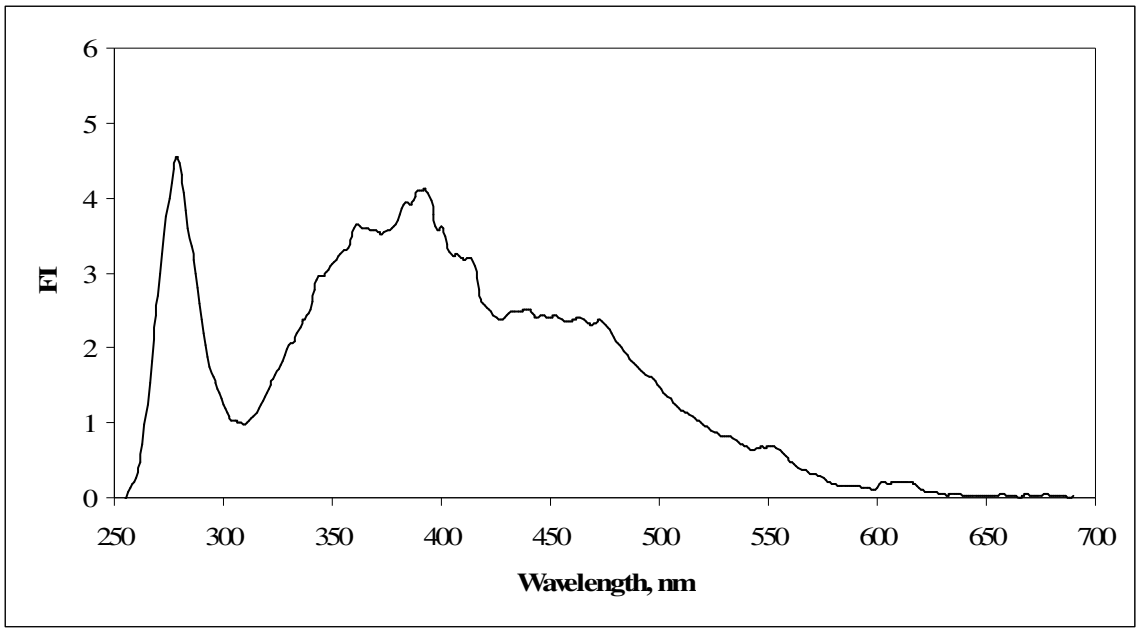

Figure 4.14. Synchronous scan fluorescence spectra of 1:3 diluted ANOM solution.

Synchronous scan fluorescence spectra of 1:3 diluted ANOM solution displayed similar fluorescence properties as recorded for 1:2 diluted ANOM solution except for their fluorescence intensity values (Figure 4.14). The maximum peak observed at 280 nm could be considered as broader than the one observed for 1:2 diluted ANOM solution. In the wavelength region of 360-410 nm, another broader peak was also observed with a FI value of 4.11. The fluorescence intensity did not change significantly in the wavelength range of 430 to 475 nm, thus this region could be considered as a broad shoulder. The trend observed in the fluorescence spectrum showed very slight changes in the wavelength region of about 550 and 610 nm and approached to zero for higher longer wavelengths than 630 nm.

4.3.7. UV-vis Spectroscopic Properties of 1:4 Diluted ANOM Solutions

The solution was constituted by 1:4 dilution of ANOM solution with distilled water. The properties of diluted 1:4 ANOM solution were shown in Table 4.5.

Table 4.5. The general properties of 1:4 diluted ANOM solution.

Physical Properties:	
Turbidity, NTU	-
Temperature, ^{o}C	30
Chemical Properties:	
pH	6.73
Chemical Oxygen Demand	
Permanganate Consumption Value, mg O_2 L^{-1}	9.10
Dichromate Method, mg O_2 L^{-1}	6.46
Total Organic Carbon, mg C L^{-1}	-
Spectroscopic Properties:	
$Color_{436}$, m^{-1}	1.65
$Color_{400}$, m^{-1}	2.21
UV_{365}, m^{-1}	3.06
UV_{280}, m^{-1}	7.86
UV_{254}, m^{-1}	9.43

As can be seen from in Table 4.5, the pH value of 1:4 diluted ANOM solution was 6.73. The $KMnO_4$ consumption value and COD values of 1:4 diluted ANOM solution were determined as 9.10 and 6.46 mg L^{-1} respectively. Moreover, 1:4 diluted ANOM solution had significantly low color forming moieties as expressed by $Color_{436}$ and $Color_{400}$ parameters with values as 1.65 and 2.21 m^{-1} respectively. On the other hand, considerably significant amounts of UV absorbing moieties were still detected as expressed by UV_{254} and UV_{280} values (Table 4.5).

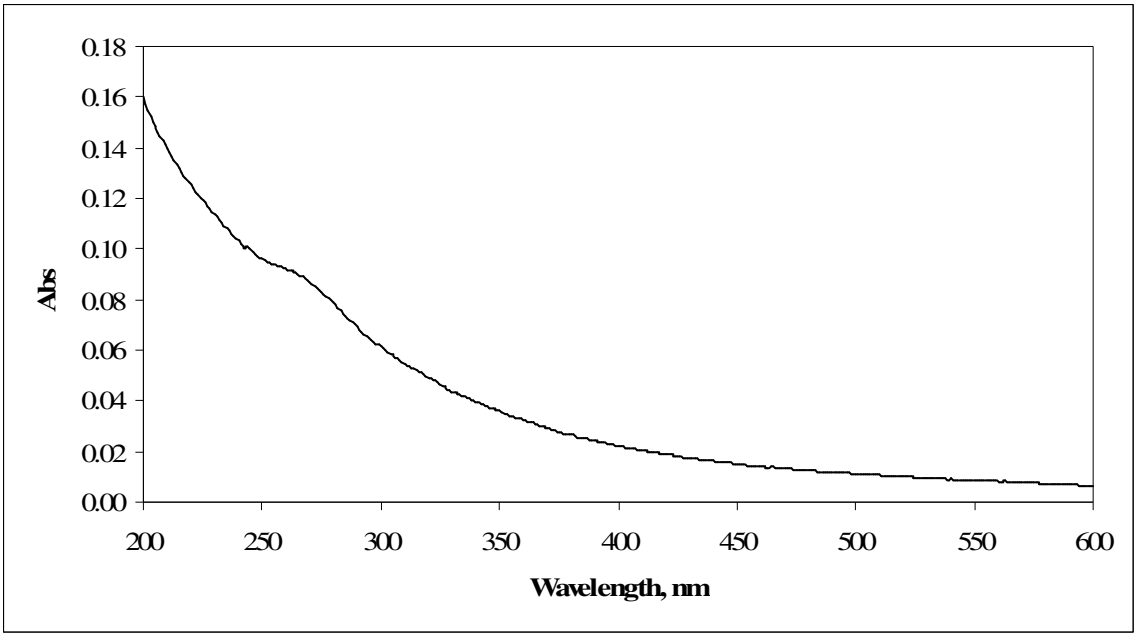

Figure 4.15. UV-vis spectra of 1:4 diluted ANOM solution.

The UV-vis spectra of 1:4 diluted ANOM solution exhibited similar absorbance properties compared to other diluted ANOM solutions of which the absorbance values gradually decreased with increasing wavelength.

4.3.8. Fluorescence Spectroscopic Properties of 1:4 Diluted ANOM Solution

Synchronous scan fluorescence spectra of 1:4 diluted ANOM solution was illustrated in Figure 4.16.

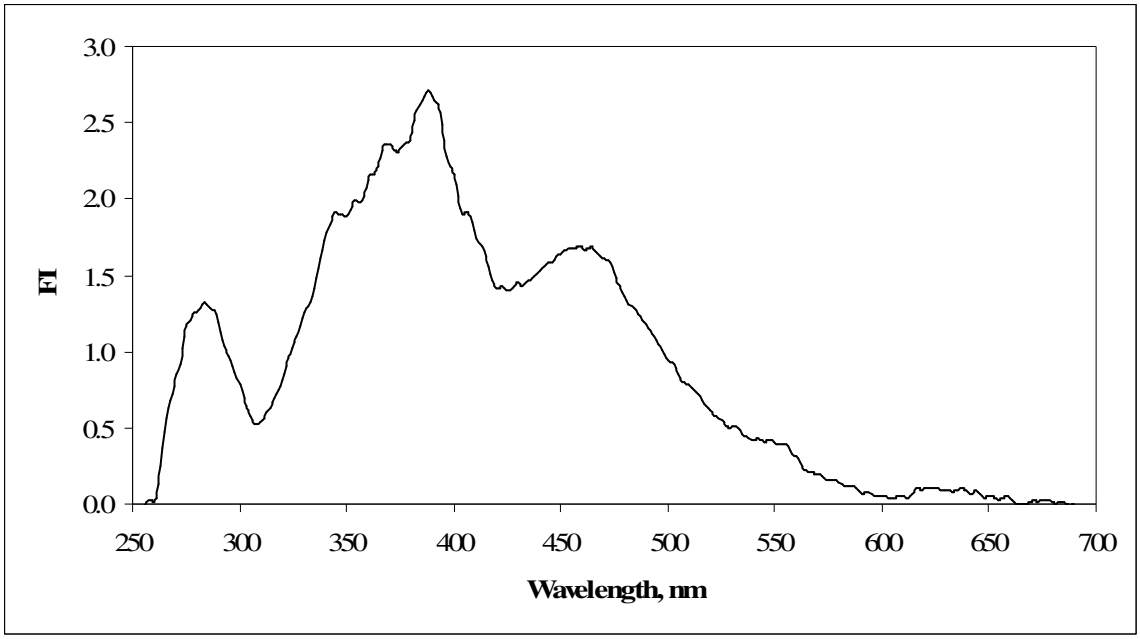

Figure 4.16. Synchronous scan fluorescence spectra of 1:4 diluted ANOM solution.

As can be seen the Figure 4.16 that 1:4 diluted ANOM solution exhibited similar trend as observed for the others despite of different peak shapes. The previous peaks were little quenched with decreasing concentration of solution but some little peaks completely turned into shoulders as around 550 nm.

The initial peak was exhibited at around 280 nm as previously however, it was not maxima. The maximum peak was detected at 388 nm wavelength with a FI value of 2.71. The discrepancy of this spectrum could be expressed by the presence of a new shoulder around 460 nm wavelength region. Following the wavelength region up to 650 nm, the spectra displayed no significant change (Figure 4.16).

4.3.9. UV-vis Spectroscopic Properties of 1:5 Diluted ANOM Solution

ANOM solution was further diluted to obtain 1:5 diluted ANOM solution with considerably low aromatic content. General properties of 1:5 diluted ANOM solution was given in Table 4.6.

Table 4.6. The general properties of 1:5 diluted ANOM solution.

Physical Properties:	
Turbidity, NTU	-
Temperature, ^{o}C	30
Chemical Properties:	
pH	6.69
Chemical Oxygen Demand	
Permanganate Consumption Value, mg O_2 L^{-1}	5.91
Dichromate Method, mg O_2 L^{-1}	4.45
Total Organic Carbon, mg C L^{-1}	-
Spectroscopic Properties:	
$Color_{436}$, m^{-1}	1.47
$Color_{400}$, m^{-1}	1.99
UV_{365}, m^{-1}	2.75
UV_{280}, m^{-1}	6.29
UV_{254}, m^{-1}	7.37

Under neutral pH condition of 1:5 diluted ANOM solution, relatively lower consumption value (5.91 mg L^{-1}) and COD (4.45 mg L^{-1}) were determined. Considering the dilution effect, the 1:5 diluted colorless ANOM solution expressed. UV_{254} and UV_{280} values were 6.29 and 7.37 m^{-1}.

The UV-vis spectra of 1:5 diluted ANOM solutions was recorded in the wavelength range of 200-600 nm and demonstrated in Figure 4.17.

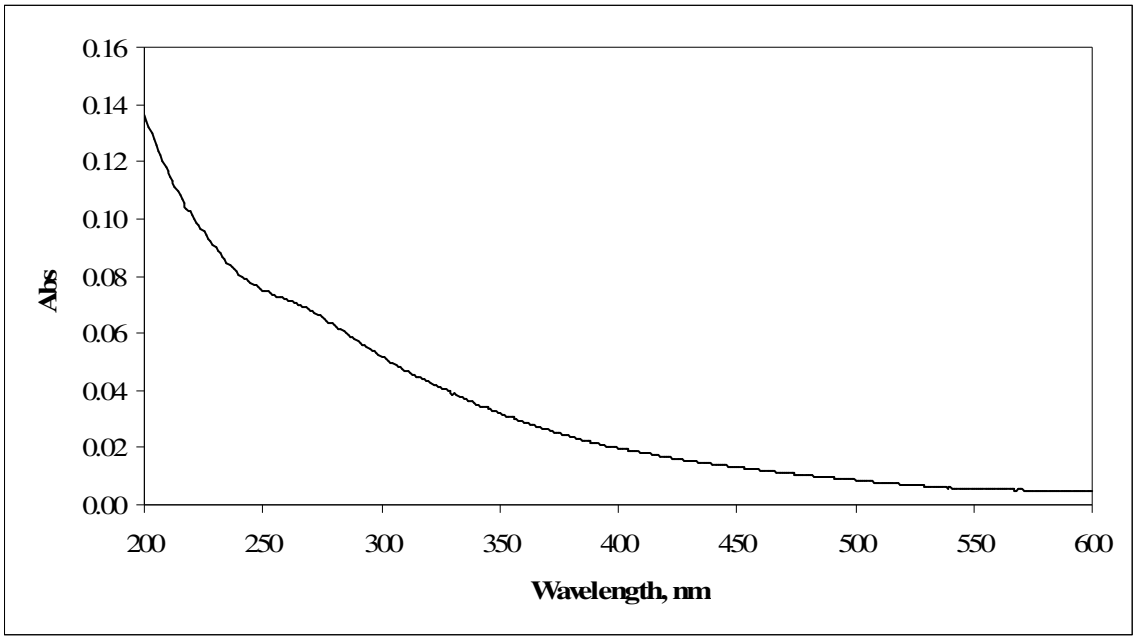

Figure 4.17. UV-vis spectra of 1:5 diluted ANOM solution.

Displaying the similar pattern of declining trend, a decrease in the absorbance values were observed with the increasing wavelengths. The respective absorbance values of 1:5 diluted solution were quite less than the others as expected. 1:5 diluted ANOM solution had a broad shoulder between 250 and 300 nm wavelength region, due to the dilution effect.

4.3.10. Fluorescence Spectroscopic Properties of 1:5 Diluted ANOM Solution

Synchronous scan fluorescence spectra of 1:5 diluted ANOM solution were presented in Figure 4.18.

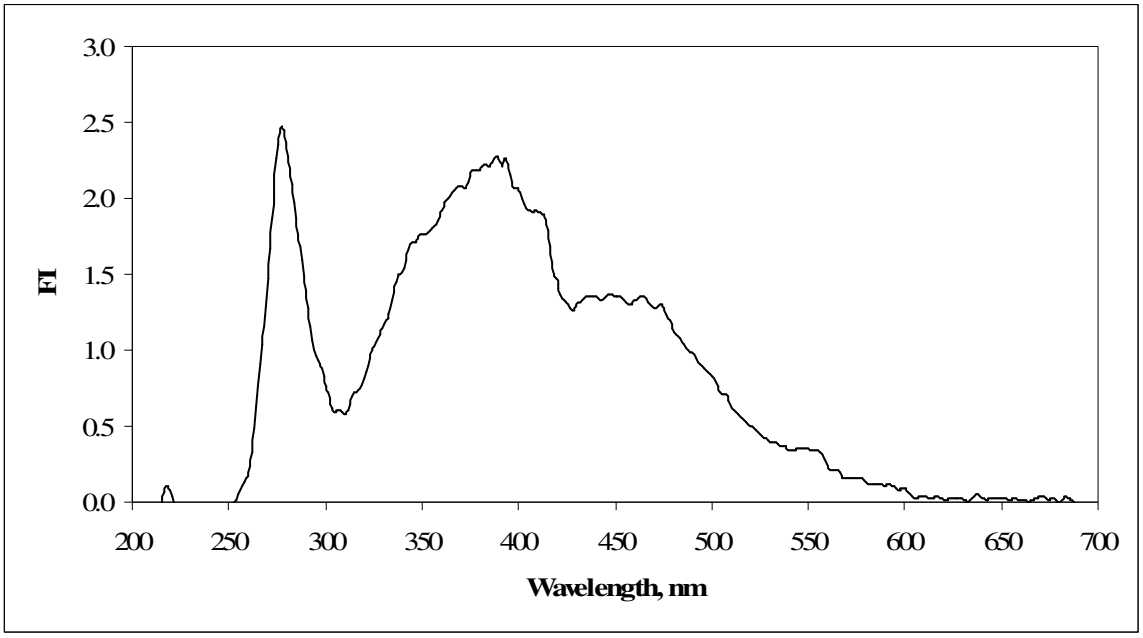

Figure 4.18. Synchronous scan fluorescence spectra of 1:5 diluted ANOM solution.

According to Figure 4.18, only the spectrum of 1:5 diluted ANOM solution exhibited a minor peak around 220 nm. On the other hand, it showed similar fluorescence properties with other diluted ANOM solutions and its intensity values were found to be very close to 1:4 diluted ANOM solution for wavelengths greater than 300 nm. In the range of 360 to 410 nm it had broad peak followed by a minor peak around 550 nm. A significant shoulder was also observed at 430 to 475 nm wavelength region. For wavelengths greater than 600 nm, the fluorescence intensity diminished to almost undetectable levels.

4.3.11. Comparison of Concentration Effects of ANOM Solution on UV-vis Spectroscopic Properties

UV- vis Spectra of all diluted solutions were demonstrated in Figure 4.19.

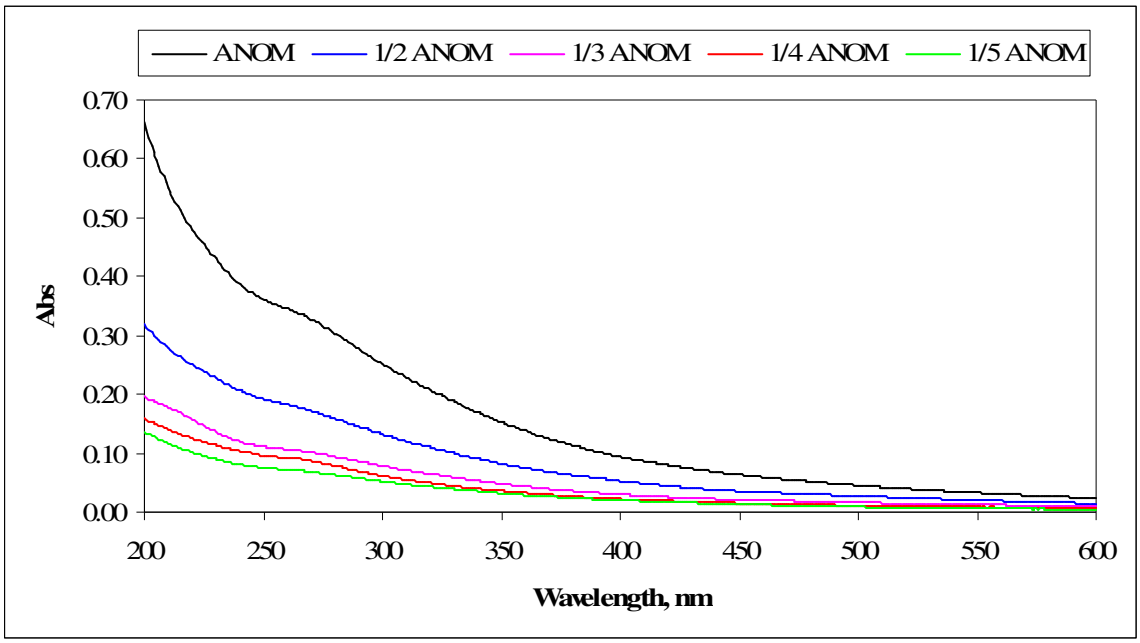

Figure 4.19. UV-vis spectra of all ANOM solutions.

In Figure 4.19, all ANOM solutions were compared; a minor change was appeared around 280 nm. At this region, the observed shoulder was removed with increasing dilutions. On the other hand, similar trend was observed according to the UV-vis spectroscopic parameters. The UV absorptivity of all solutions decreased with increasing wavelengths. Apart from the dilution effect, no distinct differences were attained for the ANOM solutions in terms of UV-vis spectroscopic evaluation.

4.3.12. Comparison of Concentration Effects of ANOM Solution on Fluorescence Spectroscopic Properties

The fluorescence spectra of all diluted and raw ANOM solutions were presented in Figure 4.20.

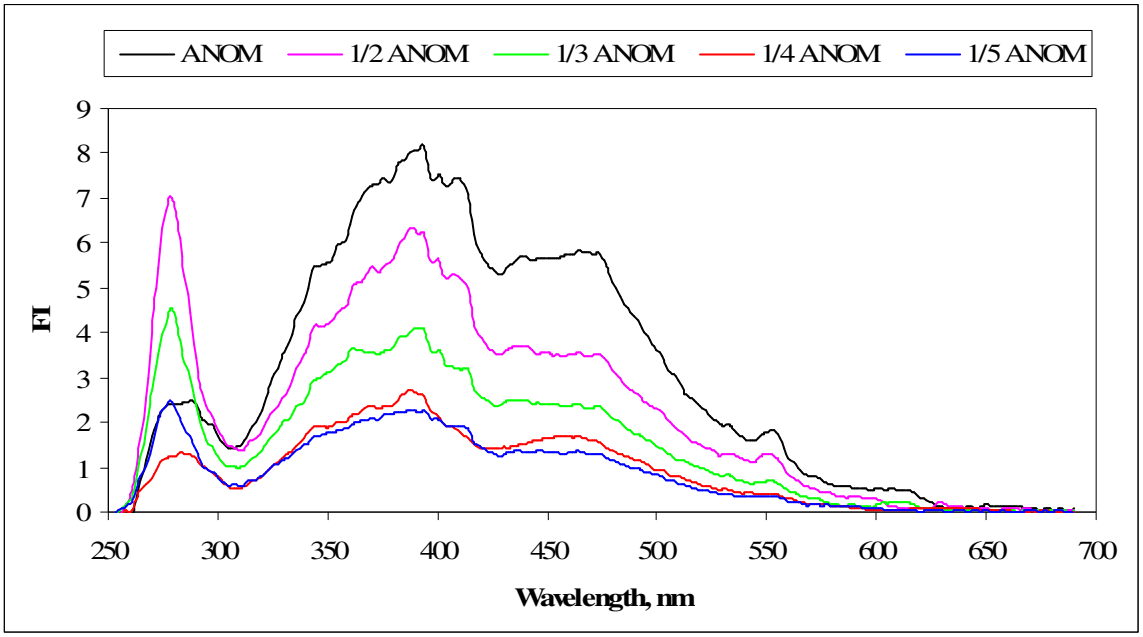

Figure 4.20. Synchronous scan fluorescence spectra of all ANOM solutions.

Comparison of the raw and diluted ANOM solutions as demonstrated in Figure 4.20 displayed different trends in FI values at about 280 nm wavelengths. In this region the solutions exhibited disordered patterns irrespective of the dilution degree.

As expected, the FI intensity of all of the ANOM solutions decreased with decreasing concentration in the region of the spectrum with wavelengths greater than 300 nm wavelengths. The data of 1:4 and 1:5 diluted ANOM solutions were very similar to each other. In this region, high intensities and slight peaks were observed around 390 nm wavelengths. In the 420-480 nm wavelength regions, the FI intensities did not change significantly but after 480 nm it decreased rapidly to 545 nm, then at around 550 nm, the emergence of a slight peak was observed clearly only for raw solution and 1:2 diluted solution (Figure 4.20).

The fluorescence intensity is based on the origin of solution and the possible presence of impurities. Fluorescence spectra have also different profiles as a function of their structural differences. According to obtained data, it can be said that in the synchronous scan spectra of ANOM solution, the concentration has a minor effect on the position of bands and shoulders,

however it alters their intensities. Further decrease of concentration leads to subsequent quenching of fluorescence intensity (Figure 4.20).

Similar findings was reported by Uyguner (2005) that the effect of concentration on the fluorescence spectra of humic substances in 10-100 mg L^{-1} concentration ranged for Aldrich humic acid and same results which had effect on the position of bands and value of intensities were reached.

4.4. Photocatalytic Degradation

4.4.1. UV-vis Spectroscopic Properties of the Molecular Size Distribution of Photocatalytic Oxidized AOM Aqueous Solution

Photocatalytic degradation of AOM aqueous solution was performed in the presence of 0.25 mg mL^{-1} TiO_2 for an irradiation period of up to 60 minutes. Approximately 20 % degradation was achieved irrespectively in irradiation time.

The molecular size distribution of oxidized AOM aqueous solution was performed using ultrafiltration stirred cell by filtering through membranes with pore sizes in the diameter of 0.45 µm to 1 kDa.

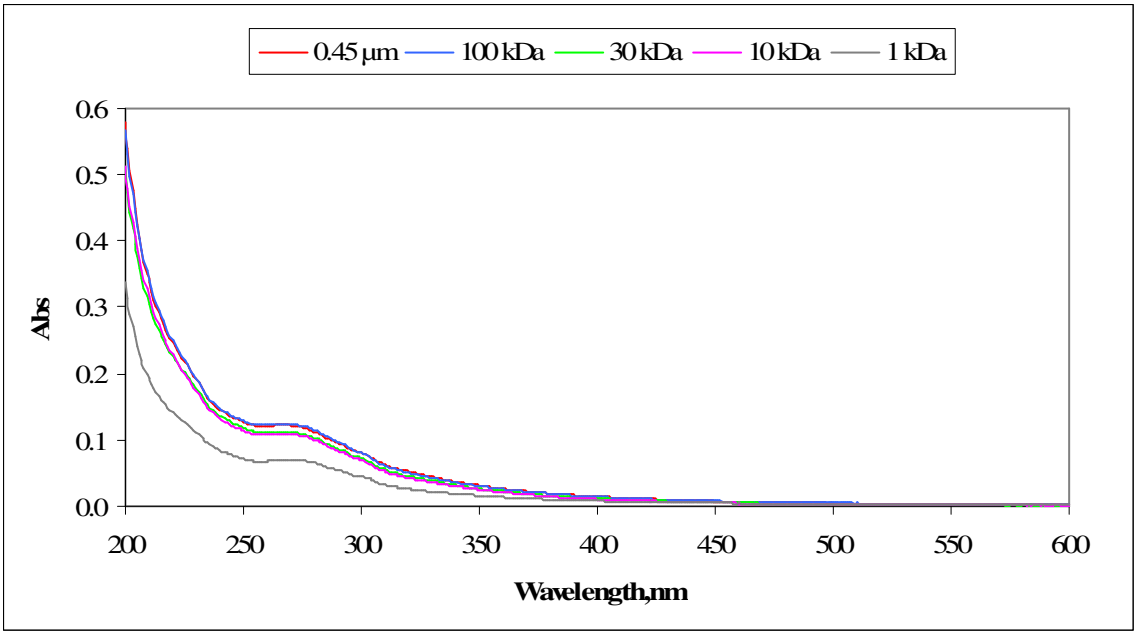

Figure 4.21. UV-vis spectra of the molecular size distribution of oxidized AOM aqueous solution.

It can be clearly seen from Figure 4.21 that, the absorbance of the oxidized AOM aqueous solution exhibited generally decreasing trend from low wavelength to the high wavelength, however the decreased trend was also observed from high size fraction to low size fraction. When aqueous solution of AOM was oxidized, 0.45 µm with 100 kDa and 30 kDa with 10 kDa sizes of absorbance values were found to be close to each other. Except for molecular size fraction of 1 kDa, all molecular sizes were distributed equally after oxidation occurred (Figure 4.22).

According to Figure 4.22, 1 kDa displayed the lowest UV-vis parameters and also differed from the others as its UV_{254} and UV_{280} values were found to be very close to each other.

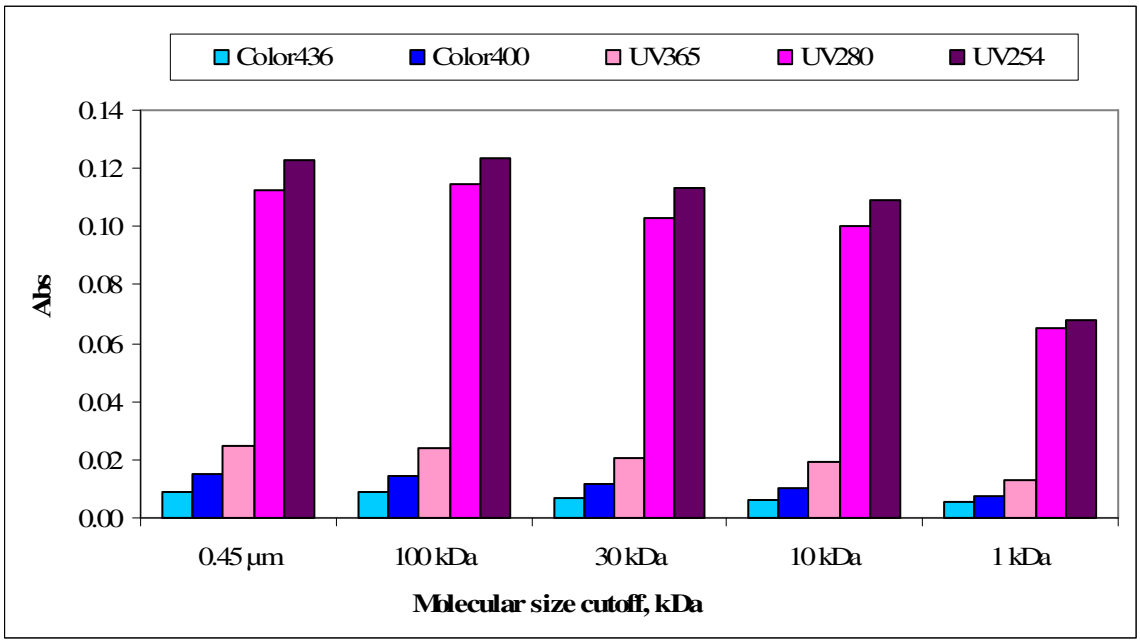

Figure 4.22. $Color_{436}$, $Color_{400}$, UV_{365}, UV_{280} and UV_{254} values for oxidized AOM aqueous solution with respect to molecular size distribution.

It was mentioned in the previous section that, the molecular size distribution profiles of the AOM aqueous solution followed general decreasing trend from high molecular size fractions to the lower molecular size fractions (Figure 4.6 and Figure 4.7). As a general trend, the absorbance values of the oxidized AOM aqueous solution also followed the same pattern of increasing absorbance values versus decreasing molecular size fractions. Similar decreasing trends were also reported in literature for humic substances (Peuravuori and Pihlaja, 1997).

4.4.2. Comparison of Molecular Size Distribution of Raw and Oxidized AOM Aqueous Solution on UV-vis Spectroscopic Properties

Substantial differences among the fractions of different molecular sizes point out the importance of the characterization of the size fractions properly in order to better understand the spectroscopic properties of oxidized AOM aqueous solution.

When the AOM aqueous solution was oxidized by the nonselective oxidation pathway of the hydroxyl radical, significant structural changes occurred in the organic matrix of the algal derived organic matter. According to its UV-vis spectroscopic parameters, it would be better assessed in following figure (Figures 4.23).

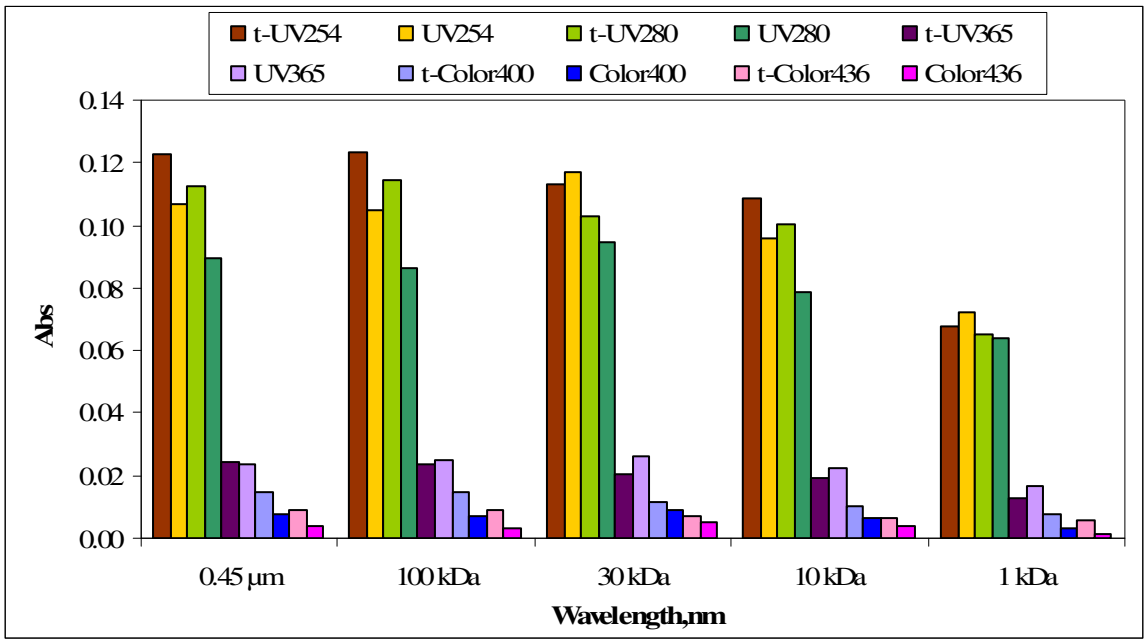

Figure 4.23. Comparison of $Color_{436}$, $Color_{400}$, UV_{365}, UV_{280} and UV_{254} with molecular size distribution of raw and treated aqueous solution of AOM (i.e. UV_{254} represents the absorbance value of raw aqueous solution of AOM at 254 nm; t-UV_{254} represents the absorbance value of oxidized AOM aqueous solution at 254 nm).

It is evident from Figure 4.23, that the effect of oxidation could be visualized in terms of higher UV_{280}/UV_{254} changes than $Color_{400}/Color_{436}$ changes irrespective of the molecular size fractions.

As can be seen in figure above, absorbance values of oxidized AOM aqueous solution observed for $Color_{436}$, $Color_{400}$, UV_{280} and UV_{254} increased after photocatalytic treatment where the degradation efficiency was irrespective of the molecular size fractions. These

increases can be explained by the formation of high molecular weight fractions (450-10 kDa) via the combination of the photoproducts originating from lower molecular size fractions and also structural change during the molecular size fractionation experiments.

The maximum increase of was observed for 1 kDa on the other hand 30 kDa had minimum increase value for $Color_{436}$. The data of $Color_{400}$ was found to be similar to $Color_{436}$ despite of less increasing rates.

The UV_{365} changes detected for the molecular size fractions of the oxidized AOM aqueous solution were found to be less than the corresponding values observed for raw AOM solution as expected. The highest UV_{365} removal (20%) was observed for 1 kDa and 30 kDa molecular size fractions. On the other hand, considerably higher UV_{254} values were attained for 0.45μm, 100kDa and 10 kDA fractions upon oxidation. All of the molecular size fractions of the photocatalytically oxidized AOM solution exhibited significantly higher UV_{280}.

The study of the molecular size distribution was researched with different humic acids by Uyguner (2005). In this study it was found that the primary effect of photocatalytic oxidation was observed in the 450-100 kDa fraction for all of the humic acids except for humic acid of terrestrial origin (RHA). According to the literature the exception of RHA was explained by the formation of high molecular weight fractions (450-100 kDa) via the combination of the photoproducts originating from lower molecular size fractions (Uyguner and Bekbolet, 2005c).

4.4.3. Fluorescence Spectroscopic Properties of the Molecular Size Distribution of Oxidized AOM Aqueous Solution

The oxidative behavior of AOM aqueous solution towards photocatalytic degradation could also be evaluated by the use of molecular size distribution profiles of which sizes differs in the range of 100 to 1 kDa. After oxidation in all size fractions, significant changes in

molecular size distribution were noted in the synchronous scan fluorescence spectra of AOM aqueous solution as figured in Figure 4.24.

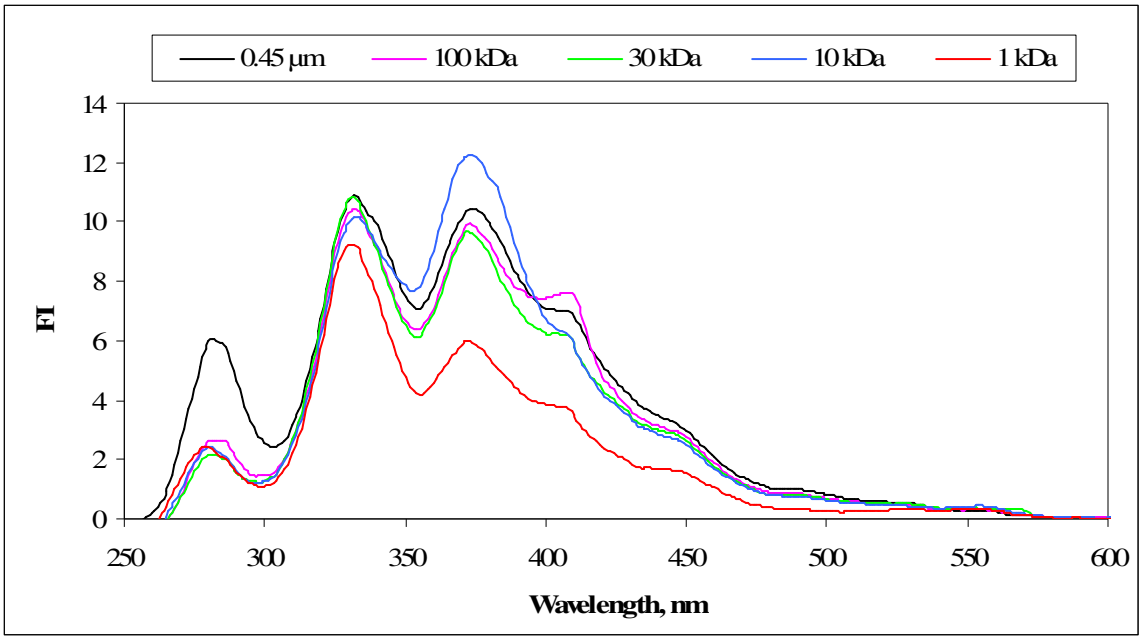

Figure 4.24. Synchronous scan spectra of molecular size distribution of oxidized AOM aqueous solution.

Compared to raw aqueous solution of AOM molecular size distribution shown in Figure 4.8, oxidation leaded to changes in the fluorescence properties as well as the structural properties in the molecular size distribution of AOM aqueous solution. Also, the broad peaks of AOM aqueous solution became narrower and sharper by the effect of oxidation (Figure 4.24).

The most significant difference was observed in the shift of the fluorescence peaks of oxidized size distribution to lower wavelength region. Another noticeable difference was in the 330-350 nm regions, the shoulder of raw aqueous solution of AOM altered as a peak when it was oxidized. Therefore, in the 330-400 nm regions, the size fractions greater than 10 kDa exhibited similar fluorescence properties, however, 10 kDa showed maxima fluorescence

intensity. The spectra of oxidized AOM solution exhibited a disordered pattern depending on the size distribution in this region and also all of the sizes had higher intensity than the sizes of raw aqueous solution of AOM. It might be concluded that the effect of oxidation on the different molecular sizes of AOM aqueous solution increased in the fluorophoric group (Figure 4.24).

From Figure 4.24, it was clearly seen that the size distribution of oxidized AOM aqueous solution had a prominence as a small shoulder about 400 nm wavelengths. Moreover, compared to the corresponding molecular size distributions of raw AOM aqueous solution, decrease in fluorescence intensity was observed in spite of the presence of the major absorbance peak at 280 nm. According to this behavior, it could be said that oxidation leaded to subsequent quenching of fluorescence intensity at 280 nm. In addition it completely quenched the peak which could be detected previously at 530 nm wavelength.

4.4.4. Photocatalytic Degradation of ANOM Solution

In this section, ANOM solution was treated by photocatalytic oxidation using TiO_2 Degussa P-25 as the photocatalyst. A representative example of the time dependent UV-vis spectra was given for the photocatalytic oxidation of ANOM solution in Figure 4.25.

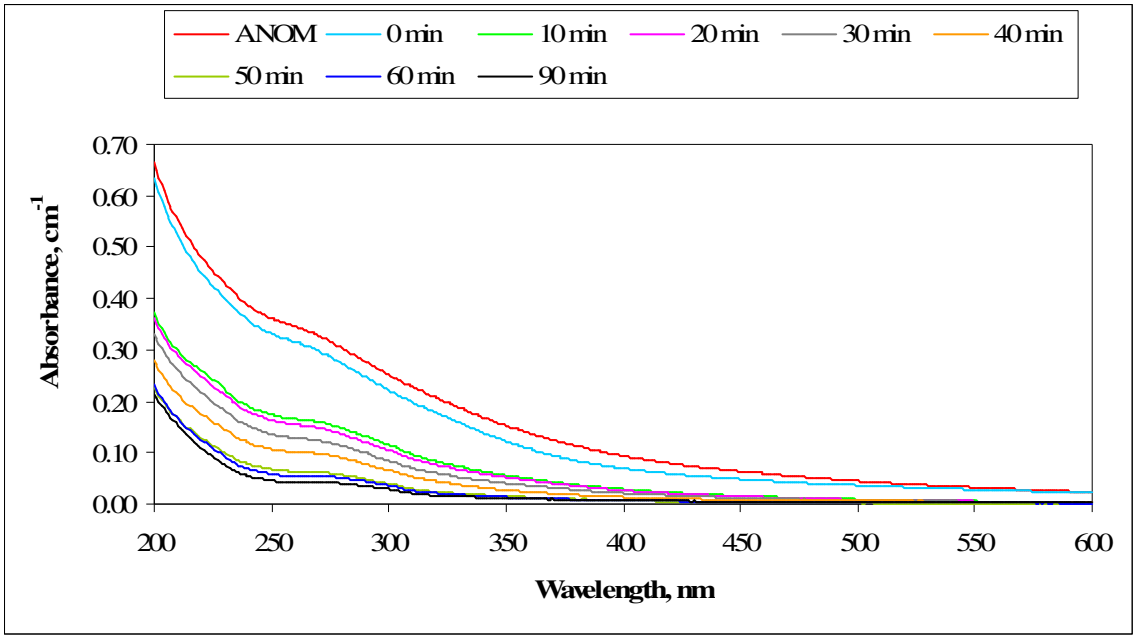

Figure 4.25. UV-vis spectra of the photocatalytic degradation of ANOM solution in the presence of 0.5 mg mL^{-1} TiO_2.

As already mentioned in the previous section, the UV-vis spectra of the raw ANOM solution displayed a decreasing trend with increasing wavelength. Oxidized ANOM solution also followed the same declining trend, as presented in Figure 4.25. Moreover, during photocatalytic oxidation process, a decrease in the absorbance values was observed with the increasing irradiation time, displaying the same basic pattern of declining trend (Figure 4.26).

Modeling of the photocatalytic removal of ANOM solution was based on pseudo first order kinetic model. The reaction kinetics was followed in terms of the specified UV-vis parameters as $Color_{436}$, $Color_{400}$, UV_{365}, UV_{280} and UV_{254}.

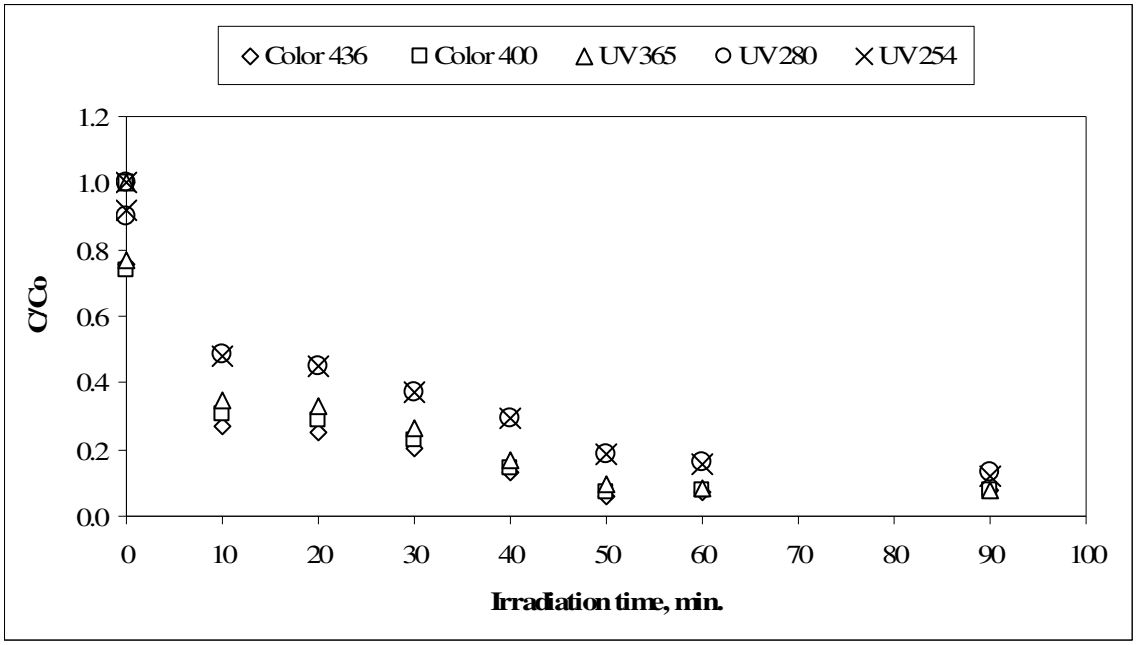

Figure 4.26. Normalized values of $Color_{436}$, $Color_{400}$, UV_{365}, UV_{280} and UV_{254} with respect to irradiation time in the presence of 0.5 mg mL^{-1} TiO_2 for ANOM solution.

The data obtained from the photocatalytic reactions of ANOM solution for $Color_{436}$, $Color_{400}$, UV_{365}, UV_{280} and UV_{254} removal efficiencies were demonstrated in Figure 4.26. The photocatalytic interaction between TiO_2 and ANOM solution resulted in initial adsorptive values of approximately 10% for UV_{280}, and UV_{254} and approximately 20% for $Color_{436}$, $Color_{400}$, and UV_{365}. In extended irradiation periods, after 60 and 90 minutes, the removal percentages were almost the same for all of UV-vis spectroscopic parameters. The UV_{280} and UV_{254} removal efficiencies were slightly lower at 60 and 90 minutes than the removal of the color forming moieties for the given time. For 90 minutes same removal efficiencies were found as 92% for $Color_{436}$, $Color_{400}$ and UV_{365}. Based on the data illustrated in Figure 4.26, the removal efficiencies (Removal, %) are presented in the following table (Table 4.7).

Table 4.7. Oxidative removal of ANOM solution upon irradiation for 30 (t_{30}), 60 (t_{60}) and 90 (t_{90}) minutes in terms of $Color_{436}$, $Color_{400}$, UV_{365}, UV_{280} and UV_{254}.

Parameter	Removal, % t_{30}	Removal, % t_{60}	Removal, % t_{90}
$Color_{436}$	80	93	92
$Color_{400}$	77	92	92
UV_{365}	74	91	92
UV_{280}	63	84	87
UV_{254}	63	84	88

According to the obtained data, although 73% removal was reached for $Color_{436}$ after 10 minutes of irradiation, only 80% removal was attained in rest 30 minutes. On the other hand, no significant increase in removal efficiency was achieved from 60 to 90 minutes of irradiation for $Color_{436}$. $Color_{400}$ removal showed the similar trend to $Color_{436}$ removal in photocatalytic reactions and their removal efficiencies were found the same after 40 minutes. In accordance with the previous results observed for humic acids $Color_{436}$ and $Color_{400}$ parameters could also be used interchangeably (Bekbolet et al., 1998).

For UV_{254} and UV_{280} more than 50% removal was observed in 10 minutes. The removal efficiencies of UV_{254} and UV_{280} showed close similarity to each other and for 60 minutes of irradiation 84% removal was achieved for both of them.

The photocatalytic degradation of ANOM solution in terms of $Color_{436}$, $Color_{400}$, UV_{365}, UV_{280} and UV_{254} can be explained by pseudo first order kinetics (Bekbolet et al., 1998; Bekbolet et al., 2002) which was explained in previous section 2.4.4.1.

According to the obtained data, the evaluation of the kinetic data for the photocatalytic removal of ANOM solution in the presence of 0.5 mg mL^{-1} Degussa P-25 TiO_2 revealed the following model parameters like reaction rate constants, half-life values and reaction rates for $Color_{436}$, $Color_{400}$, UV_{365}, UV_{280} and UV_{254} as presented in Table 4.8.

Table 4.8. Pseudo first order reaction rate constants (k, min^{-1}), half-life values ($t_{1/2}$, min) and reaction rates (R, $m^{-1}min^{-1}$) of photocatalytic degradation of ANOM solution (related correlation coefficient, r^2>0.64).

Parameter	k (min^{-1})	$t_{1/2}$ (min)	R ($m^{-1}min^{-1}$)
$Color_{436}$	$2.68x10^{-2}$	26	0.1881
$Color_{400}$	$2.75x10^{-2}$	25	0.2582
UV_{365}	$2.77x10^{-2}$	25	0.3623
UV_{280}	$2.17x10^{-2}$	32	0.6595
UV_{254}	$2.25x10^{-2}$	31	0.7972

According to Table 4.8, $Color_{436}$, $Color_{400}$ and UV_{365} removal rate constants were almost equal to each other (≈$2.70xl0^{-2}$ min^{-1}) and corresponding half-life values were approximately 25 minutes. The removal rate for UV_{254} was calculated ≈0.8 $m^{-1}min^{-1}$ and found to be 20% more than removal rate of UV_{280}. The half-life values of UV_{280} and UV_{254} were calculated as 32 and 31 min respectively. These values were not significantly different from each other with respect to color forming moieties and UV absorbing centers. On the other hand, it can be said that in color forming centers the degradation rate was higher than in UV absorbing centers as expected.

As it was generally observed during photocatalytic oxidation, the ANOM solution that was also consisted of aromatic components would transform into more simple and colorless moieties. After the photocatalytic oxidation, the decrease observed for UV_{280} and UV_{254}

indicated the degradation of the aromatic sites of the organic skeleton of the ANOM solution besides that the decrease in $Color_{400}$ and $Color_{436}$ would be an indication of a rapid decolorization.

4.4.5. Photocatalytic Degradation of 1:2 Diluted ANOM Solution

Photocatalytic degradation of 1:2 diluted ANOM solution was carried out in the presence of 0.25 mg mL^{-1} TiO_2 and during reaction periods up to 90 minutes. All data were presented in following Figure 4.27.

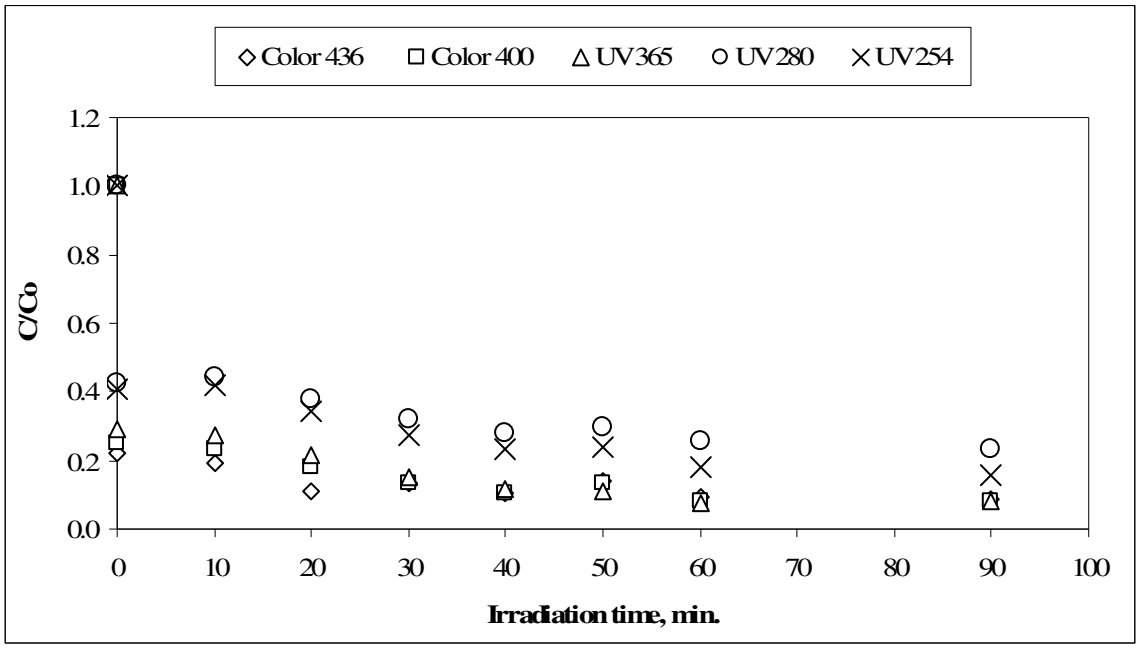

Figure 4.27. Normalized values of $Color_{436}$, $Color_{400}$, UV_{365}, UV_{280} and UV_{254} with respect to irradiation time in the presence of 0.25 mg mL^{-1} TiO_2 for 1:2 diluted ANOM solution.

According to Figure 4.27, initial adsorption values were as high as about 70% for $Color_{436}$, $Color_{400}$ and about 60% for UV_{280} and UV_{254}. On the other hand, in 10 minutes of irradiation time, the removal efficiencies of UV_{280} and UV_{254} slightly increased because of the probable adsorption-desorption process. The oxidative removal of 1:2 diluted ANOM solution

followed a rather slow degradation profile. The removal data of photocatalytic degradation of 1:2 diluted ANOM solution was evaluated in terms of the efficiencies achieved for irradiation periods of 30, 60 and 90 minutes and was given Table 4.9.

Table 4.9. Oxidative removal of 1:2 diluted ANOM solution upon irradiation for 30 (t_{30}), 60 (t_{60}) and 90 (t_{90}) minutes in terms of $Color_{436}$, $Color_{400}$, UV_{365}, UV_{280} and UV_{254}.

Parameter	Removal, % t_{30}	Removal, % t_{60}	Removal, % t_{90}
$Color_{436}$	87	91	91
$Color_{400}$	86	92	92
UV_{365}	85	92	92
UV_{280}	68	74	77
UV_{254}	73	82	84

As it was obviously seen in Table 4.9, $Color_{436}$, $Color_{400}$ and UV_{365} removal percentages were very close to each other. All of them reached more than 90% in 60 and 90 minutes. Their degradation efficiencies did not change significantly after 60 and 90 irradiation times. Moreover, removal efficiency of UV_{280} was less than UV_{254} for each irradiation period.

As mentioned in the previous section, the photocatalytic degradation of ANOM solution was carried out by using 0.5 mg mL^{-1} TiO_2 but 0.25 mg mL^{-1} TiO_2 was used for 1:2 diluted ANOM solution. Because of the different amount of TiO_2 loading, the photocatalytic degradation rates of the ANOM and 1:2 diluted ANOM solutions were not compared directly, therefore, the aerial rate values were calculated for both of them. Aerial rate is defined as the pseudo first order rate with reference to the surface area of the photocatalyst.

Kinetic modeling of photocatalytic degradation of 1:2 diluted ANOM solution revealed pseudo first order rate constant k as 0.0176 min^{-1} and reaction rate R as 0.329 $m^{-1}min^{-1}$ for UV_{254}.

The aerial rates of the photocatalytic degradation of ANOM solution were found to be 1.16 $m^{-1}min^{-1}m^{-2}$ and 0.956 $m^{-1}min^{-1}m^{-2}$ for 1:2 diluted ANOM solution. The comparison of the aerial rates did not reflect any significant difference due to the concentration and loading effects.

4.4.6. Photocatalytic Degradation of 1:3 Diluted ANOM Solution

Photocatalytic degradation of 1:3 diluted ANOM solution was carried out in the presence of 0.25 mg mL^{-1} TiO_2 during reaction periods up to 60 minutes. According to the obtained data, $Color_{436}$, $Color_{400}$, UV_{365}, UV_{280} and UV_{254} removal efficiencies were illustrated in Figure 4.28 and Table 4.9.

As mentioned in previous sections, the degradation efficiencies did not significantly change between 60 and 90 minutes. Therefore, in this part, the irradiation times were chosen 60 minutes.

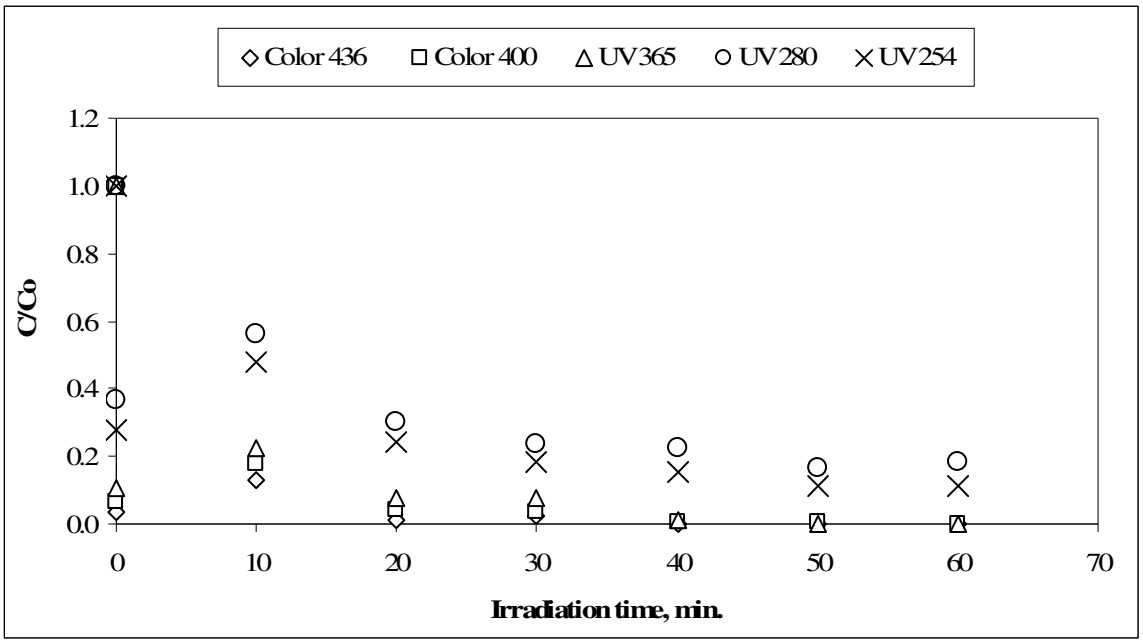

Figure 4.28. Normalized values of $Color_{436}$, $Color_{400}$, UV_{365}, UV_{280} and UV_{254} with respect to irradiation time in the presence of 0.25 mg mL^{-1} TiO_2 for 1:3 diluted ANOM solution.

According to Figure 4.28, initial adsorption values were as high as about 60% and 70% for UV_{280} and UV_{254}, respectively. The initial adsorptions of color forming moieties ($Color_{436}$ and $Color_{400}$) were found to be more than 90% revealing a strong preadsorption phenomenon. On the other hand, the removal due to the fast adsorption-desorption process was also observed in 10 minutes as was attained for 1:2 diluted ANOM solution. But adsorption-desorption value differences of 1:3 diluted solution were higher than 1:2 diluted solution. After 10 minutes, a normal decreasing trend was observed for UV_{280} and UV_{254}. UV_{254} removal followed a similar trend with UV_{280} removal but the UV_{254} removal efficiency was more than removal efficiency of UV_{280} as it was 1:2 diluted ANOM solution.

As it is obviously seen in Figure 4.28, the photocatalytic interaction between TiO_2 and 1:3 diluted ANOM solution resulted in approximately 100% removal in 30 minutes. After 40 minutes, the degradation efficiencies achieved were almost 100% for $Color_{436}$, $Color_{400}$ and

UV_{365}. After 30 minutes of irradiation period, the detected values could be accepted as negligible.

In the Figure 4.28, the $Color_{436}$ removal was almost complete upon irradiation for 20 minutes. In extended irradiation periods up to 60 minutes, oxidative degradation of UV_{280} and UV_{254} could still be observed, attaining 83% and 89% removal percentages, respectively (Table 4.10).

Table 4.10. Oxidative removal of 1:3 diluted ANOM solution upon irradiation for 30 (t_{30}) and 60 (t_{60}) minutes in terms of $Color_{436}$, $Color_{400}$, UV_{365}, UV_{280} and UV_{254}.

Parameter	Removal, % t_{30}	Removal, % t_{60}
$Color_{436}$	97	100
$Color_{400}$	97	100
UV_{365}	92	100
UV_{280}	76	82
UV_{254}	82	89

The previous experimental data for $Color_{436}$ and $Color_{400}$ showed similar removal efficiency values for 1:2 diluted ANOM solution but 1:3 diluted ANOM solution values were the same for $Color_{436}$ and $Color_{400}$. By comparison between 1:2 diluted and 1:3 diluted ANOM solutions, the removal of $Color_{436}$ and $Color_{400}$ indicated that the difference was not exceeding 11% after 30 minutes of photocatalysis. While the initial adsorption values of 1:2 diluted solution for the UV absorbing centers (UV_{280} and UV_{254}) were almost 2 times greater than color forming centers ($Color_{436}$ and $Color_{400}$), the values of 1:3 diluted solution were approximately 10 times.

4.4.7. Photocatalytic Degradation of 1:4 Diluted ANOM Solution

Photocatalytic degradation of 1:4 diluted ANOM solution was carried out in the presence of 0.25 mg mL^{-1} TiO_2 during reaction periods up to 40 minutes. The degradation time was chosen depending on dilution and the degree of detectable absorbance values. The obtained data were presented in Figure 4.29.

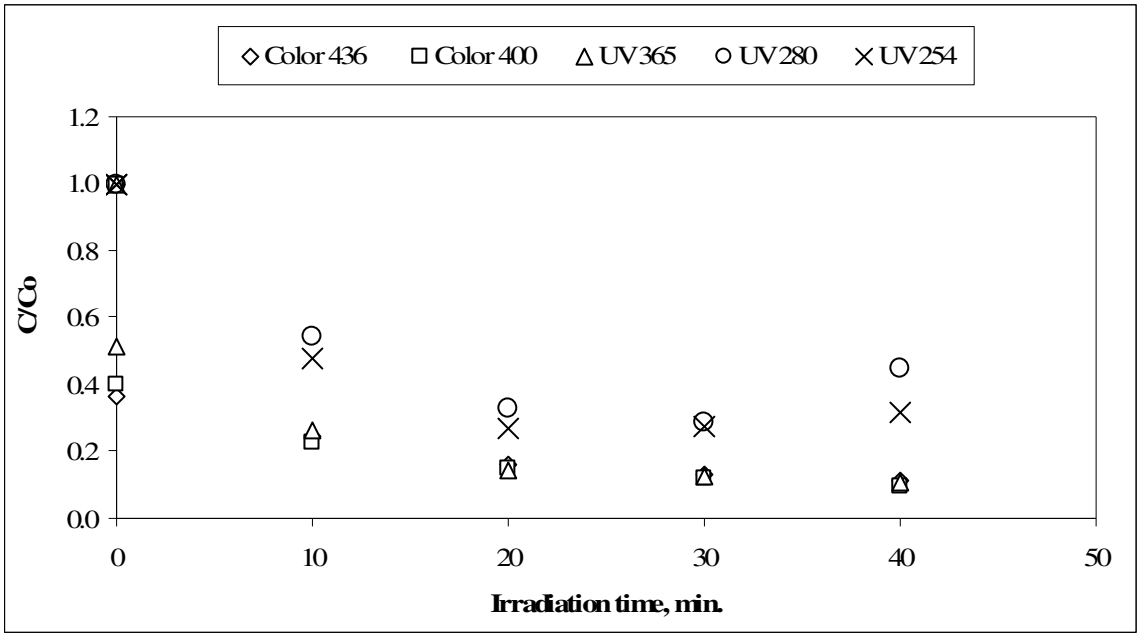

Figure 4.29. Normalized values of $Color_{436}$, $Color_{400}$, UV_{365}, UV_{280} and UV_{254} with respect to irradiation time in the presence of 0.25 mg mL^{-1} TiO_2 for 1:4 diluted ANOM solution.

The data obtained from the photocatalytic reactions of 1:4 diluted ANOM solution for $Color_{436}$, $Color_{400}$, UV_{365}, UV_{280} and UV_{254} removal efficiencies were demonstrated in Figure 4.41. $Color_{436}$, $Color_{400}$ and UV_{365} removal efficiencies exhibited a similar declining trend. According to the figure (Figure 4.29), initial adsorption values were about 60% and 50% for $Color_{400}$ and UV_{365} respectively. As reported in the previous sections, all of the diluted ANOM solutions indicated initial adsorption values for all UV-vis parameters. 1:4 diluted ANOM solution differed from the others because initial adsorptions of UV_{280} and UV_{254} were almost

zero. Moreover, previous solutions generally showed desorption properties in 10 minutes but 1:4 diluted ANOM solution followed expected degradation trend. In extended irradiation periods, no significant removal efficiency was attained besides the maximum degradation observed in 30 minutes.

Table 4.11. Oxidative removal of 1:4 diluted ANOM solution upon irradiation for 30 (t_{30}) minutes in terms of $Color_{436}$, $Color_{400}$, UV_{365}, UV_{280} and UV_{254}.

Parameter	Removal, % t_{30}
$Color_{436}$	87
$Color_{400}$	88
UV_{365}	88
UV_{280}	72
UV_{254}	73

In the presence of 0.25 mg mL^{-1} TiO_2, removal efficiencies values of 1:4 diluted solution revealed that the difference between 30 and 40 minutes was 2% for $Color_{436}$, $Color_{400}$ and UV_{365}.

4.4.8. Photocatalytic Degradation of 1:5 Diluted ANOM Solution

Photocatalytic degradation of 1:5 diluted ANOM solution was carried out in the presence of 0.25 mg mL^{-1} TiO_2 during reaction periods up to 30 minutes. In this experiment, the irradiation times were chosen as 30 minutes because after 30 minutes the absorbance values were not detected. The data were demonstrated in Figure 4.30.

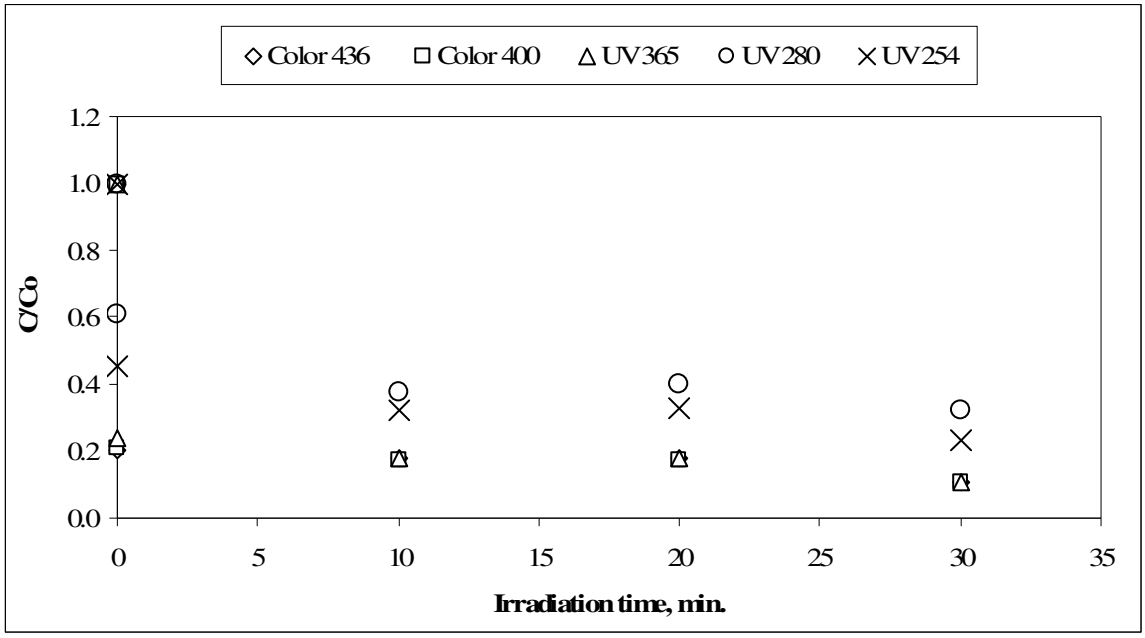

Figure 4.30. Normalized values of $Color_{436}$, $Color_{400}$, UV_{365}, UV_{280} and UV_{254} with respect to irradiation time in the presence of 0.25 mg mL^{-1} TiO_2 for 1:5 diluted ANOM solution.

As shown on the Figure 4.30, few data obtained for degradation of 1:5 diluted ANOM solution during 30 minutes degradation period. Degradation was not measured after 30 minutes of irradiation because the solution was more diluted displaying no significant UV-vis parameters.

In this solution, initial adsorption values of $Color_{436}$, $Color_{400}$ and UV_{365} were not changed significantly, they all had the same value as %80. During the photocatalytic oxidation, the removal percentage differences between initial time and end of the reaction time were about 10% for $Color_{436}$, $Color_{400}$ and UV_{365}. Also, they had similar removal efficiencies after 10 minutes.

As can be seen from figure (Figure 4.30), the initial adsorption values of UV_{280} and UV_{254} were 40% and 55% respectively. Their removal percentages were also slightly increased in 20 minutes. It could be explained by an effective initial adsorption-desorption processes.

Table 4.12. Oxidative removal of 1:5 diluted ANOM solution upon irradiation for 30 (t_{30}) minutes in terms of $Color_{436}$, $Color_{400}$, UV_{365}, UV_{280} and UV_{254}.

Parameter	Removal, % t_{30}
$Color_{436}$	89
$Color_{400}$	89
UV_{365}	89
UV_{280}	68
UV_{254}	77

The removal efficiencies of $Color_{436}$, $Color_{400}$, and UV_{365} were found to be the same for irradiation period of 30 minutes during photocatalytic degradation process representing an effective oxidation process. In comparison to the previously presented data, the removal efficiency achieved for UV_{254} was almost 10 % higher than UV_{280} for 1:5 diluted ANOM solution.

4.5. Adsorption Effects in Photocatalysis

In this study, batch adsorption experiments were also carried out to evaluate the effect of the adsorptive effects of ANOM solution onto TiO_2. The amount of TiO_2 used in adsorption experiments were selected according to the photocatalyst loadings used in photocatalysis experiments as 0.2, 0.5, 0.8 and 1.0 mg mL^{-1}. The data achieved by the adsorption experiments were fitted to the Freundlich adsorption equation which is the most commonly used nonlinear adsorption equilibrium model.

As it can be seen from below figures, q_A versus C_e graphs were plotted for ANOM solution based on Freundlich adsorption model. q_A is the amount of solute adsorbed per unit weight of solid adsorbent, C_e is the concentration of ANOM solution remaining in the aqueous phase after adsorption, and C_i is the initial concentration of ANOM solution. The data for $Color_{436}$, UV_{365}, UV_{280} and UV_{254} were presented in Figures 4.31, 4.32, 4.33 and 4.34.

According to the obtained data from above figures, adsorption trend of $Color_{436}$ with UV_{365} and adsorption trend of UV_{280} with UV_{254} displayed similar features.

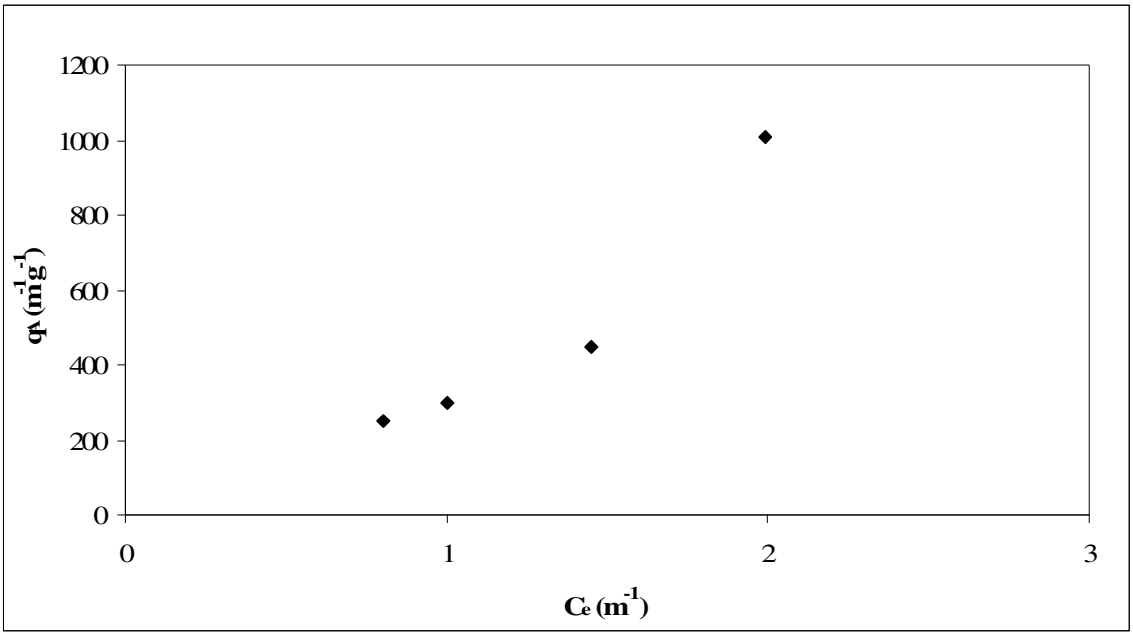

Figure 4.31. $Color_{436}$ adsorption curve of ANOM solution on Degussa P25.

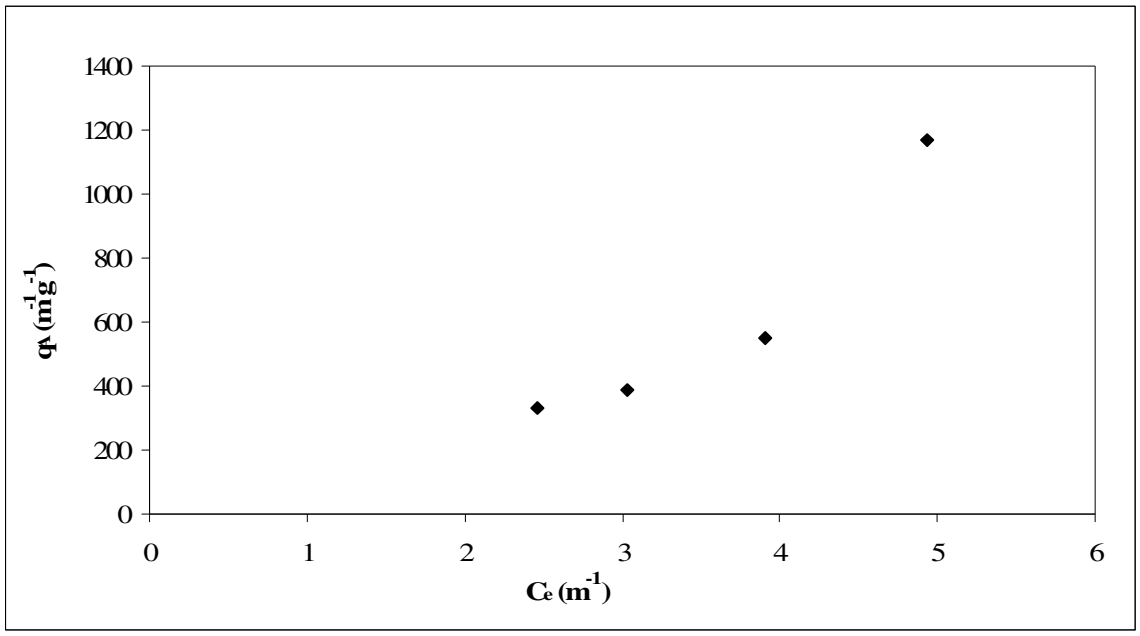

Figure 4.32. UV_{365} adsorption curve of ANOM solution on Degussa P25.

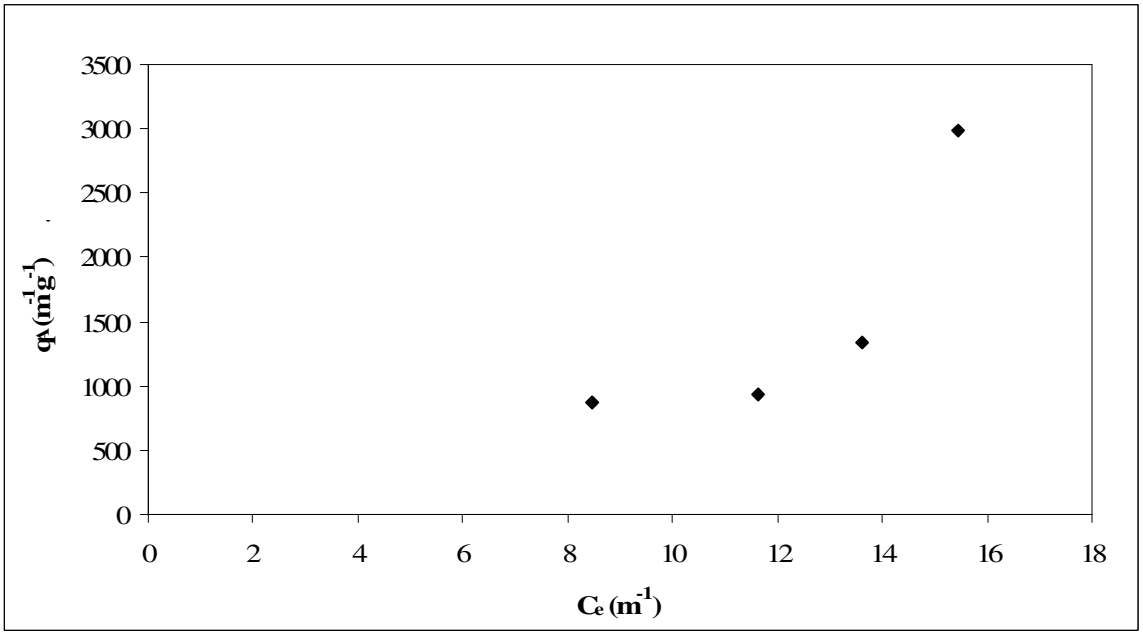

Figure 4.33. UV_{280} adsorption curve of ANOM solution on Degussa P25.

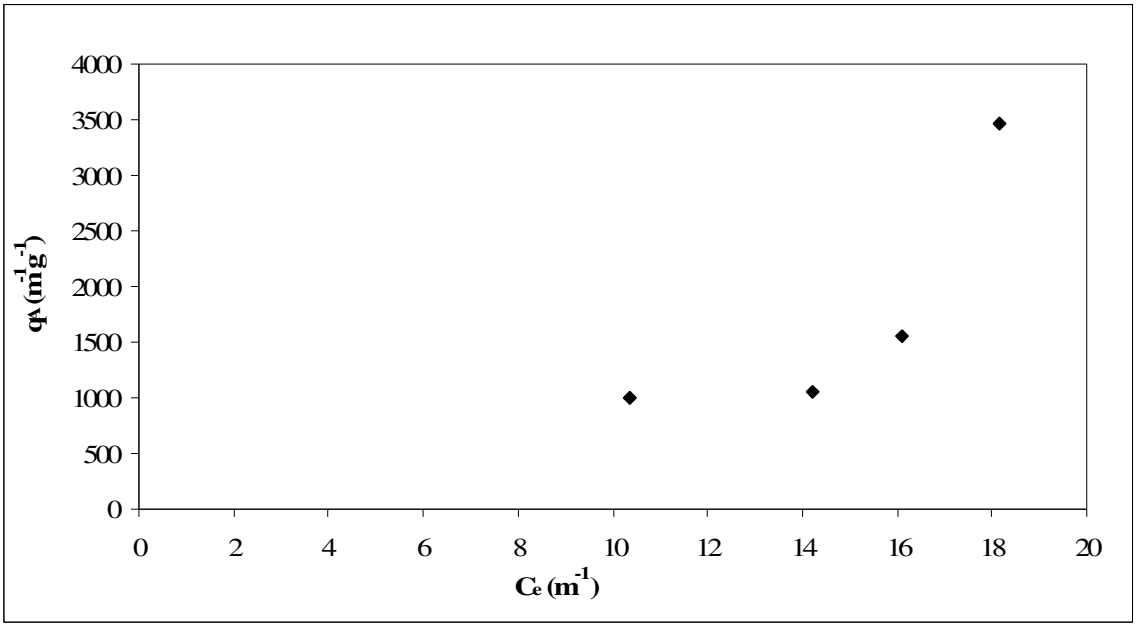

Figure 4.34. UV_{254} adsorption curve of ANOM solution on Degussa P25.

For comparison purposes the Freundlich parameters, K_F (adsorption capacity) and 1/n (adsorption intensity) values obtained from the adsorption experiments of ANOM solution were given in Table 4.13.

Table 4.13. The adsorption coefficients for ANOM solution (related correlation coefficient, r^2>0.64).

	K_F	1/n
$Color_{436}$	313.5	1.49
UV_{365}	59.68	1.77
UV_{280}	16.15	1.78
UV_{254}	9.677	1.90

As it can be seen from Table 4.13, The UV absorbing centers exhibited lower adsorption capacity (K_F) than the color forming centers. K_F values decreased with in relation to the UV-vis parameters as specified by the absorbance values recorded with respect to the wavelengths. However, 1/n values followed the opposite behavior. A plausible explanation could be the structural diversity of the ANOM solutions. As it was mentioned before ANOM solution was obtained from extracted algal organic matter and humic acid. Moreover, previous studies showed that humic acid can be adsorbed easily on the photocatalyst surface but aqueous solution of AOM was not as easily adsorbed as humic acid because of complex structure of AOM. Beside the colorless features of AOM aqueous solution, humic acid gives yellow-brownish color to the ANOM solution. According to adsorption capacity of $Color_{436}$ and UV_{254}, it can be said that adsorption of humic acid was higher than adsorption of aqueous solution of AOM.

Table 4.13 exhibited that 1/n values were found to be higher than 1, indicating strong concentration dependency and favorable adsorption intensity.

In the adsorption process, there is an equilibrium which is defined as the distribution of solute between the liquid and solid phases in critical time. The main difference between initial adsorption removal and adsorption efficiency is reaching equilibrium over time. As it mentioned in materials and methods section (i.e. 3.2.6) adsorption experiments were run for 24 hours because of practical reasons. Preliminary adsorption experiments showed that the equilibration was reached in 16 h, however, no major deviation was observed in 24 h period (Bekbolet et al., 2002; Uyguner and Bekbolet, 2004b).

The adsorption data was evaluated in terms of adsorption efficiency (%) and was given in Table 4.14.

Table 4.14. Adsorption efficiency of ANOM solution on Degussa P25.

TiO_2 loading (mg mL^{-1})	$Color_{436}$ %	UV_{365} %	UV_{280} %	UV_{254} %
0.2	72	54	49	49
0.5	79	64	55	55
0.8	86	72	62	60
1.0	88	77	72	71

According to Table 4.14, no significant differences were observed in adsorption efficiency (%) of UV_{254} and UV_{280}. The ANOM solution was adsorbed over 49% onto the TiO_2 particles. The maximum efficiency was observed at 436 nm. As expected, the efficiency increased with increasing loading TiO_2.

In Suphandag (1998) study, the adsorption effects of TiO_2 on the degradability of natural organic matter, namely, humic acid, by photocatalytic oxidation were investigated depending on pH conditions. According to obtained data that the adsorption capacity of TiO_2 decreased with increasing pH. For example, when the pH values were at 7 and 9, the adsorption efficiencies were found to be % 25 and 19, respectively. In this study the adsorption experiments were carried out with ANOM solution which had 6.54 pH values. At this pH, in the presence of 0.2, 0.5, 0.8 and 1.0 mg mL^{-1} TiO_2, the adsorption efficiencies were calculated as 72%, 79%, 86% and 88% for $Color_{436}$, respectively.

According to Uyguner (1999) study, adsorption of humic acid exhibited a declining trend. Also, adsorption process was not favored by color forming centers because the color forming centers exhibited lower 1/n values than the UV absorbing centers for humic acid. On the other hand, the minimum K_F constants were determined for the UV absorbing centers.

5. CONCLUSIONS

In this study, photocatalytic degradation of AOM aqueous solutions was investigated with respect to their UV-vis and fluorescence properties as representatives to natural organic matter in drinking water supplies.

Considering the complexity of the AOM aqueous solution, it was fractionated into well defined subcomponents of defined molecular sizes using ultrafiltration through membranes in the range of 0.45 μm-100 kDa. In addition, the spectroscopic properties of each size fraction were characterized and compared by UV-vis and fluorescence spectroscopy. Moreover, the structural characteristics of the ANOM solutions relative to changes during photocatalytic oxidation were monitored by UV-vis spectroscopy.

According to the molecular size distribution results, the samples followed similar patterns between size fractions of 0.45 μm to 30 kDa. As a general trend, the absorbance values of the fractionated aqueous solution of AOM increased with decreasing molecular size, except for size fractions 30 kDa. In general, the size fractions of 30 kDa expressed different fluorescence and UV-vis characteristics because of structural change during the molecular size fractionation experiments. The absorbance values of all molecular size of oxidized AOM solution were similar, except for size fractions of 1 kDa. The efficient removal was observed for less than 10 kDa size fractions.

The oxidative degradation of AOM/ANOM solution with 0.25 mg mL^{-1} TiO_2 followed the pseudo first order kinetics. Defined absorbance parameters values during photocatalytic oxidation exhibited a decreasing trend over irradiation time. Higher removal rates have been achieved with $Color_{436}$ and $Color_{400}$ values than UV_{254} and UV_{280} values for all the photocatalytic process.

During photocatalytic oxidation experiments for irradiation time of 60 minutes UV_{254}, removal of AOM aqueous solution was achieved approximately 20% in presence of 0.25 mg mL^{-1} $TiO_{2,}$ and 30% removal in presence of 0.50 mg mL^{-1} $TiO_{2,}$. While for ANOM solution higher removal percentage has been achieved 63% during 30 minutes. The other studied solutions were carried out with the same amount of TiO_2 as 0.25 mg mL^{-1} and with irradiation time of 30 minutes which was investigated adequately for all the diluted solutions. The removal efficiencies which were 70-80% did not change significantly for the diluted solutions. Investigation of the initial adsorptive effects prior to photocatalysis revealed nonconsistent results with respect to dilution effects.

In this study, adsorption experiments were also performed to evaluate the effect of adsorption intensity on the photocatalytic degradation rates and results were expressed based on Freundlich constants. Experiments were held in four different amounts of TiO_2 investigating the effect of amount of TiO_2 on adsorption by means of structural changes.

A significant increase was detected with increasing concentration of TiO_2 amount in adsorption process. Further increase was also obtained for increasing wavelengths. Adsorptive removals of ANOM solution were calculated for $Color_{436}$, in the presence of 0.2, 0.5, 0.8 and 1.0 mg mL^{-1} TiO_2 72%, 79%, 86% and 88% respectively. As experiments carried out with the same TiO_2 amounts, the adsorptive removals of UV_{254} were found to be 49%, 55%, 60% and 71%, respectively.

REFERENCES

Akhlaq, M.S., Schuchann, H.P., Von Sonntag, C., 1990. Degradation of the polysaccharide alginic acid: A comparison of the effects of UV light and ozone. Environmental Science and Technology, 24, 379-383.

Amon, R., Benner, R., 1996. Photochemical and microbial consumption of dissolved organic carbon and dissolved oxygen in the Amazon River system. Geochimica et Cosmochimica Acta, 60, 1783-1792.

Arai, H., Arai, M., Skumoto, A., 1986. Exhaustive degradation of humic acid in water by simultaneous applications of radiation and ozone. Water Research, 20(7), 885-891.

APHA, AWWA, WPCF, 1998. Standard Methods for the Examination of Water and Wastewater, 20th Ed., American Public Health Association, Washington DC.

Azam, F., 1998. Microbial control of oceanic carbon flux: the plot thickens. Science, 280, 694-696.

Backlund, P., 1992. Degradation of aquatic humic material by ultraviolet light. Chemosphere, 25(12), 1869-1878.

Bahnemann, D., Cunningham, J., Fox, M.A., Pelizetti, E., Pichat, P., Serpone, N., 1994. Photocatalytic Treatment of Waters. In Helz, G.R., Zep, R.G., Crosby, D.G.(Eds), Aquatic and Surface Photochemistry, 261-316, Lewis Publishers, USA.

Bas, T., 2001. Humic acid and oxide surface interactions: Adsorption, desorption and surface charge effects, M.S. Thesis, Boğaziçi University.

Bekbolet, M., 1996. Destructive removal of humic acids in aqueous media by photocatalytic oxidation with illuminated titanium dioxide. Journal of Environmental Science and Health, A31 (4), 845-858.

Bekbolet, M., Araz, C.V., 1996. Inactivation of *Escherichia coli* by photocatalytic oxidation. Chemosphere, 32, 959-965.

Bekbolet, M., Balcioglu, I., 1996. Photocatalytic degradation kinetics of humic acid in aqueous TiO_2 dispersions: The influence of hydrogen peroxide and bicarbonate ion. Water Science and Technology, 34, 73-80.

Bekbolet, M., Ozkosemen, G., 1996. A preliminary investigation on the photocatalytic degradation of a model humic acid. Water Science and Technology, 33, 189-194.

Bekbolet, M., Boyacioglu, Z., Ozkaraova, B., 1998. The influence of solution matrix on the photocatalytic removal of color from natural waters. Water Science and Technology, 38, 155-162.

Bekbolet, M, 1999. Photocatalytic Treatment of Drinking Water: Influence of Aqueous Medium Characteristics. The Fourth International Conference on TiO_2 Photocatalytic Purification and Treatment of Water and Air, Albuquerque, 24-28 May 1999, 5, 19-20.

Bekbolet, M., Suphandag, A.S., Uyguner, C.S., 2002. An investigation of the photocatalytic efficiencies of TiO2 powders on the decolorization of humic acids. Journal of Photochemistry and Photobiology A: Chemistry, 148, 121-128.

Benjamin, B.B., 2002. Water Chemistry, McGraw- Hill, Inc., New York.

Bertilsson, S., Tranvik, L.J., 1998. Photochemically produced carboxylic acids as substrates for freshwater bacteriaplankton. Limnology and Oceanography, 43, 885-895.

Black, A.R., Singley, J.E., Whittle, G.P., Maudling, J.S., 1963. Stoichiometry of the coagulation of color-causing organic compounds with ferric sulphate. Journal of American Water Works Association, 55, 1347-1366.

Bolto, B., Abbt-Braun, G., Dixon, D., Eldridge, R., Frimmel, F., Hesse, S., King, S., Toifl, M., 1999. Experimental evaluation of cationic polyelectrolyte for removing natural organic matter from water. Water Science and Technology, 40(9), 71-79.

Bolto, B., Dixon, D., Eldridge, R., King, S., 2002. Removal of THM precursors by coagulation or ion exchange. Water Research, 36, 5066-5073.

Bouteleux, C., Saby, S., Tozza, D., Cavard, J., Lahoussine, V., Hartemann, P., Mathieu, L., 2005. *Escherichia coli* behavior in the presence of organic matter released by algae exposed to water treatment chemicals. Applied and Environmental Microbiology, 71(2), 734-740.

Boyacioglu, Z., 1997. Photocatalytic Degradation of Humic Acids in Aqueous Solutions, M.S. Thesis, Boğaziçi University.

Cabaniss, S.E., Zhou, Q., Maurice, P.A., Chin, Y-P., Aiken, G.R., 2000. A long normal distribution model for the molecular weight of aquatic fulvic acids. Environmental Science and Technology, 34, 1103-1109.

Camel, V., Bermond, A., 1998. The use of ozone and associated oxidation processes in drinking water treatment. Water Research, 32(11), 3208-3222.

Chen, Y., Schnitzer, M., 1976. Viscosity measurements on soil humic substances. Soil Science Society of America Journal, 40, 866-872.

Chin, Y.P., Aiken, G., O'Loughlin, E., 1994. Molecular weight, polydispersity, and spectroscopic properties of aquatic humic substances. Environmental Science and Technology, 28, 1853-1858.

Choudry, G.G., 1982. Interaction of Humic Substances with Environmental Chemicals. The Handbook of Environmental Chemistry, 2, 103-128, Springer-Verlag, Berlin.

Chow, C.W.K., Panglisch, S., House, J., Drikas, M., Burch, M.D., Gimbel, R., 1997. A study of membrane filtration for the removal of cyanobacterial cells. Aqua, 46(6), 324-334.

Cleuvers, M., Altenburger, R., Ratte, H.T., 2002. Combination effect of light and toxicity in algal tests. Journal of Environmental Quality, 31, 539-546.

Cloete, V., Villiers, D., Engelbrecht, W.J, Wessels, G.F.S, 1999. Photocatalytic Treatment of Humic Substances in Raw Natural Water Destined for Drinking Purposes," The Fourth International Conference on TiO_2 Photocatalytic Purification and Treatment of Water and Air, Albuquerque, 24-28 May 1999, 5, 108-109.

Cottrell, M.T., Kirchman, D.L., 2000. Natural assemblages of marine protobacteria and members of the *Cytophaga-Flavobacter* cluster consuming low- and high-molecular weight DOM. Applied and Environmental Microbiology, 66, 1692-1697.

Covert, J.S., Moran, M.A., 2001. Molecular characterization of estuarine bacterial communities that use high- and low-molecular weight fractions of dissolved organic carbon. Aquatic Microbial Ecology, 25, 127-139.

Dincer, B., 1998. Comparison of the Photocatalytic Efficiency of Various Forms of Titanium Dioxide by Using Humic Acid as a Model Compound, M.S. Thesis, Boğaziçi University.

Dominguez-Bocanegra, A.R., Guerrero-Legarreta, I., Martinez-Jeronimo, F., Tomasin-Campocosio, A., 2004. Influence of environmental and nutritional factors in the production of astaxanthin from *Haematococcus pluvialis*. Bioresource Technology, 92(2), 209-214.

Edzwald, J.K., Becker, W.C., Wattier, K.L., 1985. Surrogate parameters for monitoring organic matter and THM precursors. Journal of American Water Works Association, 77(4), 122-132.

Edzwald, J.K., 1993. Coagulation in drinking water treatment particles, organics and coagulants. Water Science and Technology, 27(11), 21-35.

Eggins, B.R., Palmer, FL., Byrne, J.A., 1997. Photocatalytic treatment of humic substances in drinking water. Water Research, 31, 1223-1226.

Eiler, A., Langenheder, S., Bertilsson, S., Tranvik, L.J., 2003. Heterotrophic bacterial growth efficiency and community structure at different natural organic carbon concentrations. Applied and Environmental Microbiology, 69, 3701-3709.

Esparza-Soto, M., Westerhoff, P., 2003. Biosorption of humic and fulvic acids to live activated sludge biomass. Water Research, 37, 2301-2310.

Fein, J.B., 2000. Quantifying the effects of bacteria on adsorption reactions in water-rock systems. Chemical Geology, 169, 265-280.

Findlay, S., Carlough, L., Crocker, M.T., Gill, H.K., Meyer, J.L., Smith, P.J., 1986. Bacterial growth on macrophyte leachate and fate of bacterial production. Limnology and Oceanography, 31, 1335-1341.

Frimmel, F.H., Abbt-Braun, G., Heumann, K.G., Hock, B., Ludemann, H.D., Spiteller, M.(Eds), 2002. Refractory Organic Substances in the Environment, Wiley-VCH, Weinheim.

Frost, P., Maurice, P.A., Fein, J.B., 2003. The effect of cadmium on fulvic acid adsorption to *Bacillus subtilis*. Chemical Geology, 200, 217-224.

Gaffney, J.S., Marley, A.N., Clark, B. (Eds), 1996. Humic and Fulvic Acids; Isolation, Structure, and Environmental Role, ACS Symposium Series 651, American Chemical Society, Chicago.

Geis, S., Fleming, K., Korthals, E., Searle, G., Reynolds, L., Karner, D., 2000. Modifications to the algal growth inhibition test for use as a regulatory assay. Environmental Toxicology and Chemistry, 19(1), 6-41.

Geller, A., 1986. Comparison of mechanisms enhancing biodegradability of refractory lake water constituents. Limnology and Oceanography, 31, 755-764.

Gilbert, E., 1988. Biodegradability of ozonation products as a function of COD and elimination by the example of humic acids. Water Resources, 22, 123-126.

Gjessing, E.T., 1976. Physical and Chemical Characteristics of Aquatic Humus, Ann Arbor Science Publishers Inc., Ann Arbor, Michigan.

Goel, S., Hozalski, R.H., Bouwer, E.J., 1995. Biodegradation of NOM: Effect of NOM source and ozone dose. Journal of American Water Works Association, 87(1), 90-105.

Gracia, R., Aragues, J.L., Ovelleiro, J.L., 1996. Study of the catalytic ozonation of humic substances in water and their ozonation byproducts. Ozone Science and Engineering, 18, 195-208.

Gregor, J.E., Nokes, C.J., Fenton, E., 1997. Optimizing natural organic matter removal from low turbidity waters by controlled pH adjustment of aluminum coagulation. Water Research, 31, 2949-2958.

Gregor, J., Marsalek, B., 2004. Freshwater phytoplankton quantification by chlorophyll a: a comparative study of *in vitro, in vivo* and *in situ* methods. Water Research, 38(3), 517-522.

Guillard, R.R.L., 1975. Culture of Phytoplankton for Feding Marine Invertebrates. In W.L. Smith, M.H., Chanley (Eds.), Culture of Marine Invertebrate Animal, 15-41, Plenum Pres, New York.

Hall, E.S., Packham, R.F., 1965. Coagulation of organic color with hydrolyzing coagulants. Journal of American Water Works Association, 57, 1149-1166.

Hatchard, C.G., Parker, C.A., 1956. A new sensitive chemical actinometer II. Potassium ferrioxalate as a standard chemical actinometer. Proceedings of Royal Society London Series A, 235, 518-536.

Hautala, K., Peravuori, J., Pihlaja, K., 2000. Measurement of aquatic humus content by spectroscopic analysis. Water Research, 34, 246-258.

Her, N., Amy, G., Yoon, J., Song, M., 2003. Novel methods for characterizing algogenic organic matter and associated nanofiltration membrane fouling. Water Science and Technology, 3, 165-174.

Her, N., Amy, G., Park, H.R., Song, M., 2004. Characterizing algogenic organic matter and evaluating associated NF membrane fouling. Water Research, 38(6), 1427-1438.

Hobbie, J.E., 1988. A comparison of planktonic bacteria in fresh and salt water. Limnology and Oceanography, 33, 750-764.

Hoehn, R.C., Barnes, D.B., Thompson, B.C., Randall, C.W., Grizzard, T.J., Shaffer, P.T.B., 1980. Algae as sources of trihalomethane precursors. Journal of American Water Works Association, 72, 344-350.

Hoehn, R.C., Dixon, K.L., Malone, J.K., Novak, J.T., Randall, C.W., 1984. Biologically induced variation in the nature and removability of THM precursors by alum treatment. Journal of American Water Works Association, 76, 134-141.

Hunt, T.R., O'Melia, C.R., 1988. Aluminum-fulvic acid interactions: Mechanisms and applications. Journal of American Water Works Association, 80, 176-186.

Hunt, A.P., Parry, J.D., Hamilton-Taylor, J., 2000. Further evidence of elemental composition as an indicator of the bioavailability of humic substances to bacteria. Limnology and Oceanography, 45, 237-241.

Jacobsen, T.R., 1978. A quantitative method for the separation of chlorophyll a and b from phytoplankton pigments by HPLC. Marine Science Community, 4, 33-47.

Jardine, P.M., Weber, N.L., McCarthy, J.F., 1989. Mechanism of dissolved organic carbon adsorption on soil. Soil Science Society of America, 53, 1378-1385.

Kaplan, L.A., Bott, T.L., 2000. Microbial heterotrophic utilization of dissolved organic matter in a piedmont stream. Limnology and Oceanography, 27, 363-377.

Karabacakoglu, E., 1998. Photocatalytic Oxidation Efficiency of Titanium Dioxide in Hard Waters, M.S. Thesis, Boğaziçi University.

Kerc, A., Bekbolet, M., Saatci, A., 2003. Effect of partial oxidation by ozonation on the photocatalytic degradation of humic acids. International Journal of Photoenergy, 5(2), 75-80.

Kerc, A., Bekbolet, M., Saatci, A., 2004. Effects of oxidative treatment techniques on molecular size distribution of humic acids. Water Science and Technology, 49(4), 7-12.

Kim, J.S., Chian, E.S.K., Saunders, F.M., Perdue, E.M., Giabbai, M.F., 1989. Characteristics of Humic Substances and Their Removal Behavior in Water Treatment. In McCarthy, P., Suffet, I.H. (Eds.), Aquatic Humic Substances, Influences on Fate and Treatment of Pollutants, 727-748, American Chemical Society, Washington DC.

Kroer, N., 1993. Bacterial growth efficiency on natural dissolved organic matter. Limnology and Oceanography, 38, 1282-1290.

Kusakabe, K., Aso, S., Hayashi, S.I., Isomura, K., Morooka, S., 1990. Decomposition of humic acid and reduction of THM formation potential in water by ozone with UV irradiation. Water Research, 24(6), 781-785.

Lake, R., Driver, S., Ewington, S., 2001. The Role of Algae in Causing *Coliform* Problems Within the Distribution System: Proceedings of the Second World Water Congress, International Water Association, Berlin, Germany.

Langlais, B., Reckhow, D.A., Brink, D., 1991. Ozone in Water Treatment Application and Engineering, Lewis Publishers, Inc., U.S.A.

Leff, L.G., Meyer, J.L., 1991. Biological availability of dissolved organic carbon along the Ogeechee River. Limnology and Oceanography, 36, 315-323.

Leff, L.G., 2000. Longitudinal changes in microbial assemblages of the Ogeechee River. Freshwater Biology, 43, 605-615.

Legrini, O., Oliveros, E., Braun, A.M., 1993. Photocatalytic processes for water treatment. Chemical Reviews, 93, 671-698.

Lindell, J.J., Graneli, W., Tranvik, L.J., 1995. Enhanced bacterial growth in response to photochemical transformation of dissolved organic matter. Limnology and Oceanography, 40, 195-199.

Liu, X., Tao, S., Deng, N., 2005. Synchronous-scan fluorescence spectra of *Chlorella vulgaris* solution. Chemosphere, 60, 1550-1554.

Mann, C.J., Wetzel, R.G., 1995. Dissolved organic carbon and its utilization in a riverine wetland ecosystem. Biogeochemistry, 31, 99-1290.

Markle, P.J., Gully, J.R., Baird, R.B., Nakada, K.M., Bottomley, J.P., 2000. Effects of several variables on whole effluent toxicity test performance and interpretation. Environmental Toxicology and Chemistry, 19(1), 123-132.

Matthews, R.W., 1991. Environment: Photochemical and Photocatalytic Processes. Degradation of Organic Compounds. In Pelizetti, E., Schiavello, M.(Eds.), Photochemical Conversion and Storage of Solar Energy, 427-449, Kluwer Academic Publishers, The Netherlands.

Maurice, P.A., Leff, L.G., 2002. Hydrogeochemical controls on the organic matter and bacterial ecology of a small freshwater wetland in the New Jersey Pine Barrens. Water Research, 36, 2561-2570.

Maurice, P.A., Manecki, M., Fein, J.B., Schaefer, J., 2004. Fractionation of an aquatic fulvic acid upon adsorption to the bacterium, *Bacillus subtilis*. Geomicrobiology Journal, 21, 1-10.

Mayer, P., Frickman, J., Christensen, E.R., Nyholm, R., 1998. Influence of growth conditions on the results obtained in algal toxicity tests. Environmental Toxicology and Chemistry, 17, 1091-1098.

McCoy, M.C., 1996. Minimizing the Economic Impact of Organics on ion exchanges Systems, 57th Annual Meeting of the International Water Conference, Pittsburgh, Pennsylvania, November 1996.

McDonald, S., Bishop, A.G., Prenzler, P.D., Robards, K., 2004. Analytical chemistry of freshwater humic substances. Analytica Chimica Acta, 527, 105-124.

Meyer, J.L., Edwards, R.T., Risley, R., 1987. Bacterial growth on dissolved organic carbon from a blackwater river. Microbial Ecology, 13, 13-29.

Meyer, J.L., Benke, A.C, Edwards, R.T., Wallace, J.B., 1997. Organic matter dynamics in the Ogeechee River, a blackwater river in Georgia, U.S.A. Journal of the North American Benthological Society. 53, 82-87.

Mobed, J.J., Hemmingsen, S.L., Autry, J.L., McGown, L.B., 1996. Fluorescence characterization of IHSS humic substances: Total luminescence spectra with absorbance correction. Environmental Science and Technology, 30, 3061-3065.

Moran, M.A., Hodson, R.E., 1990. Bacterial production on humic and nonhumic components of dissolved organic carbon. Microbial Ecology, 13, 13-29.

Moran, M.A., Sheldon, W.M., Zepp, R.G., 2000. Carbon loss and optical property changes during long-term photochemical and biological degradation of estuarine dissolved organic matter. Limnology and Oceanography, 45, 1254-1264.

Myklestad, S.M., Swift, E., 1998. A new method for measuring soluble cellular organic content and a membrane property, T_m, of planktonic algae. European Journal of Phycology, 33, 333-336.

Ogura, N., 1975. Further studies on decomposition of dissolved organic matter in coastal seawater. Marine Biology, 31, 101-111.

O'Melia, C.R., Becker, W.C., Au, K.K., 1999. Removal of humic substances by coagulation. Water Science and Technology, 40, 47-54.

Otsuki, A., Takamura, N., 1987 .Comparison of chlorophyll A concentrations measured by fluorometric HPLC and spectrophotometric methods in highly eutrophic small Lake

Kasumiagura. Internationale Vereinigung fuer Theoretische und Angewandte Limnologie, 23, 944-51.

Ozkovalak, N., 2005. Interactions Betweeen Azo Dyes and Selenium in Their Toxicity to *Dunalielle tertiolecta* and *Vibrio fischeri*, M.S. Thesis, Boğaziçi University.

Peuravuori, J., Pihlaja, K., 1997. Molecular size distribution and spectroscopic properties of aquatic humic substances. Analytica Chimica Acta, 337, 133-149.

Peuravuori, J., Koivikko, R., Pihlaja, K., 2002. Characterization, differentiation and classification of aquatic humic matter separated with different sorbents: Synchronous scanning fluorescence spectroscopy. Water Research, 36, 4552-4562.

Pullin, M.J., Cabaniss, S.E., 1995. Rank analysis of the pH dependent synchronous fluorescence spectra of six standard humic substances. Environmental Science and Technology, 29, 1460–1467.

Pullin, M.J., Cabaniss, S.E., 2001. Colorimetric flow-infection analysis of dissolved iron (II) and total iron in natural waters containing dissolve organic matter. Water Research, 35, 363-372.

Rice, J.A., MacCarty, P., 1991. Statistical evaluation of the elemental composition of humic substances. Organic Geochemistry, 17, 635-648.

Rump, H.H., Krist, H., 1992. Laboratory Manual for the Examination of Water, Wastewater and Soil, Second Ed., VCH, USA.

Sabater, F., Meyer, J.L., Edwards, R.T., 1993. Longitudinal patterns of dissolved organic carbon concentration and suspended bacterial density along a blackwater river. Biogeochemistry, 21, 73-93.

Santos, E. B. H., Filipe, O. M. S., Duarte, R. M. B. O., Pinto, H., Duarte A. C., 2001. Fluorescence as a tool for tracing the organic contamination from pulp mill effluents in surface waters. Acta Hydrochimica et Hydrobiologica, 28, 364-371.

Saunders, G., 1976. The role of terrestrial and aquatic organisms in decomposition processes. In Anderson, J., Macfadyen, A. (Eds), Decomposition in fresh water, 341-374, Blackwell, Oxford.

Scheck, C.K., Frimmel, F.H., 1995. Degradation of phenol and salicylic acid by ultraviolet radiation/ hydrogen peroxide/ oxygen. Water Resource, 29(10), 2346-2352.

Schwertmann, U., Cornell, R.M., 1991. Iron oxides in the laboratory. VCH, New York.

Sen, S., 2004. Effects of Oxidation, Photocatalytic Oxidation, and Sequential Oxidation on Coagulation of Humic Acids, M.S. Thesis, Boğaziçi University.

Senesi, N., 1990. Molecular and quantitative aspects of the chemistry of fulvic acid and its interactions with metal ions and organic chemicals Part II: The fluorescence spectroscopy approach. Analytica Chimica Acta, 232, 77-106.

Senesi, N., Miano, T.M., Provenzano, M.R., Brunetti, G., 1991. Characterization, differentiation, and classification of humic substances by fluorescence spectroscopy. Soil Science, 152, 259-271.

Servais, P., Anzil, A., Ventresque, C., 1989. Simple method for determination of biodegradable dissolved organic carbon in water. Applied and Environmental Microbiology, 55, 2732-2734.

Singh, B.R., 1984. Sulfate adsorption by acid forest soils: Sulfate adsorption isotherms and comparison of different adsorption equation in describing sulfate adsorption. Soil Science, 138, 189-197.

Slawinska, D., Polewski, K., Rolewski, P., Plucinski, P., Slawinski, J., 2002. Spectroscopic studies on UVC-induced photodegradation of humic acids. Electronic Journal of Polish Agricultural Universities, 5(2), 1-13.

Sondergaard, M., Middelboe, M., 1995. A cross-system analysis of labile dissolved organic carbon. Marine Ecology Progress Series, 118, 283-294.

Suffet, I.H., MacCarty, P.(Eds), 1989. Aquatic Humic Substances, Influences on Fate and Treatment of Pollutants, American Chemical Society, Washington DC.

Suphandag, A.S., 1998. Adsorption Capacity of Natural Organic Matter on Semi-Conductor Powders. M.S. Thesis, Boğaziçi University.

Suphandag, A.S., 2006. Evaluation of Natural organic Matter-Metal Oxide Adsorption Isotherms under Influential Structural Concepts, Ph.D. Thesis, Boğaziçi University.

Stephan, D., Lobbes, J.M., Rainer, R., Jurgen, R., 1998. Ultraviolet fluorescence excitation and emission spectroscopy of marine algae and bacteria. Marine Chemistry, 62, 137-156.

Stephenson, R.J., Duff, S.J.B., 1996. Coagulation and precipitation of a mechanical pulping effluent-I. Removal of carbon, color and turbidity. Water Research, 30, 781-792.

Strickland, J.D.H., Parsons, T.R., 1972. Pigment analysis-a practical handbook of seawater analysis. Bulletin Fisheries Research Board of Canada, 167, 185-205.

Takahashi, N., Nakai, T., Satoh, Y., Katoh, Y., 1995. Ozonolysis of humic acid and its effect on decoloration and biodegradability. Ozone Science and Engineering, 17, 511-525.

Thurman, E.M., 1985. Organic Geochemistry of Natural Waters. Martinus Nijhoff/Junk, Boston.

Tipping, E.(Eds), 2002. Cation Binding by Humic Substances, Cambridge University Press, Cambridge, UK.

Traina, S.J., Novak, J., Smeck, N.E., 1990. An ultraviolet absorbance method of estimating the percent aromatic carbon content of humic acids. Journal of Environmental Quality, 19, 151-153.

Tranvik, L.J., 1990. Bacterioplankton growth on fractions of dissolved organic carbon of different molecular weights from humic and clear waters. Applied and Environmental Microbiology, 56, 1672-1677.

Tulonen, T., Salonen, T.C., Arvola, L., 1992. Effects of different molecular weight fractions of dissolved organic matter on growth of bacteria, algae and protozoa from highly humic lakes. Hydrobiology, 229, 239-252.

Tulonen, T., 2004. Role of Allochtonous and Autochthonous Dissolved Organic Matter (DOM) As a Carbon Source for Bacterioplankton in Boreal Humic Lakes. Ph.D. Thesis, University of Helsinki.

U.S.EPA., 1993. Short-term Methods for Estimating the Chronic Toxicity of Effluents and Receiving Waters to Freshwater Organisms. Environmental Monitoring Systems Laboratory. Cincinnati, OH. EPA-600/4-90/027F.

Uyguner, C.S., Bekbolet, M., 2004a. Photocatalytic degradation of natural organic matter: Kinetic considerations and light intensity dependence. International Journal of Photoenergy, 6, 73-80.

Uyguner, C.S., Bekbolet, M., 2004b. Evaluation of humic acid, chromium (VI) and TiO2 ternary system in relation to adsorptive interactions. Applied Catalysis B: Environmental, 49, 267-275.

Uyguner, C.S., 2005. Elucidation of the Photocatalytic Removal Pathways of Humic Substances: Progress towards Mechanistic Explanations. Ph.D. Thesis, Boğaziçi University.

Uyguner, C.S., Bekbolet, M., 2005a. Implementation of spectroscopic parameters for practical monitoring of natural organic matter. Desalination, 176, 47-55.

Uyguner, C.S., Bekbolet, M., 2005b. Evaluation of humic acid photocatalytic degradation by UV-vis and fluorescence spectroscopy. Catalysis Today, 101, 267-274.

Uyguner, C.S., Bekbolet, M., 2005c. A comparative study on the photocatalytic degradation of humic substances of various origins. Desalination, 176, 167-176.

Van Benschoten, J.E., Edzwald, J.K., 1990. Chemical aspects of coagulation using aluminum Salts-II. coagulation of fulvic acid using alum and polyaluminum chloride. Water Research, 24, 1527-1535.

Van Loon, G.W., Duffy, S.J., 2000. Environmental Chemistry, Oxford University Press, Oxford.

Vik, E.A, Eikeorokk, B., 1989. Coagulation Process for Removal of Humic Substances from Drinking Water. In McCarthy, P., Suffet I.H.(Eds.), Aquatic Humic Substances, Influences on Fate and Treatment of Pollutants, 385-408, American Chemical Society, Washington, D.C.

Vilge-Ritter, A., Masion, A., Boulange, T., Rybacki, D., Bottero, J.Y., 1999. Removal of natural organic matter by coagulation-flocculation: A pyrolysis-GC-MS study. Environmental Science and Technology, 33, 3027-3032.

Volk, C.J., Volk, C.B., Kaplan, L.A., 1997. Chemical composition of biodegradable dissolved organic matter in streamwater. Limnology and Oceanography, 42, 39-44.

Westerhoff, P., Chen, W., Esparza, M., 1999. Organic Compounds in the Environment: Fluorescence Analysis of a Standard Fulvic Acid and Tertiary Treated Wastewater, Technical Report.

Wetzel, R.G., Hatcher, P.G., Bianchi, T.S., 1995. Natural photolysis by ultraviolet irradiance of recalcitrant dissolved organic matter to simple substrates for rapid bacterial metabolism. Limnology and Oceanography, 40, 1369-1380.

Wetzel, R.G., 1998. Aquatic Humic Substances: Ecology and Biogeochemistry. In Hessen, D.O., Tranvik, L.J.(Eds), Springer-Verlag, Berlin.

Widrig, D.L., Gray, K.A., Mcauliffe, K., 1996. Removal of Algal-Derived Organic Material by Preozonation and Coagulation: Monitoring Changes in Organic Quality by Pyrolysis- GC-MS. Water Research, 30(11), 2621-2632.

Yildirim, H., 2000. Contribution of Ionic Strength to the Interaction of Natural Organic Matter and Metal Oxide Surface. Ph.D. Thesis, Boğaziçi University.

Young, K.C., Maurice, P.A., Docherty, K.M., Bridgham, S.D., 2004. Bacterial degradation of dissolved organic matter from two northern Michigan streams. Geomicrobiology Journal, 21, 521-528.

Young, K.C., 2005. Utilization of Natural Organic Matter (NOM) Substrates by Bacteria. Ph.D. Thesis, University of Notre Dame.

Zhou, H., Smith, D.W., 2002. Advanced technologies in water and wastewater treatment. Journal of Engineering Science, 1, 247-264.

Zhou, J.L., Banks, C.J., 1993. Mechanism of humic acid color removal from natural waters by fungal biomass biosorption. Chemosphere, 27, 607-620.

Zhou, Q., Maurice, P.A., Cabaniss, S.E., 2001. Size fractionation upon adsorption of fulvic acid on goethite: Equilibrium and kinetic studies. Geochimica et Cosmochimica Acta, 5, 803-812.

REFERENCES NOT CITED

Kerc, A., 2002. Oxidation of Aqueous Humic Substances by Ozonation. Ph.D. Dissertation, Boğaziçi University.

Sacan, M.T., Balcioglu, I.A., Ercan, C., 1999. Laboratory bioaccumulation of copper, lead and selenium in the marine alga *Dunaliella tertiolecta* metal pair situation. Toxicological and Environmental Chemistry, 76, 17-27.

Sacan, M.T., Balcioglu, I.A., 2006. A case study on algal response to raw and treated effluents from an aluminum plating plant and a pharmaceutical plant. Ecotoxicology and Environmental Safety, 64, 234-243.

Sawyer, C.N., McCarty, P.L., Parkin, G.F., 2003. Chemistry for Environmental Engineering and Science, Fifth Ed., McGraw-Hill, Inc., Singapore.

Tchobanoglous, G., Burton, F. L., 1991. Wastewater Engineering: Treatment, Disposal and Reuse, Third Ed., McGraw-Hill, Inc., Singapore.

http://io.uwinnipeg.ca/~simmons/ysesp/iso5.htm -Algal Culture Methods.